CHROMIUM(III) INTERACTION WITH TRANSFERRIN AND TRANSFERRIN RECEPTOR

by

KYLE CARTER EDWARDS

JOHN B. VINCENT, COMMITTEE CHAIR
DAVID A. DIXON
CAROLYN J. CASSADY
MICHAEL K. BOWMAN
PATRICIA A. SOBECKY

A DISSERTATION

Submitted in partial fulfillment of the requirements
for the degree of Doctor of Philosophy
in the Department of Chemistry
in the Graduate School of
The University of Alabama

TUSCALOOSA, ALABAMA

2021

ABSTRACT

Transferrin (Tf) appears to transports trivalent chromium via endocytosis. The release of chromium(III) from human serum transferrin has been examined under conditions mimicking an endosome during endocytosis. At pH 4.5 and 5.5, the release of Cr(III) from Tf occurs rapidly from the C-lobe binding site and slowly from the N-lobe binding site. The loss of N-lobe bound Cr(III) under these conditions is accelerated by the presence of a anionic chelating ligand. When Cr(III)-loaded transferrin is added to soluble transferrin receptor (sTfR), the loss of Cr(III) from both binding sites becomes rapid at acidic pH, more rapid than from either site in the absence of the receptor. Loss of Cr(III) from the Tf-sTfR complex is easily sufficiently rapid for Tf to serve as the physiological transporter of Cr(III) from the bloodstream to the tissues. Studies have also found that $Cr(III)_2$-Tf can exist in multiple conformations giving rise to different spectroscopic properties and different rates of Cr(III) release. Time-dependent spectroscopic studies of the binding and release of Cr(III) from human serum Tf have been used to identify three conformations of $Cr(III)_2$-Tf. The conformation formed between 5 and 60 minutes after the addition of Cr(III) to apoTf at pH 7.4 resembles the conformation of $Cr(III)_2$-Tf in its complex with sTfR and loses Cr(III) rapidly at endosomal pH. Loss of Cr(III) from Cr_2-Tf and Cr_2-Tf-sTfR in the presence of apo-chromodulin (LMWCr) results in accumulation of Cr(III) bound to LMWCr and is rapid when sTfR is present indicating the species can form under endosomal conditions and may be the next carrier in the Cr(III) transport pathway. Techniques used throughout the projects were also applied to $Mn(III)_2$-Tf, and the first parallel mode EPR signal for Mn(III)-Tf is reported, which could prove valuable for future studies.

DEDICATION

This dissertation is dedicated to everyone who helped me and guided me through the trials and tribulations of creating this manuscript. In particular, my family offered encouragement and support, my close friends offered camaraderie and fellowship, and my advisors offered mentorship and guidance throughout my time at The University of Alabama.

LIST OF ABBREVIATIONS AND SYMBOLS

Al	aluminum
ASP	aspartic acid
Bi	bismuth
BLI	bio-layer interferometry
cm	centimeters: 10^{-3} meter
CHAPS	(3-((3-cholamidopropyl) dimethylammonio)-1-propanesulfonate)
CHO	Chinese hamster ovary cells
CNBr	Cyanogen bromide activated agarose
Co	cobalt
Cr	chromium
$[Cr(pic)_3]$	chromium picolinate
CW-EPR	continuous-wave electron paramagnetic resonance: a form of EPR experiment in which the frequency of radiation is held constant and the magnetic field is varied

d	unit of time: day
D	aspartic acid
DTT	dithiothreitol
E	glutamic acid
ESEEM	electron spin echo envelope modulation: A type of pulsed EPR experiment in which modulation in the decay of the electron spin echo is dependent upon nuclear hyperfine frequencies
EPR	electron paramagnetic resonance
Fe	iron
G	glycine
Ga	gallium
HCl	hydrochloric acid
Hepes	2-[4-(2-hydroxyethyl)piperazin-1-yl]ethanesulfonic acid
Hep G2	human liver cancer cells
HIS	histidine
hr	unit of time: hour
G	magnetic field in gauss

g	proportionality factor of an electron whose value is dependent on the environment and can be taken as a ratio of the microwave frequency and a constant over the magnetic field
k	rate constant of a process
KCl	potassium chloride
Kd	dissociation constant
kD	kilodalton
KISAB	kinetically significant anion binding site located on the N-lobe of serum transferrin
KPi	potassium phosphate
LMWCr	the oligopeptide low-molecular-weight chromium-binding substance otherwise known as chromodulin
M	molar
MCT	monocarboxylate transporter
min	unit of time: minute
mM	millimolar: 10^{-3} molar
Mn	manganese
ms/ms	tandem mass spectrometry
mT	milliteslas
NaCl	sodium chloride

NaOH	sodium hydroxide
nm	nanometers: 10^{-9} meter
nM	nanomolar: 10^{-9} molar
PDB	protein database file
PMSF	phenylmethylsulfonyl fluoride
SD	standard deviation
sTfR	the extracellular portion of transferrin receptor lacking the transmembrane region
t	time
Tf	the protein transferrin
TfR	the protein transferrin receptor
TfR2	an analogue protein to transferrin receptor that possess lower affinity for Tf
Ti	titanium
TYR	tyrosine
U	uranium
UV	ultraviolet radiation
UV-Vis	ultraviolet and visible radiation
w/v	weight per volume
ε	extinction coefficient from Beer's Law

µM	micromolar: 10^{-6} molar
°C	degree Celsius
Δ	change in
Å	angstrom: 10^{-10} meters
~	approximately equal to
<	less than
>	greater than
±	plus or minus

ACKNOWLEDGMENTS

I would like to take this opportunity to thank the many colleagues, friends, and faculty members that have assisted me on this research project. I am most indebted to John Vincent, the chairman of this dissertation, for his advice, tutelage, wisdom, and expertise not only in chromium research, but also in nuisances of the higher academia. I would also like to thank all of my committee members, David Dixon, Carolyn Cassady, Michael Bowman, and Patricia Sobecky, for their invaluable input, inspiring questions, and support of both the dissertation and my academic progress. I would like to extend special thanks to Molly Lockart, Michael Bowman, and Brad Pierce for their assistance in training and use of the EPR facilities at The University of Alabama, without which much of this research would be impossible. I would like to extend additional thanks to Courtney Petersen and Matthew Thompson for their expertise and time in the collaborative efforts to obtain the first X-ray crystal structure of a Cr(III)-containing transferrin. I would also like to extend thanks to Patrick Frantom for his expertise in kinetic modeling and his assistance in recent works. Lastly, I would like to thank my peers and coworkers who made time at Alabama enjoyable and enriching.

CONTENTS

LIST OF TABLES

LIST OF FIGURES

INTRODUCTION

1. Background

Research investigating trivalent chromium's, Cr(III)'s, potential role as a biomolecule was often flawed due to the misunderstandings of the active form of Cr(III) and how it is transported throughout the body. Initially, Cr(III)'s biochemical role was thought to be as an essential component in glucose metabolism. A supposedly pioneering study in the 1950's in which rats were fed a *Torula* yeast-based diet found the rats developed glucose intolerance, presumably due to a lack of some essential trace element [1]. Trace elements were reintroduced one by one to the rat's diet until glucose tolerance was restored [2]; the trace element found to restore glucose metabolism was Cr(III) [3]. However, the amount of Cr(III) being introduced to the diet, and if the diet was Cr(III) deficient in the first place requires scrutiny. The amount of Cr(III) initially in the diet was not reported such that the amount of Cr supplementation compared to dietary Cr is unclear. Given the trace element composition of the diet was not reported, no potential dietary stress from deficiency of a trace element can be established. Furthermore, the rats were maintained in steel wire mesh cages, which could provide Cr(III) to the rats as they gnaw on the cages. Nevertheless, this series of studies set the stage for decades of research into Cr(III)'s supposed role as 'glucose tolerance factor'; which contributes to current claims of Cr(III)'s ability to enhance body mass loss due to its interactions with glucose metabolism [4].

Cr(III)'s postulated role in carbohydrate and lipid metabolism has generated significant scientific and commercial interest in the element. Commercial sales of Cr(III) supplements are significant, accounting for 4% of all mineral supplements sold [4]. This interest is not totally without merit as some studies have indicated that Cr(III) potentiates the action of insulin, which may be helpful in improvement of diabetes symptoms (discussed below). Additionally, some studies have also indicated Cr(III) may improve lean muscle gain or improved body mass loss; however, these studies require critical evaluation.

Cr(III) is purported to have a therapeutic potential in cases of insulin resistance. Cr(III) has been suggested to have a role in stimulating tyrosine kinase activity primarily in the form Cr_4-LMWCr (Low-molecular-weight-binding-substance). LMWCr is an oligopeptide complexed with Cr(III) that has been isolated from numerous mammals and is the form of Cr(III) excreted in urine. Yamamoto and coworkers first reported that LMWCr may have a role in potentiating the action of insulin in rat adipocytes [5]. Cr_4-LMWCr in the presence of insulin enhanced the rate of radiolabeled-glucose conversion to ^{14}CO and incorporation of the label into lipids compared to insulin alone by 20-30% [6]. Further work would show that the Cr_4-LMWCr complex results in a 3-8 fold insulin dependent stimulation in tyrosine kinase activity in rat fat cells [7]. Another study found in CHO cells, immortalized ovary cells from hamsters with increased insulin receptor expression, that regardless of the form of Cr(III) added to cells in serum, kinase activity is enhanced by ~40% in trials with added Cr(III) due to increased tyrosine phosphorylation of insulin receptors [8]. Similar results to these have been obtained in liver, skeletal muscle, and other cells from rats, hamsters, and rabbits [9]. Other metabolic pathways involved in glucose homeostasis have also been implicated (endoplasmic reticulum stress, AMP-activated protein

kinase, protein tyrosine phosphatase 1B). However, the majority of studies are correlative, and explicit molecular mechanisms to explain the causality of Cr(III)'s effects are speculated but unproven [10-12].

The results of clinical studies of chromium in alleviating diabetic symptoms in humans remains mixed; meta-analysis on randomized controlled clinical trials investigating Cr(III) supplementation in improving glycaemia among diabetic patients is complicated due to the poor quality of many studies. Out of the eight meta-studies conducted recently, fasting blood glucose levels (the most commonly reviewed biomarker) were shown to have been significantly affected by Cr(III) in five of them [13-20]. The most recent pooled analysis on 28-randomized trials concluded Cr(III) supplementation did appear have an effect on fasting plasma glucose levels ($p=0.008$) and hemoglobin A1c ($p=0.0002$) in patients with Type-2 diabetes; however, the effects were small (< 5%) indicating chromium supplementation is only suitable in conjunction to traditional pharmacological treatment and of questionable clinical significance [20]. Some explanations have been offered to reconcile the mixed studies; however, not enough is known on the molecular mechanisms of Cr(III) to offer more than conjecture. As it stands, not enough evidence exists to offer formal practicing guidelines for the use of Cr(III) supplementation in any form as a therapeutic treatment in lowering blood glucose or other risk factors in diabetes; however, consistent and reproducible results demonstrating Cr(III)'s effects in promoting the action of insulin in rat models is promising for potential future applications in humans. Reconciling the effects observed in animal models with those from human clinical studies emphasizes the need of understanding Cr(III)'s biochemistry moving forward.

Numerous studies have investigated the effects of Cr(III) supplementation on body mass composition/body mass loss in adults with mixed results; a recent survey of all body mass

composition studies to date is provided by Ref 21. Out of 31 different studies investigating the effects of Cr(III) supplementation of body composition, only 10 studies observed either an increase in fat-free mass or a decrease in fat mass associated with increase Cr(III) intake [21]. Though these studies are somewhat limited in subjects, the consensus of these studies appears to be that Cr(III) supplementation has no effect on body mass and composition. The results of these studies are somewhat difficult to compare due to the inconsistent (and often poor) experimental design varying in sample size, duration, and evaluation of Cr(III) nutritional status. Four of the studies used a sample size of only 6 adults, resulting in weak statistical strength despite two of the studies reporting favorable effects by Cr(III). The duration of the studies was also inconsistent, ranging from 6-64 weeks with the majority (~84%) taking place in 14 weeks or less. These flawed experimental parameters exemplifies complications stemming from the lack of understanding of Cr(III)'s biochemistry. How Cr(III) is stored, its uptake its efficacy, its transportation throughout the body, and its bioactive forms are critical when evaluating how these experiments should be designed and the strength of their conclusions. For example, if Cr(III) is only stored in a highly labile pool (i.e. Tf) with high turnover after introduction (i.e. ~100 min), supplementation occurring immediately prior to an exercise routine may have different effects than a dose administered hours beforehand. Currently, little evidence exists to support Cr(III) as having an effect in body composition changes in humans.

Regularly, studies fail to take into account how the Cr(III) is being introduced into an organism and what form it takes. $CrCl_3$ as the inorganic salt can be considered the most basic form of Cr(III) used as a supplement; other supplements include $Cr(picolinate)_3$, $[Cr(pic)_3]$, Cr nicotinate, and chromium propionate. Several studies have investigated the uptake mechanism of Cr(III) in its various forms used as nutritional supplements. With few exceptions, most organic

Cr(III) derivatives share the same uptake efficiency (~2%) as $CrCl_3$ [22, 23]. Most studies investigating the uptake mechanism of Cr(III) using these various supplements have found the absorption to be unsaturable over a wide range of dosage suggesting passive diffusion to be the uptake mechanism [24]. One study does exist which suggests active transport is involved in the uptake of Cr(III) [25]. An inverse uptake efficiency of Cr(III) by the intestine at high and low doses was observed in women, but not men, suggesting a non-passive uptake mechanism in women only; this study not been reproduced and lacks proper statistical analysis [25].

Several case studies have been conducted in which patients on total parenteral nutrition, a diet in which nutrients are added directly into veins bypassing gastrointestinal absorption, exhibited glucose intolerance and were supplemented with Cr(III) in efforts to restore glucose tolerance/insulin sensitivity [26-32]. While the dosages varied, the highest dosages were in the 100 ug/d range, compared with ~30 ug/d as the recommended dietary adult intake of Cr(III). However, as total parenteral nutrition is an intravenous diet, the dosage used in these studies were approximately 300 to 3,000 times the average Cr(III) dietary uptake as very little of the recommended oral intake of 30 ug/d is absorbed to the bloodstream while 100 % of the Cr(III) is in the bloodstream when administered intravenously [33]. Consequently, the action of Cr(III) in these studies cannot be taken as resulting from typical dietary levels of Cr(III) and instead demonstrates potential therapeutic effects resulting from extremely high doses of Cr(III).

The intestinal uptake of Cr(III) in its various forms is fairly well understood; however, recent studies have drawn scrutiny on the transport of Cr(III) through the bloodstream and subsequent introduction into cells. Cr(III)'s fate after uptake in the intestines is ultimately excretion in urine complexed with the small oligopeptide low-molecular-weight chromium-binding substance, LMWCr (otherwise known as chromodulin); however, its transport to cells,

the form Cr(III) takes in cells, and the mechanism of its potential activity within cells are poorly understood.

2. Cr(III) Transport by Tf/TfR

Cr(III) has long been thought to be transported by the protein transferrin (Tf). The Tf-Cr(III) interaction was originally proposed by Schwarz; Schwarz observed for rats fed radiolabeled $^{51}CrCl_3$ that 90% of the blood Cr(III) immunoprecipitated with the β-globulin fraction; at least 70% of the chromium bound to transferrin [34]. Further radiolabeling studies have demonstrated that $^{51}Cr_2$-Tf injected into blood of rats results in >50% of the Cr(III) being transported into tissues within 30 minutes [35]. Binding of Cr(III) to transferrin has also been demonstrated to be rapid under physiological conditions (i.e. in the presence of 25 mM bicarbonate) and to be essentially complete in 20 minutes [36].

Recently, Cr(III) was demonstrated to not accumulate over 24 hours in liver cancer cells when $Cr(III)_2$-Tf was added to the growth media [37]. Cr(III) was preloaded into Tf and the Cr-Tf was introduced to HepG2 cells (liver cancer cells). After being incubated with the cells for 24 hrs, samples in which the Cr(III) would be able to load in the binding pocket of Tf were shown to have a lower uptake of Cr(III) than just Cr(III) alone. The inability for Cr(III) from Tf to enter the cells was postulated to result from Cr(III) release from the Tf binding site being slower than the endosome cycle and the binding of Cr(III) to Tf was postulated to 'detoxify' Cr(III) by trapping it in the Tf. The postulate is in disagreement with a study investigating monocarboxylate transport (MCT) inhibition on the cellular accumulation of Cr(III) in mouse C2C12 muscle cells; in this study, Cr(III) and Fe(III) were similarly added to cellular media as their transferrin complexes [38]. The study concluded that MCTs were not involved in transport of Cr(III) due to Cr(III) accumulation in cells not being affected by MCT inhibitors (i.e. the

investigators observed Cr(III) accumulation in cells). This discrepancy begs the question if Cr(III) can be released from Tf within an endosomal cycle as required if Tf is to be the physiological transporter of Cr(III) in the blood stream.

Fe(III) is known to be released from Tf during the endocytosis process, and numerous studies on the Fe-Tf interaction have demonstrated different factors that have an effect on Fe(III)'s release from Tf during endocytosis. These effects could also be involved in the release of Cr(III) from Tf. Fe(III) has been shown to have heterogeneous rates of release from the different lobes of transferrin [39], and the release of the metal has been shown to affected by complexation with transferrin's receptor protein (transferrin receptor (TfR)). The presence of biological chelating ligands have been demonstrated to accelerate the release of Fe(III) from Tf during acidification [40]. Additionally, the endocytosis process requires approximately 15 min, such that release of the Fe(III) must be complete with 15 min otherwise it could not be transported from the endosome to the cytoplasm within that time period. For Fe(III) after its release from Tf, this involves the reduction of Fe(III) to Fe(II) and subsequent removal of Fe(II) via divalent metal transporter channel.

3. Tf/TfR Cycle and General Overview of Endocytosis

Tf is a plasma glycoprotein with a molecular weight of 79.5 kilodalton (kD). Tf possesses two metal binding sites located on two separate lobes, the N- and C-lobe; each lobe binds a single metal ion. The metal is typically trivalent with a large charge to size ratio. The binding sites have the same protein-provided ligands: 2 tyrosinate, 1 histidine, and 1 aspartate, with additional coordination provided by a synergistic anion (physiologically bicarbonate) located in a nearby anion binding pocket (Figure 1.1). In humans, the two lobes have approximately 40 % sequence homology; however, the metal binding constants for the two lobes differ [41]. Metal-

bound Tf (holo-Tf) typically has a higher affinity for the receptor protein TfR than apo-Tf, and holo-Tf will typically bind tightly at the surface of a cell at pH 7.4. The holo-Tf-TfR complex will then be internalized via endocytosis; the process is summarized in Figure 1.2. The acidification of the resulting endosome to pH 4.5-5.5 dramatically lowers the Tf's affinity towards the metal, which facilitates the metal's release from the Tf-TfR complex and the metal's subsequent removal from the endosome. The endosome remerges with the cell membrane, returning the Tf-TfR complex to pH 7.4, which recycles the now apo-Tf back to serum.

TfR is a transmembrane protein consisting of two homologous lobes (~90 kDa per lobe) linked via a disulfide bridge; each lobe is capable of binding two Tf molecules. The extracellular portion of TfR can be cleaved via trypsin yielding a 70 kDa fragment capable of tightly binding two molecules of transferrin; this extracellular fragment of TfR is soluble and denoted soluble transferrin receptor (sTfR) (Figure 1.3). The sTfR molecule has been used in numerous Tf-TfR affinity studies investigating the binding affinity of various metallated Tfs with the receptor and is widely considered a good model for the physiological endosomal process [42]. The binding of $Fe(III)_2$-Tf to TfR has been shown to accelerate the rate of release of Fe(III) from Tf when acidified [43]. TfR has been shown to bind $Cr(III)_2$-Tf; however, the effect TfR binding has on the release of Cr(III) from Tf has not been investigated [44].

TfR was long believed to be a single receptor protein; however, recently a second protein has been reported as a receptor for Tf, TfR2. The extra cellular domain of TfR2 is 45% identical to TfR and similar in structure and function. TfR2 has been found to be primarily expressed in hepatocytes [41]. TfR affinity for holo-Tf is more than 25 times greater than that of TfR2. TfR is known to be species specific with human receptor failing for form complexes with bovine Tf (and vice versa); curiously, human TfR2 can interact with both bovine and human Tf [45]. TfR2 mRNA

is unaffected by iron loading or iron chelation but is upregulated by holo-Tf suggesting that the protein's main function is not primarily iron uptake [46]. Expression of TfR2 is low compared to TfR, and TfR is used throughout the experiments in later chapters.

The recycling of transferrin receptor is known to be insulin sensitive. The movement of TfR between the plasma membrane and vesicles is enhanced by the administration of insulin. The effect is likely due compartmentalization of TfR in Glut4 vesicles, which, upon insulin stimulation, move into the cell [47, 48]. TfR is often located on the cellular membrane nearby insulin receptor and is incorporated into vesicles alongside them. This is likely the reason for the insulin stimulated movement of Cr(III) into tissues that has been observed in rat models and can be attributed Cr(III)'s 'second-messenger' like behavior[49]. This insulin interaction with the transferrin cycle is well studied, and disorders in iron metabolism are regular complications in cases of insulin resistance (i.e. type 2 diabetes) [48].

4. Experiments to Study Cr(III)-Tf Interaction

No previous study has explicitly investigated the feasibility of Cr(III) release from Tf within the times required for an endosomal cycle. The approach proposed to answer if Tf can feasibly release Cr(III) during endocytosis is to investigate Cr(III)-Tf interactions in a replicated endosomal environment without cells to remove confounding factors such as cell types, interactions, etc. Electron paramagnetic resonance (EPR) spectroscopy has been chosen as a primary method in the investigation as previous studies have demonstrated Cr(III) centers in each lobe of Tf can be unambiguously assigned and monitored independently [36]. Additional conditions such as the presence of biological chelating ligands, complexation with TfR, etc. ,which might effect the release of Cr(III) from Tf can also be incorporated into the experimental design to determine their effects on the release of Cr(III) from Tf.

The binding of Cr(III) and its acid induced dissociation will also be monitored using UV-Vis spectroscopy in tandem with continuous wave (CW)-EPR. The perturbation of the tyrosine residues present in the binding sites of Tf manifest in changes in the absorption at 245 nm, which can be used to monitor metal binding/release as well structure changes that effect those residues. Additionally, crystals of Cr(III)-Tf will be grown and compared to other metal Tf structures to compare similarities or distortions that may be present in the protein structure, which could affect metal binding/dissociation behavior compared to other metal binding behaviors exhibited by the protein.

REFERENCES

1. Mertz, W.; Schwarz, K. Impaired intravenous glucose tolerance as an early sign of dietary necrotic liver degeneration. *Arch. Biochem. Biophys.* 1995, 58, 504

2. Schwarz, K.; Mertz, W. A glucose tolerance factor and its differentiation from factor 3. *Arch. Biochem. Biophys.* 1957, *72*, 515

3. Schwarz, K.; Mertz, W. Chromium(III) and the glucose tolerance factor. *Arch. Biochem. Biophys.* 1959, *85*, 292

4. National Business Journal. Supplement Business Report; 2017.71–73. San Diego, CA

5. Yamamoto, A.; Wada, O.; Ono T. A low-molecular-weight, chromium-binding substance in mammals. *Toxicol. Appl. Pharmacol.* 1981, *59*, 515

6. Wang, Z. Q.; Zhang, X. H.; Russell, J. C.; Hulver, M.; Cefalu, W. T. Chromium picolinate enhances skeletal muscle sellular insulin signaling in vivo in obese, insulin-resistant JCR:LA-Cp Rats. *J. Nutr.* 2006, *136*, 415

7. Davis, C. M.; Vincent, J. B. Chromium oligopeptide activates insulin receptor tyrosine kinase activity. *Biochemistry* 1997, *36*, 4382

8. Wang, H.; Kruszewski, A.; Brautigan, D. L. Cellular chromium enhances activation of insulin receptor kinase. *Biochemistry* 2005, *44*, 8167

9. Hua, Y.; Clark, S.; Ren, J.; Sreejayan N., molecular mechanisms of chromium in alleviating insulin resistance. *J. Nutr. Biochem.* 2012, *23*, 313

10. Zhao, P.; Wang, J.; Ma, H.; Xiao, Y.; He, L.; Tung, C.; Wang, Z.; Zheng, Q.; Dolence, E. K.; Nair, S.; Ren, J.; Li, J. A newly synthetic chromium complex-chromium potential mechanisms $(D\text{-Phenylalanine})_3$ activates AMP-activated protein kinase and stimulates glucose transport. *Biochem. Pharmacol.* 2009, *77*, 1002

11. Davis, C. M.; Sumrall, K. H.; Vincent, J. B. A biologically active form of chromium may activate a membrane phosphotyrosine phosphatase (PTP). *Biochemistry* 1996, *35*, 12963

12. Sreejayan, N.; Dong, F.; Kandadi, M. R.; Yang, X.; Ren, J. Chromium alleviates glucose intolerance, insulin resistance, and hepatic er stress in obese mice. *Obesity* 2008, *16*, 1331

13. Althuis, M. D.; Jordan, N. E.; Ludington, E. A.; Wittes, J. T. Glucose and insulin responses to dietary chromium supplements: a meta-analysis. *Am. J. Clin. Nutr.* 2002, *76*, 148

14. Balk, E. M.; Tatsioni, A.; Lichtenstein, A. H.; Lau, J.; Pittas, A. G. Effect of chromium supplementation on glucose metabolism and lipids: a systematic review of randomized controlled trials. *Diabetes Care* 2007, *30*, 2154

15. Patal, P. C.; Cardino, M. T.; Jimeno, C. A. A meta-analysis on the effect of chromium picolinate on glucose and lipid profiles among patients with type 2 diabetes mellitus. *Philipp. J. Intern. Med.* 2010, *48*, 32

16. Abdollahi, M.; Farshchi, A.; Nikfar, S.; Seyedifar, M. Effect of chromium on glucose and lipid profiles in patients with type 2 diabetes; a meta-analysis review of randomized trials. *J. Pharm. Pharm. Sci.* 2013, *16*, 99

17. Bailey, C. H. Improved meta-analytic methods show no effect of chromium supplements on fasting glucose. *Biol. Trace Elem. Res.* 2014, *157*, 1

18. Suksomboon, N.; Poolsup, N.; Yuwanakorn, A. Systematic review and meta-analysis of the efficacy and safety of chromium supplementation in diabetes. *J. Clin. Pharm. Ther.* 2014, *39*, 292

19. Yin, R. V.; Phung, O. J. Effect of chromium supplementation on glycated hemoglobin and fasting plasma glucose in patients with diabetes mellitus. *Nutr. J.* 2015, *14*, 14.242

20. Huang, H.; Chen, G.; Dong, Y.; Zhu, Y.; Chen, H. Chromium supplementation for adjuvant treatment of type 2 diabetes mellitus: results from a pooled analysis. *Mol. Nutr. Food Res.* 2017, *62*, 1700438

21. Lukaski, H. Effects of chromium(III) as a nutritional supplement. the nutritional biochemistry of chromium(III). *John Wiley & Sons: Chichester*. 2019. 61

22. Anderson, R. A.; Polansky, M. M.; Bryden, N. A.; Patterson, K. Y.; Veillon, C.; Glinsmann, W. H. Effects of chromium supplementation on urinary Cr excretion of human subjects and correlation of Cr excretion with selected clinical parameters. *J. Nutr.* 1983, *113*, 276

23. Donaldson, R. M., Jr.; Barreras, R. F. Intestinal absorption of trace quantities of chromium. J. *Lab. Clin. Med.* 1966, *68*, 484

24. Dowling, H. J.; Offenbacher, E. G.; Pi-Sunyer, F. X. Absorption of inorganic, trivalent chromium from the vascularly perfused rat small intestine. *J. Nutr.* 1989, *119*, 1138

25. Anderson, R. A.; Kozlovsky, A. S. Chromium intake, absorption and excretion of subjects consuming self-selected diets. *Am. J. Clin. Nutr.* 1985, *41*, 1177

26. Jeejeebhoy, K. N.; Chu, R. C.; Marliss, E. B.; Greenberg, G. R.; Bruce-Robertson, A. Chromium deficiency, glucose intolerance, and neuropathy reversed by chromium supplementation, in a patient receiving long term total parenteral nutrition. *Am. J. Clin. Nutr.* 1977, *30*, 531

27. Freund, H.; Atamian, S.; Fischer, J. E. Chromium deficiency during total parenteral nutrition. *JAMA* 1979, *241*, 496

28. Brown, R. O.; Forloines-Lynn, S.; Cross, R. E.; Heizer, W. D. Chromium deficiency after long-term total parenteral nutrition. *Dig. Dis. Sci.* 1986, *31*, 661

29. Verhage, A. H.; Cheong, W. K.; Jeejeebhoy, K. N. Neurologic symptoms due to possible chromium deficiency in long-term parenteral nutrition that closely mimic metronidazole-induced syndromes. *JPEN* 1996, *20*, 123

30. Tsuda, K.; Yokoyama, Y.; Morita, M.; Nakazawa, Y.; Onishi, S. Selenium and chromium deficiency during long-term home total parenteral nutrition in chromic idiopathic intestinal pseodoostruction. *Nutrition* 1998, *14*, 291

31. Wongseelashote, O.; Daly, M. A.; Frankel, E. H. High insulin requirement versus high chromium requirement in patients nourished with total parenteral nutrition. *Nutrition* 2004, *20*, 318

32. Anderson, R. A.; Borel, J. S.; Polansky, M. M.; Bryden, N. A.; Majerus, T. C.; Moser, P. B. Chromium intake and excretion of patients receiving total parenteral nutrition: effects of supplemental chromium. *J. Trace Elem. Exp. Med.* 1988, *1*, 9

33. Stearns, D. M. Is chromium a trace essential element? *Biofactors* 2000, 11, 149–162

34. Hopkins, L. L., Jr.; Schwarz, K. Chromium(III) binding to serum proteins, specifically siderophilin. *Biochim. Biophys. Acta* 1964, *90*, 484

35. Clodfelder, B. J.; Vincent, J. B. The time-dependent transport of chromium in adult rats from the bloodstream to the urine. *J. Biol. Inorg. Chem.* 2005, *10*, 383

36. Deng, G.; Wu, K.; Cruce, A. A.; Bowman, M. K.; Vincent, J. B. Binding of trivalent chromium to serum transferrin is sufficiently rapid to be physiologically relevant. *J. Inorg. Biochem.* 2015, *143*, 48

37. Levina, A.; Nguyen Pham, T. H.; Lay, P. A. Binding of Cr(III) to transferrin could be involved in detoxification of dietary chromium(III) rather than transport of an essential trace element. *Angew. Chem. Int. Ed.* 2016, *55*, 8104

38. Rhodes, N.; LeBlanc, P. A.; Rasco, J. F.; Vincent, J. B. monocarboxylate transporters are not responsible for Cr^{3+} transport from endosomes. *Biol. Trace Elem. Res.* 2012, 148, 409

39. Bali, P.; Aisen, P. Receptor-modulated iron release from transferrin: differential effects on N- and C-terminal sites. *Biochemistry*. 1991, *30*, 9947

40. El, J.M.; Chanine, H.; Fain, D. The mechanism of iron release from transferrin slow-proton-transfer-induced loss of nitrilotriacetatoiron(III) complex in acidic media. *Eur. J. Biochem.* 1994, *223*, 581

41. Kawabata, H. Transferrin and transferrin receptors update. *Free Radic Biol Med.* 2019, *133*, 46

42. Turkewitz, A.P.; Amatruda, J. F.; Borhani, D.; Harrison, S. C.; Schwartz, A. L. A high yield purification of the human transferrin receptor and properties of its major extracellular fragment. *J. Biol. Chem,* 1988, *263*, 8318

43. Steere, A. N.; Byrne, S. L., Chasteen, N. D.; Mason, A. B. Kinetics of iron release from transferrin bound to the transferrin receptor at endosomal pH. *Biochim. Biophys. Acta.* 2012, *1820*, 326

44. Bonvin, G.; Bobst, C.E.; Kaltashov, I.A. Interaction of transferrin with non-cognate metals studied by native electrospray ionization mass spectrometry. *Int. J. Mass Spectrom.* 2017, *420*, 74

45. Kawabata, H.; Tong, X.; Kawanami, T.; Wano, Y.; Hirose, Y.; Sugai, S.; Phillip Koeffler, H. Analyses for binding of the transferrin family of proteins to the transferrin receptor 2 *British Journal of Haematology* 2004, *127*, 464

46. Nakamaki, T.; Kawabata, H.; Saito, B.; Matsunawa, M.; Suzuki, J.; Adachi, D.; Tomoyasu, S.; Phillip Koeffler, H. Elevated levels of transferrin receptor 2 mRNA, not transferrin receptor 1 mRNA, are associated with increased survival in acute myeloid leukaemia *B. J. of Haematol.* 2004, *125*, 42

47. Biswas, S.; Tapryal, N.; Mukherjee, R.; Kumar, R.; Mukhopadhyay, C. K. Insulin promotes iron uptake in human hepatic cell by regulating transferrin receptor-1 transcription mediated by hypoxia inducible factor-1 *Biochim. Biophys. Acta* 2013, *1832*, 293

48. Fernandez-Real, J. M.; Lopez-Bermejo, A.; Ricart, W. Cross-talk between iron metabolism and diabetes *Diabetes* 2002, *51*, 2348

49. Vincent, J. B. Is the pharmacological mode of action of chromium(III) as a second messenger? *Biol. Trace Elem. Res.* 2015, *166*, 7

50. Gkouvatsos, K.; Papanikolaou, G.; Pantopoulos K. Regulation of iron transport and the role of transferrin *Biochim. Biophyc. Acta*, 2012, 1820, 188

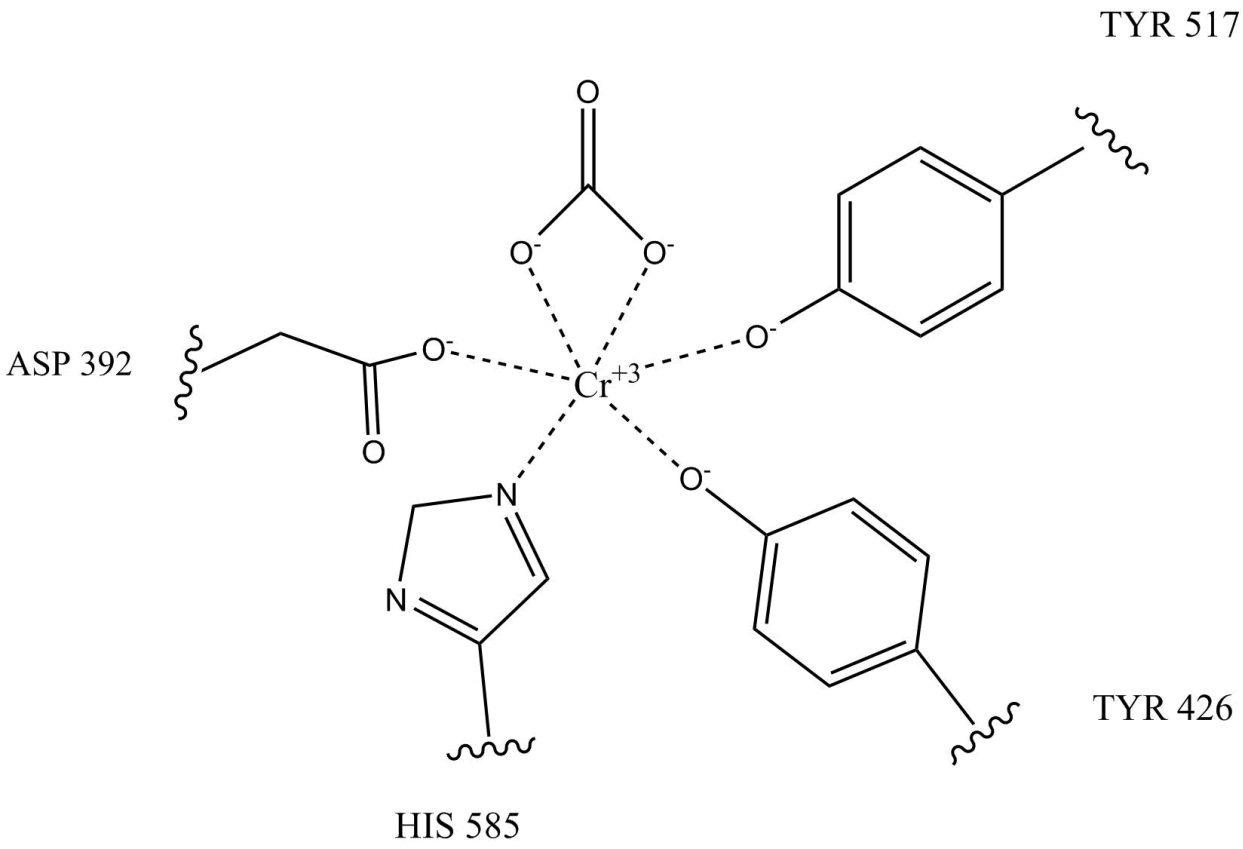

Figure 1.1. Binding site of human serum Tf with Cr(III) present.

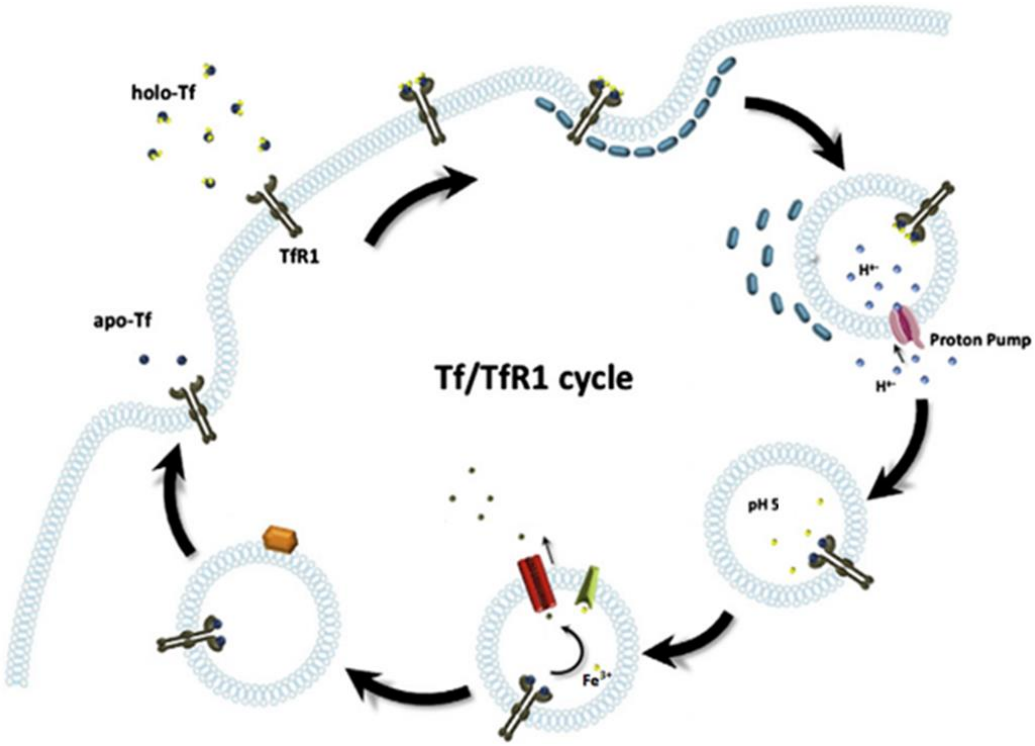

Figure 1.2. Tf/TfR cycle summarization. Figure adapted from ref 50.

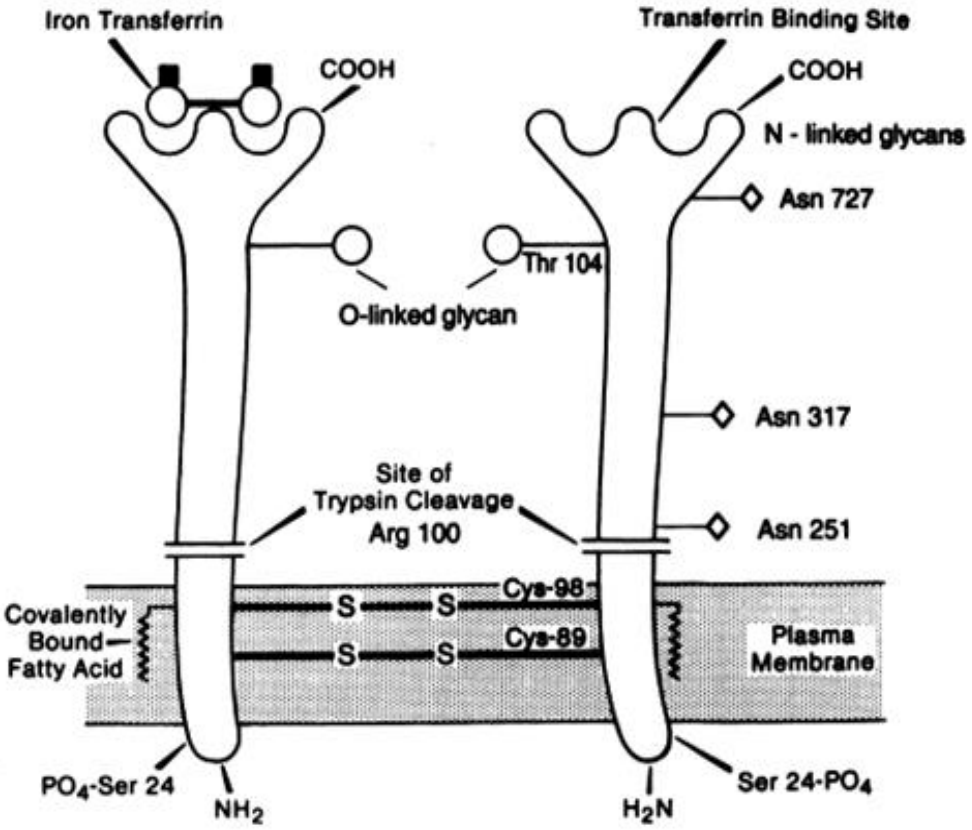

Figure 1.3. Transferrin receptor 1 with bound iron loaded transferrin. Figure adapted from Ref

RELEASE OF CR(III) FROM TRANSFERRIN IN THE PRESENCE OR ABSENCE OF POTENTIAL CHELATING LIGANDS

1. Introduction

Transferrin (Tf) is a plasma glycoprotein consisting of two similar lobes, the C lobe and N lobe; each lobe contains a single metal binding site composed of two tyrosines, one aspartate, and one histidine residue [1]. As its name implies, transferrin's primary function is to bind Fe(III) and transport it through the blood to cells, and transferrin is considered the major iron transporter in mammals [1]. Tf's metal binding sites are notoriously promiscuous and are known to bind several alternative metal ions with a similar charge/ionic radius to that of Fe(III) (i.e. Cr(III), Mn (III), etc.); however, Tf's highest metal binding affinity is for Fe(III), for which it is selective under biological conditions [2]. The presence of an additional synergistic carboxylate is necessary for metal binding and is supplied by an outside cofactor (typically (bi)carbonate) located in an anion binding site near the metal binding site [2].

Despite only composing a small pool of the body's total iron (~4 mg), Tf undergoes very efficient iron turnover (approximately 24 mg/day) through an endosomal mediated pathway requiring transferrin receptor (TfR) [3]. Iron entering the serum transferrin pool will remain on average 90 min before being transferred to the intracellular labile iron pool via receptor mediated endocytosis[1]. In humans, the lobes of Tf share ~60% sequence homology. Both metal binding sites have the same protein provided ligands; yet, the two binding sites exhibit significantly different metal binding affinity [2]. Tf has a very strong affinity for Fe(III) with a $K_1=10^{20}$ M^{-1} at

pH 7.4 and 37°C, although the binding affinity drops rapidly with decreased pH [3]. TfR will tightly bind holo-Tf at biological pH, and the TfR-holoTf complex with the surrounding membrane will form an endosomal vesicle in which the pH is subsequently lowered to ~5 [3]. The acidification prompts release of Fe(III) from the Tf-TfR complex; the Fe(III) is reduced to Fe(II) and removed from the endosome via divalent metal transporter proteins. After the endosome recombines with cell membrane, the now apo-Tf is released from TfR with the return to pH 7.4. While Cr(III) was once thought to be essential as Glucose Tolerance Factor, Cr(III) has been demonstrated to not be essential trace element but may provide therapeutic benefits in large supranutritional doses [4]. Some studies have demonstrated that coadminstration of Cr(III) with insulin improves the uptake of both into specific tissues and improves fasting glucose levels [4-7]. Furthermore, Cr(III) is speculated to upregulate the insulin signaling pathway through improved tyrosine kinase activity when interacting in the form of Cr(III) bound to low-molecular-weight chromium-binding substance (LMWCr), otherwise known as chromodulin [5,6,7]. However, while promising, these effects are not well understood, and the experiments are not consistently reproducible. No long term study has been conducted utilizing Cr(III) supplementation in the context of glucose metabolism, and the short term studies clinical studies that have been conducted have observed varied results. Another study found supplementation of Cr(III) results in a statistically significant decrease in fasting plasma glucose levels [8], although the results are in question as another study found no statistically significant benefit of Cr(III) supplementation [9]. Meta analyses on the supplementation of Cr(III) have found for studies in which a statistically significant effect was observed that the effect was small enough to not expect a clinically relevant outcome [4]. The mixed results from the studies stem from a lack of

understanding about Cr(III) biochemistry and methodological errors in dosage, administration, or preparation of the Cr(III) supplement.

Cr(III) has been proposed to enter the cell in a similar fashion to Fe(III) as a result of Tf's moderate affinity (K_d = ~10^{13} M^{-1}) for the ion at pH 7.4. Although Cr(III) is not competitive with Fe(III) for Tf binding, serum Tf is only partially saturated with Fe(III) at about 30% or $Fe_{0.6}$-Tf, leaving many vacant binding sites for other metals [3]. Additionally, ^{51}Cr(III) intravenously injected as Cr_2-Tf into rats results in rapid Cr(III) accumulation in tissues (within 30 min) [10, 11]. This movement of Cr(III) into cells was also demonstrated to be insulin sensitive. The short time between injection and accumulation in cells is consistent with the endosomal uptake mechanism. Delivery of ^{51}Cr(III) has been found to be ~33 % of that ^{57}Fe(III) when added as Cr_2-Tf to C2C12 murine skeletal muscle cells [12]. Again, the timeframe of the cellular uptake of Cr(III) was rapid with ~50 % of Cr(III) appearing in endosomal fractions of the cell 30 min to 1 hr after ^{51}Cr(III) addition, ~50 % Cr was in the cytosolic fraction [12]. Cr(III) when added to serum not as Cr_2-Tf but in forms including $CrCl_3$ with labile ligands forms some interactions with other serum proteins such as albumin, although the majority does bind with Tf [13].

Cr-Tf binding/dissociation kinetics have not been studied in detail until recently. Many early studies investigating Cr_2-Tf prepared samples through incubation of Tf with Cr(III) over a two-week period [14]. Cr_2-Tf was thus thought not to be physiologically relevant due to the long incubation times required for Cr-Tf to come to equilibrium. Recently however, the rate of Cr(III) binding to Tf was demonstrated to be first order in bicarbonate [15]. Previous i*n vitro* studies readily demonstrated Tf binds Fe(III) or Cr(III) concomitantly with equal equivalents of bicarbonate [14]. When Cr(III) is loaded in Tf in the presence of 25 mM bicarbonate (the

physiological level of bicarbonate in serum), binding to Tf was rapid and reached equilibrium within 15 min [15]. Thus, the binding of Cr(III) to Tf is sufficiently rapid to be physiologically relevant.

Another recent study investigating Cr(III) accumulation in a human liver cancer cell line (HepG2) found that only when Cr(III) was added with Fe_2-Tf did Cr(III) accumulation occur [16]. In trials in which the Cr(III) was allowed to incubate with Tf, forming Cr_2-Tf, before being added to the cell, Cr was not detected in cells and was concluded not to accumulate. The same study using bio-layer interferometry (BLI) compared Fe_2-Tf, Cr_2-Tf, and apo-Tf binding and release from transferrin receptor (TfR) in simulated endosomal conditions [16]. Cr_2-Tf binding to TfR (k_1=3.9 ± 0.3 nM, k_2 = 18 ± 2 nM) was found to be faster than apo-Tf (k_1 = 5.1 ± 0.6 nM, k_2 = 50 ± 5 nM) and slower than Fe_2-Tf (k_1= 1.5 ± 0.1 nM, k_2= 7.8±0.5 nM) (similar to results found using surface plasmon resonance [17]). However, the behavior of Cr_2-Tf was found to deviate from that of Fe_2-Tf in the post acidification step; (the now apo) Fe_2-Tf dissociated from the TfR when returned to pH 7.4 whereas the Cr_2-Tf sample showed little or no dissociation from TfR. The release of Cr(III) from Tf was speculated to be too slow to occur during the acidification step, and the Cr(III) remained, proposedly crosslinking the Tf to TfR and explaining the lack of dissociation [16]. However, the cell type used in this study may have been problematic as hepatic cells typically have lower levels of Fe(III) turnover through endocytosis, or the serum free conditions that the experiment was conducted under may have lacked a critical component of the cycle. Additionally, the use of BLI is potentially problematic as the technique is sensitive to conformation changes at the probe surface. BLI immobilizes a protein on the tip of a probe. White light is reflected off this immobilized layer of protein and an internal reference layer which generates an interference pattern. When the immobilized layer binds protein, an

increase in the optical thickness of the probe tip occurs which shifts the interference pattern. This interference pattern is measured and used to generate a binding/dissociation curve between the bound protein and the immobilized protein layer. Transitions between acidic/neutral steps in which the Tf/TfR immobilized on the probe surface will undergo changes independent of metal binding/release confound changes associated with metal binding/release, making it unclear how the metal behaves. Separate studies investigating Cr(III) accumulation in skeletal cells (C2C12) found that Cr(III) rapidly accumulated in endosomal fractions (~15 min) and cystolic fractions (30 min-1 hr)[12]. The Cr(III) was introduced as Cr_2-Tf and Cr(III) accumulation into the cell was uninhibited by monocarboxylate transport inhibitors. Thus, the pathway for Cr(III) entry into the cell is still unclear, with some studies suggesting it follows the endosomal Tf-TfR pathway, while others suggest Cr(III) non-specifically binds to the outside of Fe_2-Tf and is incorporated not bound in Tf metal sites.

To monitor the status of Cr(III) bound to Tf, CW-EPR was utilized to observe the status of Cr(III) throughout a simulated endosomal cycle. CW-EPR has been used to monitor Cr(III)-Tf before and has been shown capable of distinguishing Cr(III) between the two binding sites (C-lobe and N-lobe metal binding site) of Tf. Thus, the rate of release of Cr(III) can be directly measured to determine if release of Cr(III) from Tf is sufficiently rapid for Cr(III) feasibly to be transported via endocytosis.

2. Experimental

2.a. Chemicals

Iron-free human serum Tf and bovine serum Tf were obtained from Aldrich (St. Louis, MO). Doubly deionized water was used throughout. All reagents were used as received unless otherwise noted. Cr(III) solutions were prepared by using $Cr(III)Cl_3 \cdot 6H_2O$. Apo-Tf

concentrations were determined by using the extinction coefficient ($\varepsilon = 9.12 \times 10^4\ M^{-1}cm^{-1}$) at 280 nm [18].

2.b. Tf Solution Preparation

Dichromic transferrin solutions were prepared by dissolving lyophilized human serum apo-Tf in a 0.1 M HEPES/25 mM HCO_3^- buffer, pH 7.4. A solution of $CrCl_3 \cdot 6H_2O$ was prepared in 0.1 M HEPES/25 mM HCO_3^- buffer, and an aliquot was added to the apo-Tf solution to achieve a ratio of 1.9 Cr:1Tf. Full 2:1 Cr:Tf loading was avoided to minimize amount of free aqueous $[Cr(H_2O)_6]^{+3}$ in solution. The solution was allowed to incubate for 48 hr to ensure full loading of Cr(III) into Tf.

2.c. EPR Spectroscopy

CW-EPR spectra were measured on a Bruker (Billerica, MA) ELEXSYS E540 X-band spectrometer with an ER 4102 ST resonator. CW spectra were measured at 9.44 GHz with a microwave power of 21.1 mW by using a magnetic field modulation frequency of 100 kHz with an amplitude of 30 gauss. Spectra were taken at liquid nitrogen temperatures with a quartz insertion dewar. All results are presented as the average of at least triplicate experiments. Error bars in figures represent standard deviation.

2.d. Data Analysis

Data analysis, calculation of averages and standard deviations, and fitting of curves to the appropriate equations was performed by using SigmaPlot 11 (SPSS, Inc., Chicago, IL). The iterative curve fitting algorithm of SigmaPlot 11 uses the Marquardt-Levenberg algorithm to find the parameters of the independent variables that provide the best fit between the data and the equation.

CW EPR spectrum processing and simulations were performed using the EasySpin package in MATLAB (Mathworks, R2017b). Polynomial fitting of the spectral baseline corrections was performed using Xepr software of the ELEXSYS. The g-values, g-strain, and weight of the simulated spectrum were fit using the "pepper" function in EasySpin.

3. Results and Discussion

As shown in Figure 2.1, the Cr(III) bound in the two metal binding sites of Tf can be readily distinguished by the position of their EPR signals. Cr(III) bound in the N-terminal lobe of human serum transferrin (pH 7.5) gives CW-EPR peaks at g = 5.22 and g = 5.66. Cr(III) bound in the C-terminal lobe of human serum transferrin (pH 7.7) has only one CW-EPR peak located at g=5.42. At pH 4.8 to 5.9, Cr(III) binds only to the N-terminal site (tight binding site). Co(III) has been demonstrated to only displace Cr(III) in the C-terminal site (weak binding site), and Fe(III) will displace C-terminal bound Cr(III) before displacing N-terminal bound Cr(III) [14]. The identity of these signals along with their corresponding lobes were established by selective displacement of the Cr(III) with other metal ions [2]. The EPR signal for Cr(III) is not uniform among the family of Transferrin proteins; for example, Cr(III) from bovine serum Tf gives a more single peak from Cr(III) located in both lobes [13]. Also notable is in lactoferrin, the Cr(III) in the C-terminal binding site gives rise to two EPR peaks, and the N-terminal Cr(III) gives rise to one (in the g=5 region) [19].

The acidification of the endosome that occurs during endocytosis was replicated by adjusting the pH of the Cr_2-Tf solutions to pH 5.5 or 4.5 (through addition of HCl) before aliquots were taken at prescribed time intervals and frozen. Samples were frozen rapidly using liquid nitrogen and stored at -80 °C prior to EPR analysis. Acidification of Cr_2-Tf to pH 5.5 results in the rapidly loss of intensity of the EPR signal from the weakly bound Cr(III) (C-lobe)

(Figure 2.2). The signal from C-terminal Cr(III)-Tf is essentially gone within 15 min; little decay in the tightly bound Cr(III)-Tf signal (N-lobe) occurs during this time. The signal from N-lobe Cr(III)-Tf takes nearly 12 hr to disappear; the signal loss is also associated with the generation of four EPR peaks between 1450 and 1150 G (Figure 2.3). These signals correspond to Cr(III) bound non-specifically to Tf and buffer components. Cr(III) added to a solution of apo-Tf already adjusted to pH 5.5 and allowed to come to equilibrium generates the same 4 signals (Figure 2.6). A separate study noted these four EPR features when Cr(III) was displaced from Tf at pH 7.4 by either Fe(III) or Co(II) (added with H_2O_2) after the Cr_2-Tf had incubated with the 2 molar equivalents of the metals for several days [14]. These features were attributed to Cr(III) non-specifically bound to the surface of Tf. The existence of these EPR features at pH 7.4 when Cr(III) is displaced from the binding site by a more competitive metal further indicates that these features arise due to Cr(III) non-specifically bound to the surface of Tf rather than distortion of the Cr(III) binding sites due to acidification. Similar to the loss of Fe(III), the loss of Cr(III) from Tf occurs at different rates for the two metal binding sites of Tf. The experiment was repeated at pH 4.5 and the results are reported in Table 1. These experiments were also repeated with the addition of anionic chelating ligands during the acidification step Figure 2.3.

Using EasySpin, the EPR spectra were fit to seven Gaussian curves corresponding to the weak binding site signal (C-terminal), the two strong binding site signals (N-terminal), and the four signals corresponding to the “nonspecific” Cr(III) signals. The areas of each (denoted EPR signal intensity) were thus determined at the series of times of when the aliquots were collected and rapidly frozen. The loss of the Cr(III) transferrin signals were fit to exponential decays, while the appearance of the signals from the non-specific binding of Cr(III) were fit to an exponential growth (Fig.’s 4-7\)

Loss of Cr(III) from the C-terminal site of Tf proceeded rapidly at both pH 5.5 (rate constant of 0.12 ± 0.01 min^{-1}) and pH 4.5 (rate constant of 0.16 ± 0.01 min^{-1}), corresponding to half-lives of 5.6 ± 0.2 and 4.2 ± 0.2 min, respectively (Figure 2.4, Table 2.1). Approximately 85 and 92% of Cr(III), respectively, should be released from the C-lobe Tf binding site within 15 min of acidification, the time frame of endocytosis. These rates are rapid compared to N-lobe Cr(III) Tf loss but are slower compared to Fe(III) loss with half -lives on the order of seconds [20]. The loss of Cr(III) from this lobe of Tf is unaffected by the presence or absence of chelating anionic ligands. Given that the EPR signals associated with the ligand Cr(III) complexes are not observed, it is unlikely that the Cr(III) from this site is being bound by the added anionic ligands. The early appearance of the non-specific Cr(III)-Tf EPR features at ~1175 and ~1400 G indicate Cr(III) in the C-site is rapidly being displaced and binding at the non-specific site which appears to have a higher affinity than those of the potential ligands as these signals do not appear.

Loss of Cr(III) from the tighter binding site (N-terminal) was slower than that of C-lobe bound Cr(III). Rate constants for the loss of N-lobe bound Cr(III) were $1.2 \times 10^{-3} \pm 1 \times 10^{-4}$ min^{-1} at pH 5.5 and $2.5 \times 10^{-3} \pm 3 \times 10^{-4}$ min^{-1} at pH 4.5 in the absence of a potential chelating ligand, tbe enhanced rate of Cr(III) loss at pH 4.5 demonstrates a more pronounced pH effect compared to loss from Cr(III) bound to the C lobe. The half-life for N-lobe Cr(III) loss is on the order of 100's of min (70-100 times slower then C-lobe bound Cr(III)) such that in 15 min only 4 % of Cr(III) is expected to be lost at pH 4.5 or 2 % Cr(III) loss at pH 5.5. The rate of appearance of the non-specific Cr(III) signals closely mirrors the rate of loss of tightly bound Cr(III) (Figure 2.6 and Figure 2.7) with the rate of growth being $1.5 \times 10^{-3} \pm 3 \times 10^{-4}$ min^{-1} and $2.7 \times 10^{-3} \pm 3 \times 10^{-4}$ min^{-1} at pH 5.5 and 4.5, respectively. However, the similarity of the rates is coincidental

and does not reflect direct conversion of N-lobe Cr(III) into non-specifically bound Cr(III). The rate of growth of the nonspecific Cr(III) signal are similarly obtained if Cr(III) is added to pre-acidified apo-Tf at pH 5.5/4.5, such that the appearance of the non-specific Cr(III) signal in Figure 2.6 and 2.7 actually reflects Cr(III) lost from both metal binding sites. This likely explains the poor quality of fit using a single exponential model for the rise in non-specific Cr(III) at pH 5.5 as the rate of growth is likely biphasic and is better modeled with a double exponential fit. Slow loss of Cr(III) from the N-terminal site of Tf is consistent with Cr(III) binding studies done at pH 5.9, which demonstrated that only N-terminal Cr(III) is bound in that pH range [2].

The presence of anionic ligands is known to accelerate the loss of Fe(III) from Tf [21]. This enhanced rate of loss by Fe(III) from transferrin has been shown to be affected by a wide variety of potential mechanisms including competition between the ligand and Tf for Fe(III) binding, replacement of the synergistic bicarbonate by the anionic ligand, and allosteric effects [22]. Fe(III) is not be released from Tf within the time of a cycle of endocytosis without the addition of anions (even those with no Fe(III) chelating ability) [21,23]. Furthermore, the rate of loss of Fe(III) from Tf has been demonstrated to not correlate with how tightly the anionic ligand binds to Fe(III), but with how well they bind to Tf [23]. Loss of Cr(III) from the N-terminal lobe of Tf can be accelerated by the presence of anionic ligands. EDTA, citric acid, and ascorbic acid all enhanced the rate of loss of Cr(III) from Tf. The increase in the rate of loss of Cr(III) from Tf was independent of the identity of the ligand, regardless of its ability to bind Cr(III), structure, or size. The rate of loss of Cr(III) was approximately doubled at both pH 4.5 and pH 5.5 for the N-lobe Cr(III). Given that the ability of the ligands to bind Cr(III) has no affect on the rate of loss and the time these anions take to come to equilibrium binding Cr(III) under these conditions, the anionic ligands are not binding to released Cr(III) or otherwise enhancing the rate of loss by

competition with Tf for Cr(III) binding. Thus, the anionic ligands are likely helping to displace the bicarbonate or could be binding at an allosteric site to enhance the rate of Cr(III) loss from N-lobe Tf.

4. Conclusion

The loss of Cr(III) from the C-lobe of Tf proceeds rapidly in the presence or absence of a anionic chelating ligand. The loss of Cr(III) from this lobe is essentially complete within 15 min, and Cr(III) can feasibly be lost within an endosomal cycle (~15 min). Loss of Cr(III) from the N-lobe of Tf occurs at a rate 70-100 times slower than that of the C-lobe, but some Cr(III) (~10%) is expected to be lost within 15 min under ideal conditions (pH 4.5 and in the presence of an anionic ligand). The presence of a chelating ligand accelerates the rate of loss by two fold; however, the rate is independent of the identity of the ligand. Because the properties of the anionic ligand did not have a significant effect on the rate of loss, the anionic ligands are speculated to help displace the synergistic bicarbonate in the anion binding pocket rather than competing with the Tf directly for binding Cr(III). Alternatively, the anionic ligands possibly could be binding to an allosteric site (the kinetically significant anion binding or KISAB site) located on the N-lobe of the protein [24]. A noted pH dependent effect was also observed for Cr(III) loss from both sites of Tf. Cr(III) loss from the C-lobe of Tf occurred slightly faster at pH 4.5 than at pH 5.5, but the effect was small (less than a two-fold increase). The rate of Cr(III) loss from the N-lobe of transferrin occurred ~ two times faster at pH 4.5 than at pH 5.5. The differing rates of Cr(III) loss from the two lobes of Tf suggests some difference between the two lobes exists to account for difference in Cr(III) binding ability. Since the metal binding sites of the two lobes are essentially identical, a difference in the overall structure or conformation of the lobes is likely the cause, rather than a difference immediately about the binding site. Complexation of Cr_2-Tf with its receptor protein may have significant effects on the rate of

Cr(III) loss from Tf during acidification as this has been observed with other metals and needs to be investigated for Cr(III). Importantly, complexation of $Fe(III)_2$-Tf with the TfR has been demonstrated to affect the rate of metal release unequally between the two lobes [25]. The lobe with the slower rate of Fe(III) loss without the receptor present is greatly accelerated in the presence of the receptor which results in Fe(III) loss to be more uniform between the two lobes [25]. Regardless, from this experiment, Cr(III) loss from Tf after acidification has been demonstrated to be sufficiently rapid to occur within endocytosis and cannot be used as an explanation for an apparent inability for Tf to transport Cr(III) into a cell. What subsequent steps are required to bind and remove Cr(III) from the endosome are unknown, and further studies will be required to map the pathway of Cr(III) from blood into tissue. Particularly, if Cr(III) does enter a cell through endocytosis, a chelating ligand would be required that can bind Cr(III) under endosomal conditions as a step into the process for Cr(III) to be removed from the endosome.

REFERENCES

1. Cazzola, M.; Huebers, H. A.; Sayers, M. H.; MacPhail, A. P.; Eng, M.; Finch, C. A. Transferrin saturation, plasma iron turnover, and transferrin uptake in normal humans. *Blood* 1985, 66, 935

2. Harris, D. C. Different metal-binding properties of the two sites of human transferrin *Biochemistry* 1977, *16*, 560

3. Kawabata, H. Transferrin and transferrin receptors update. *Free Radic Biol Med*. 2019, 133, 46

4. Huang, H.; Chen, G.; Dong, Y.; Zhu, Y.; Chen, H. Chromium supplementation for adjuvant treatment of type 2 diabetes mellitus: results from a pooled analysis. *Mol. Nutr. Food Res*. 2017, 62, 1700438

5. Davis, C. M.; Vincent, J. B. Chromium oligopeptide activates insulin receptor tyrosine kinase activity. *Biochemistry* 1997, 36, 4382

6. Wang, H.; Kruszewski, A.; Brautigan, D. L. Cellular chromium enhances activation of insulin receptor kinase. *Biochemistry* 2005, 44, 8167

7. Hua, Y.; Clark, S.; Ren, J.; Sreejayan N., Molecular mechanisms of chromium in alleviating insulin resistance. *J. Nutr. Biochem*. 2012, 23, 313

8. Yin, R. V.; Phung, O. J. Effect of chromium supplementation on glycated hemoglobin and fasting plasma glucose in patients with diabetes mellitus. *Nutr. J.* 2015, 14, 14.242

9. Bailey, C. H. Improved meta-analytic methods show no effect of chromium supplements on fasting glucose. *Biol. Trace Elem. Res*. 2014, 157, 1

10. Clodfelder, B. J., Vincent, J. B. The time-dependent transport of chromium in adult rats from the bloodstream to the urine. *J. Biol. Inorg. Chem.* 2005, 10, 383

11. Clodfelder, B. J., Emamaullee, J., Hepburn, D. D., Chakov, N. E., Nettles, H. S., Vincent, J. B. The trail of chromium(III) in vivo from the blood to the urine: the roles of transferrin and chromodulin. *J. Biol. Inorg. Chem.* 2001 6, 608

12. Rhodes, N. R.; LeBlanc, P. A.; Rasco, J. F.; Vincent, J. B. Monocarboxylate transporters are not responsible for Cr^{3+} transport from endosomes *Biol. Trace Elem. Res*. 2012, 148, 409

13. Tkaczyk, C.; Huk, O. L.; Mwale, F.; Antoniou, J.; Zukor, D. J.; Petit, A.; Tabrizian, M. Investigation of the binding of Cr(III) complexes to bovine and human serum proteins: a proteomic approach *J. Biomed. Mater. Res. A.* 2010, 94, 214

14. Aisen, P., Aasa, R., Redfield A. G. Chromium, manganese, and cobalt complexes of transferrin. *J. Biol. Chem.* 1969 244, 4628

15. Deng, G.; Wu, K.; Cruce, A. A.; Bowman, M. K.; Vincent, J. B. Binding of trivalent chromium to serum transferrin is sufficiently rapid to be physiologically relevant *J. Biol. Inorg. Chem.* 2015, 143, 48

16. Levina, A.; Nguyen Pham, T. H.; Lay, P. A. Binding of Cr(III) to transferrin could be involved in detoxification of dietary chromium(III) rather than transport of an essential trace element. *Angew. Chem. Int. Ed*. 2016, 55, 8104

17. Giannetti, A. M.; Snow, P. M.; Zak, O.; Björkman, P. J. Mechanism for multiple ligand recognition by the human transferrin receptor *PLoS Biology* 2003, 1

18. Deng, G.; Dyroff, S. L.; Lockart, M.; Bowman, M. K.; Vincent, J. B. The effects of the glycation of transferrin on chromium binding and the transport and distribution of chromium in vivo *J. Inorg. Biochem.* 2016, 164, 26

19. Ainscough, E. W.; Brodie, A. M.; Plowman, J. E.; Bloor, S. J.; Loehr, J. S.; Loehr, T. M. Studies on human lactoferrin by electron paramagnetic resonance, fluorescence, and resonance raman spectroscopy *Biochemistry* 1980, 19, 4072

20. Byrne, S. L.; Chasteen, N. D.; Steere, A. N.; Mason, A. B. The unique kinetics of iron release from transferrin: the role of receptor, lobe-lobe interactions and salt at endosomal pH *J. Mol. Biol.* 2010, 396, 130

21. Carver, F. J.; Frieden, E. Factors affecting the adenosine triphosphate induced release of iron from transferrin *Biochemistry* 1978, 17, 167

22. Harris, W. R. Anion binding properties of the transferrins. Implications for function *Biochim Biophys Acta Gen Subj* 2012, 1820, 348

23. Foley, A. A.; Bates, G. W. Factors affecting the adenosine triphosphate induced release of iron from transferrin *Biochim Biophys Acta* 1988, 965, 154

24. Byrne, S. L.; Steere, A. N.; Chasteen, N. D.; Mason, A. B. Identification of a kinetically significant anion binding (KISAB) site in the N-lobe of human serum transferrin *Biochemistry* 2010, 49, 4200

25. Steere, A. N.; Byrne, S. L.; Chasteen, N. D.; Mason, A. B. Kinetics of iron release from transferrin bound to the transferrin receptor at endosomal pH *Biochim Biophys Acta Gen Subj* 2012, 1820, 326

Table 2.1. Dissociation constants and corresponding half-lives for Cr(III) dissociation from the weak Cr(III) binding site of transferrin in the absence of chelating ligands at pH 5.5 and 4.5. Dissociation constants and corresponding half-lives for Cr(III) dissociation from the tight Cr(III) binding site of transferrin in the presence or absence of chelating ligands at pH 5.5 and 4.5. SD – standard deviation.

Rate Constants for Cr(III) Dissociation at pH 5.5

Chelating Ligand	*k* (min^{-1})	SD (min^{-1})	$t_{1/2}$ (min)
EDTA	0.0025	0.0002	2.8*10^2
Citrate	0.0027	0.0003	2.6*10^2
Ascorbate	0.0027	0.0003	2.6*10^2
None	0.0012	0.0001	5.8*10^2

Rate Constants for Cr(III) Dissociation at pH 4.5

Chelating Ligand	*k* (min^{-1})	SD (min^{-1})	$t_{1/2}$ (min)
EDTA	0.0048	0.0004	1.4*10^2
Citrate	0.0049	0.0004	1.4*10^2
Ascorbate	0.0054	0.0007	1.3*10^2
None	0.0025	0.0003	2.8*10^2

Rates Constants for Cr(III) Dissociation from Weak Binding Site

	k (min^{-1})	SD (min^{-1})	$t_{1/2}$ (min)
pH 4.5	0.16	0.01	4.2
pH 5.5	0.12	0.01	5.6

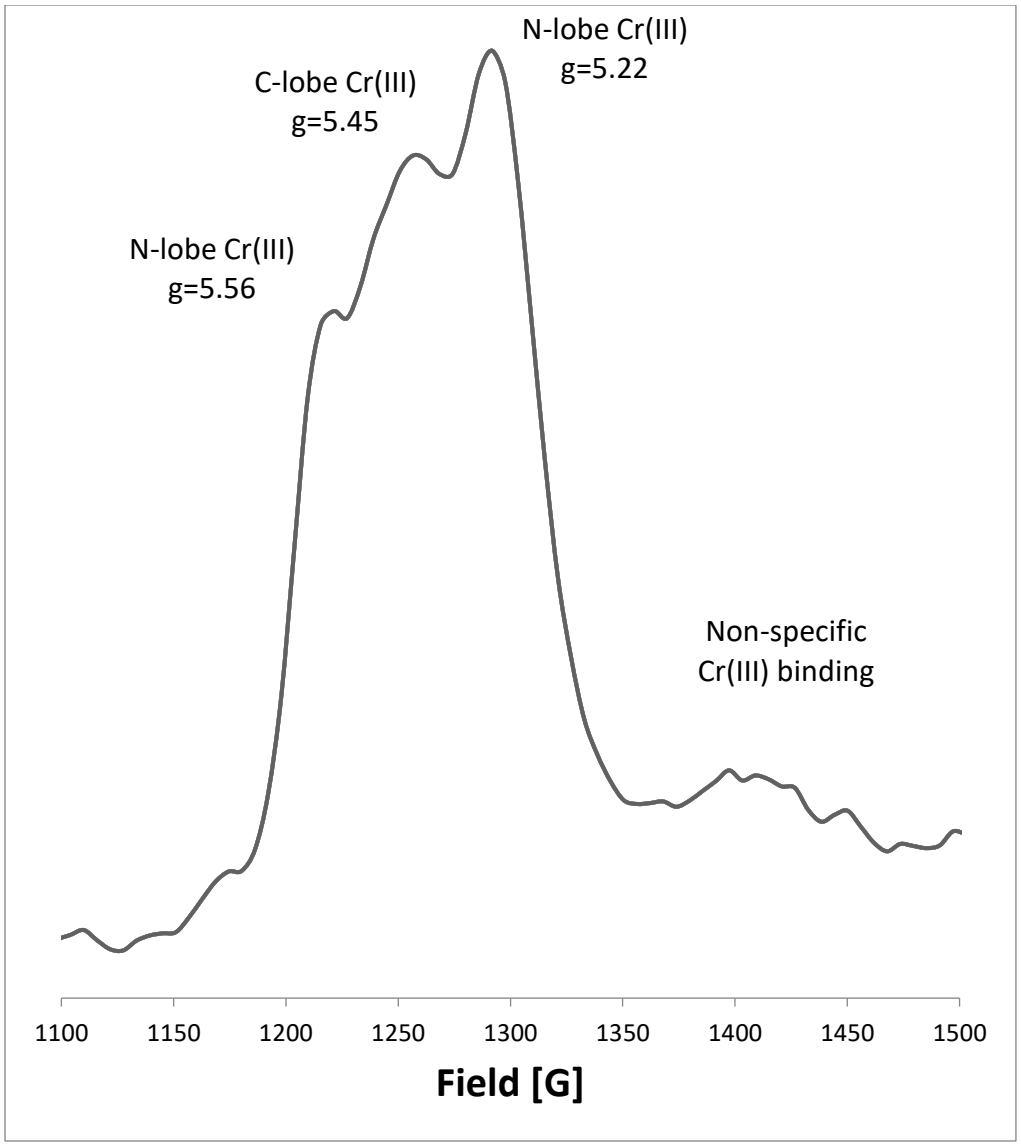

Figure 2.1. EPR spectra of Cr_2-transferrin in 100 mM HEPES with 25 mM HCO_3^- at pH 7.4. Peaks at 1220 and 1285 G (g = 5.1 and g = 5.6) correspond to Cr(III) in the N-terminal tight binding site. The peak at 1250 G (g = 5.4) corresponds to Cr(III) in the C-terminal weak binding site. Cr(III) added as $CrCl_3 \bullet 6H_2O$ and allowed to incubate for 48 hr at 4 °C

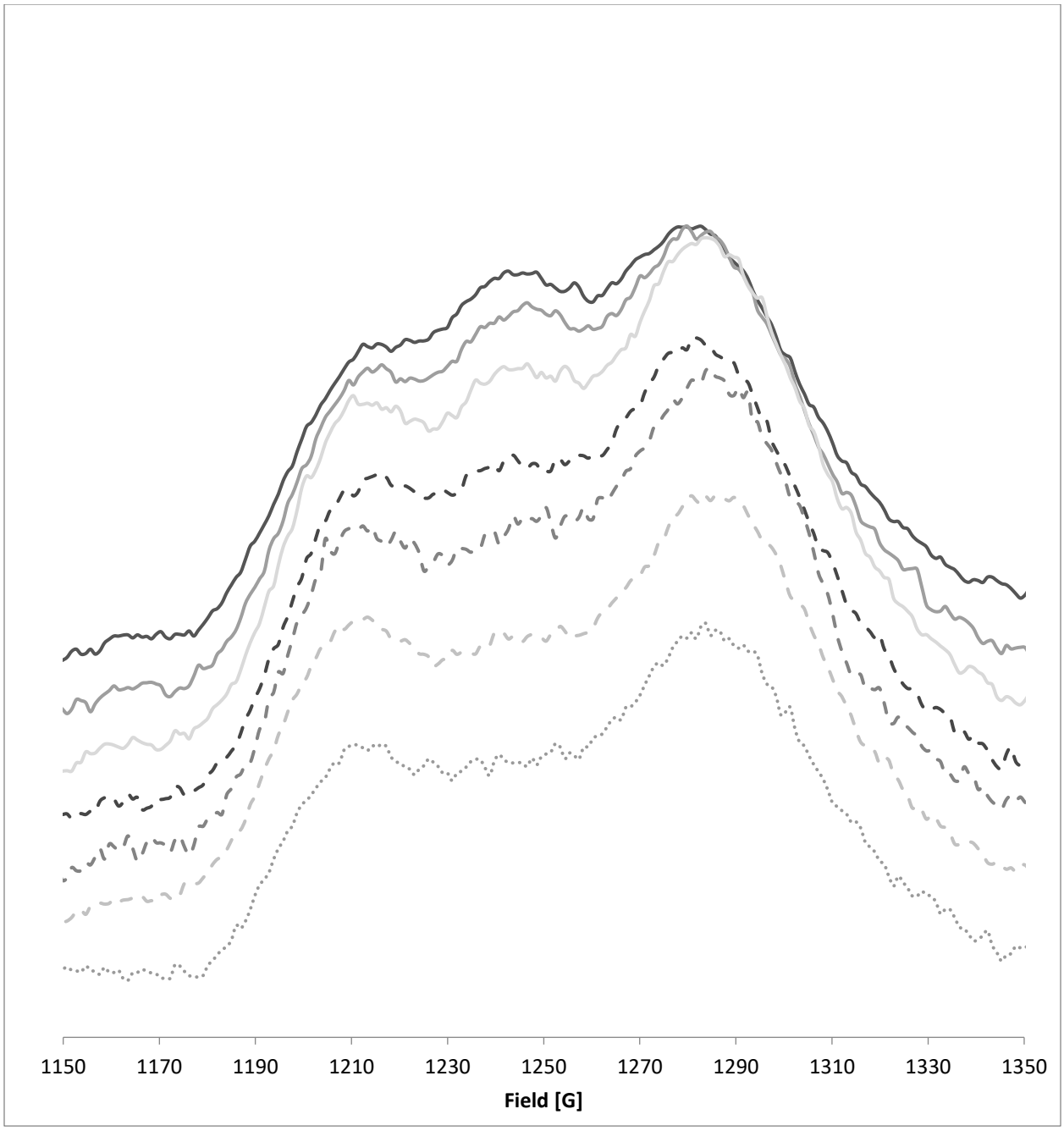

Figure 2.2. Cr_2-Tf in 100 mM HEPES\25 mM HCO_3^- at 37°C, pH 5.5 over 15 mins in the absense of a chelating agent. Spectra descending in 2.5 min intervals beginning at 0 min (top solid black) to 15 min (bottom dotted). Spectra offset to illustrate loss of central (Type 2) peak.

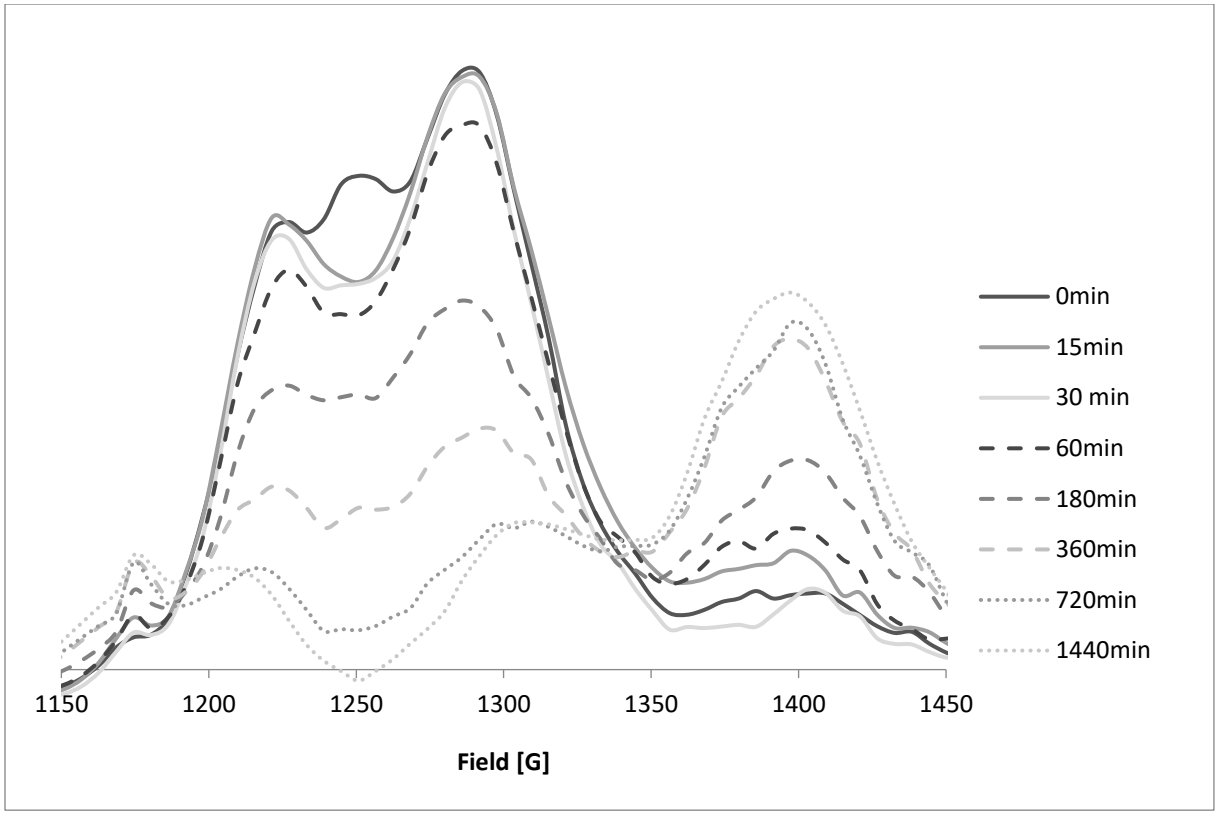

Figure 2.3. Cr_2-Tf in 100 mM HEPES\25 mM HCO_3^- at 37 °C, pH 5.5 over 24 hr in the presence of 1 mM EDTA. Peaks at 1220 and 1285 G (g= 5.1 and g=5.6) correspond to tightly bond N-terminus Cr-Tf. Peak at 1250 G (g=5.4) corresponds to weakly bound C-terminus Cr-Tf.

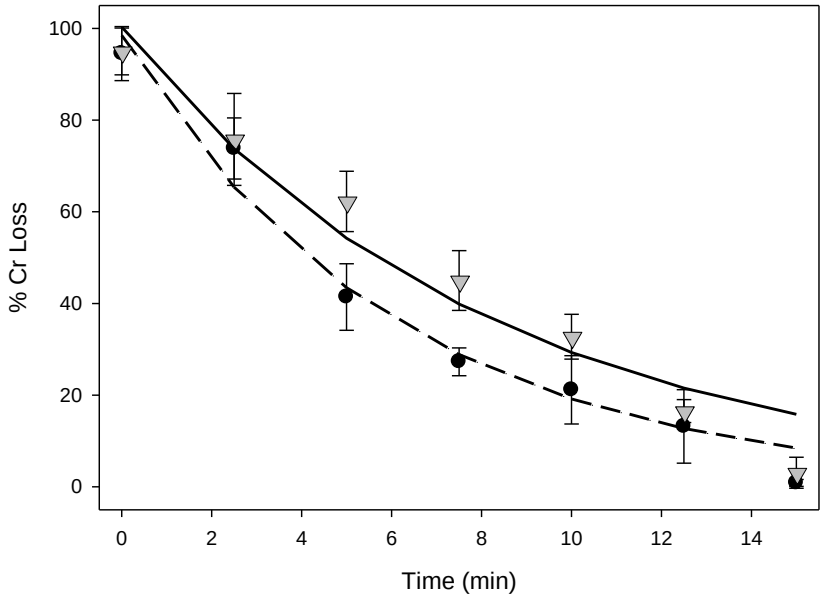

Figure 2.4. Loss of C-terminal Cr(III) signal over 15 min in the absence of a potential anionic ligand. Black circles, pH 4.5; gray triangles, pH 5.5.

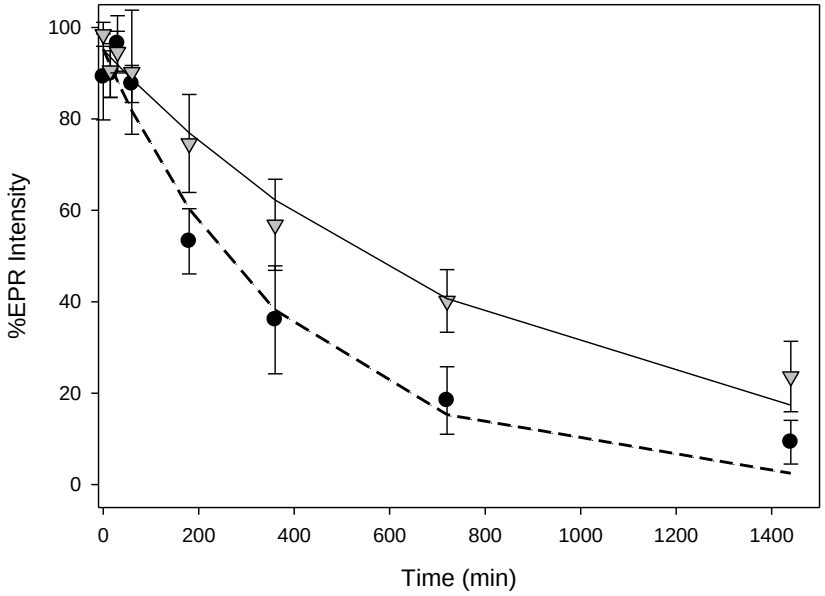

Figure 2.5. Loss of N-terminal Cr(III) signal over 24 hr in the absence of a potential anionic ligand at pH 4.5 and 5.5. Black circles, pH4.5; gray triangles, pH 5.5

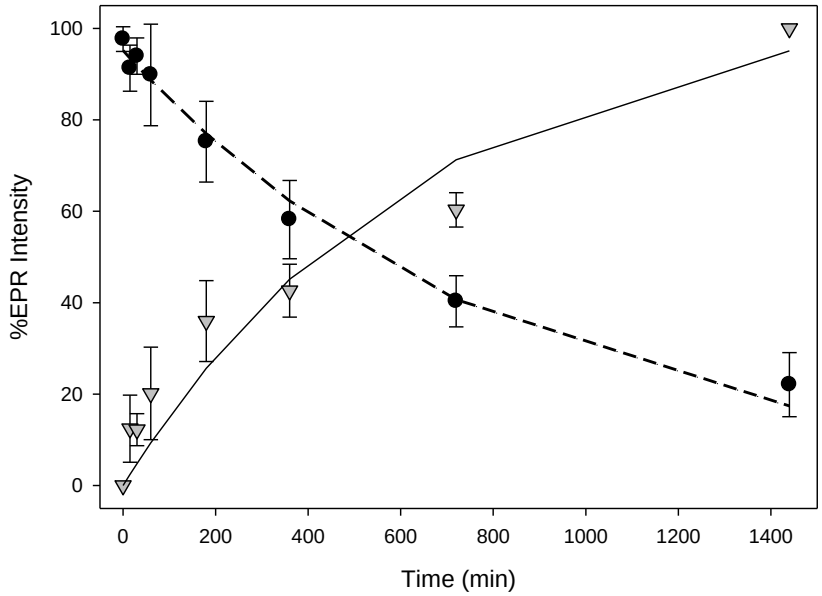

Figure 2.6 Loss of N-terminal Cr(III) signal and increase in non-specific Cr(III) signal over 24 h in the absence of a potential anionic ligand at pH 5.5. Black circles, N-terminal Cr(III); gray triangles, non-specific Cr(III).

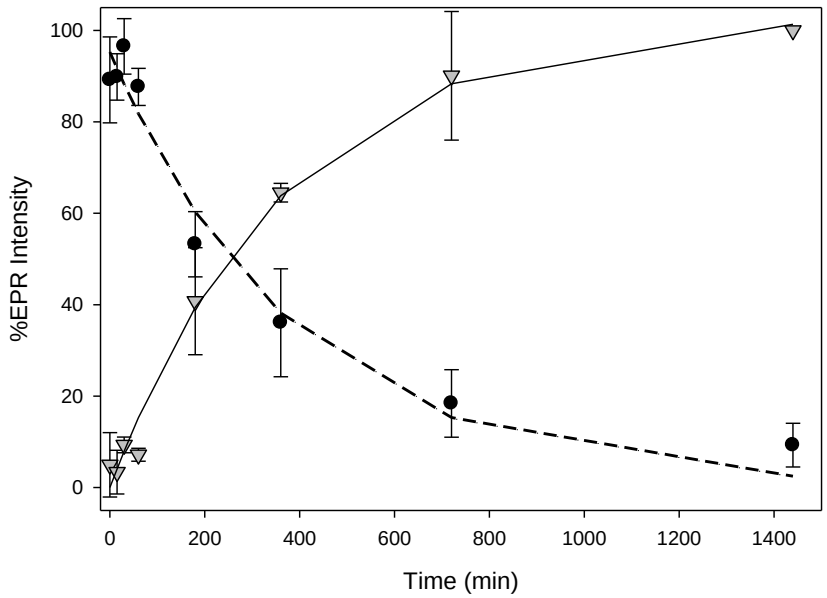

Figure 2.7. Loss of N-terminal Cr(III) signal and increase in non-specific Cr(III) signal over 24 h in the absence of a potential anionic ligand at pH 4.5. Black circles, N-terminal Cr(III); gray triangles, non-specific Cr(II)

RELEASE OF CR(III) FROM TRANSFERRIN IN THE PRESENCE/ABSENCE OF SOLUBLE TRANSFERRIN RECEPTOR

1. Introduction

Iron is a vital element for life, mostly due to its useful redox properties and natural abundance. The availability of Fe(III) is severally limited in aerobic conditions requiring specialized systems to transport the ion. Transport of Fe(III) is accomplished in vertebrates by the transferrin class of proteins. Human serum transferrin (Tf) is a glycoprotein composed of two lobes (C lobe and N lobe) that bind a single Fe(III) apiece. The metal binds alongside a synergistic ion, typically (bi)carbonate. Tf has a high affinity for Fe(III) among other metals at pH 7.4, but this affinity is drastically lowered at pH 5.5, which facilitates the ion's removal in the endosome.

Tf is only one of the critical proteins in the transferrin cycle. For the protein and the bound metal ions to be internalized into a cell, Tf must first bind with its receptor protein, transferrin receptor (TfR). TfR is a 180 kDa transmembrane protein; TfR exists as a homodimer on the cellular membrane. Each subunit possesses a Tf binding site, which is capable of binding a Fe_2-Tf at pH 7.4. Fe_2-Tf binds to TfR with high affinity at pH 7.4 (K_{d1}, K_{d2} of ~0.0002 nM, ~3.8 nM) with apo-Tf having a much weaker interaction with TfR at pH 7.4 (K_{d1}, K_{d2} of ~50 nM, ~340 nM) [1]. At pH 5.5, apo-Tf is bound more tightly by TfR (K_{d1}, K_{d2} of ~0.001 nM, ~0.042 nM)[1]. The differences in affinity at the two pHs allow for TfR to bind holo-Tf selectively from serum and ensures that after the metal release at low pH that apo-Tf stays bound until it is retuned to blood stream where it is released and recycled back into serum.

TfR is loosely composed of two domains, the short cytoplasmic N-terminal tail (residues 1-67) and the extra cellular stalk region responsible for binding holo-Tf (~70 kDa). The extracellar portion of TfR can be cleaved by trypsin which yields an active soluble form of the protein, soluble transferrin receptor (sTfR). The serum receptor has been isolated and purified from human serum and exhibits a molecular mass of 85 kDa with its 1-19 residues matching 101-119 residues of the intact receptor[2]. The truncated form of the receptor is the extracellular 'stalk' region containing the holo-Tf binding sites and lacking the cytoplasmic and transmembrane domains of the native receptor. The sTfR protein is found circulating naturally in human sera and is regularly used as a diagnostic of iron status in patients. The affinity of Fe_2-Tf of sTfR is slightly lower than that of TfR; however, Fe_2-Tf is still readily bound by sTfR [2,3]. The affinity for Fe_C-Tf or Fe_N-Tf for the soluble receptor is unknown, although changes in affinity of the intact receptor with different forms of Tf are known. Cooperativity exists between the lobes of TfR, and the binding of Fe_2-Tf to one lobe will strengthen the binding at the second lobe [4]. In sera, holo-Tf and sTfR circulate bound together, and precipitation of Tf significantly diminishes the receptor immunoreactivity [5]. The binding of holo-Tf with sTfR does not significantly impact iron circulation as sTfR circulates at a much lower concentration than Tf.

TfR has a high affinity for the diferric form of Tf but will bind monoferric Tf at lower affinity. A study demonstrated using electrospray ionization mass spectroscopy that the monoferric forms of Tf where unable to displace the diferric form but were easily able to displace the apo-Tf bound from TfR (Fe_2-Tf$\gg Fe_N$-Tf$\approx Fe_C$-Tf > apo-Tf) [6]. The binding of TfR to Fe_2-Tf has been demonstrated to have a different effect on the rate of release of Fe(III) from the unique lobes as discussed in more detail below.

The binding of Fe(III) to Tf has been shown to increase the affinity of Tf towards TfR, and Fe2-Tf has been shown to undergo conformational changes that contribute to the increased affinity [7]. These conformational changes primarily involve the shift from the 'open' apo-state of Tf to a 'closed' conformation after metal binding, in which the lobes of Tf become more compact. Metal ions other than the native Fe(III) are known to alter the binding of holo-Tf to TfR. Certain ions, such as Al(III), when bound to Tf are known to disrupt the affinity for the holo-Tf towards TfR such that affinity is close to that of apo-Tf[8]. Transferrin loaded with Bi(III), Co(III), $[U(VI)O_2]^{2+}$, or Ga(III) will still bind TfR [8]. Notably, Cr(III) loaded Tf has been shown to bind TfR; however, the binding mechanism differs from native Fe(III) [9, 10]. Typically, for Fe(III) loaded Tf, the C-lobe of Tf will bind first to the helical domain of TfR followed by the N-lobe binding to the protease domain [11]. Ga_2-Tf and Bi_2-Tf bind only in one step, implying only one lobe interaction, presumably through the C-lobe. Co_2-Tf and $[UO_2]_2$-Tf have both be observed to bind to TfR in two steps [8]. Co_2-Tf, $[UO_2]_2$-Tf, Ga_2-Tf, and Bi_2-Tf can all been internalized; however, the binding of metal loaded Tf to TfR does not guarantee metal delivery to the cell. The rate of binding of the metal loaded Tf to TfR and dissociation of metal from Tf-TfR complex must be considered to determine if metal delivery via endocytosis is feasible. In the case of $[UO_2]_2$-Tf, the binding of $[UO_2]_2$-Tf with TfR is very weak, and cellular internalization of $[UO_2]^{2+}$ via endocytosis cannot be considered physiologically viable. In addition, $In(III)_2$-Tf has been shown to bind to TfR readily; however, the transfer of In(III) to the cell is not accomplished via endocytosis as the release of the metal from the Tf-TfR complex is too slow to occur during endocytosis (~15 min) [12].

The identity of the anion bound to Tf nearby the metal binding pocket also appears to have an effect on the ability for the metal to be released during endocytosis. Under physiological

conditions, the anion bound to Tf in the body is (bi)carbonate. Without the presence of bicarbonate, many metals will not bind with Tf, including Fe(III). Several other biologically relevant anions have been shown to also bind in this pocket (as well as bind to the metal while bound to Tf). For example, citrate, oxalate, and malonate have all been demonstrated to bind with Tf and interact with metal [13]. The identity of the anion has been demonstrated to potentially interfere with Fe_2-Tf binding to TfR1, and the metal release post the acidification step in endocytosis. Citrate, when bound in the anion binding pocket, has little impact on the ability for Fe_2-Tf to bind to TfR1 or for the metal to release after endocytosis; however, oxalate loaded Fe_2-Tf will bind to TfR1 with slightly lower affinity, but the Tf protein will not dissociate from TfR1 following the acidification step [14]. Presumably the Fe_2-Tf-oxalate is not allowing the metal to dissociate during the acidification step (previous studies have demonstrated the first step in the metal dissociation is the protonation with subsequent removal of the bicarbonate anion which leaves the metal in a distorted tetrahedral environment), which is why the Tf may not dissociate from TfR1 after acidification; however, the results are not definitive [8].

Tf exists in serum only partially saturated with Fe(III) under normal iron conditions (~40% apo, ~33% monoferric, ~27% diferric), leaving it capable of binding alternative metals [15]. Several nonferric metal ions have been discovered to bind to Tf; however, many bind at considerably lower affinity than Fe(III) and in non-canonical states [16]. Alternative metals loaded into Tf typically decrease the affinity of Tf for TfR compared to Fe_2-Tf; however, many of these alternative metal Tf's bind at higher affinity than apo-Tf. One such metal, Cr(III), has been shown to bind to Tf, and Tf might be the physiological transporter of Cr(III) [17]. The transport of Cr(III) is of particular interest as the ion may provide therapeutic benefits in insulin resistant individuals, but the active forms of Cr(III) and the mechanism of this action are still

unclear [18-21]. Previously, Cr(III) loss from the C-lobe of Tf was shown to be fast enough to occur during endocytosis; however, loss of Cr(III) for the N-lobe of Tf was significantly slower. TfR has previously been shown to accelerate the loss of Fe(III) from the lobes unequally through what is suspected to be an imposed conformation by the receptor onto the protein. Thus, the effect of the presence of TfR on the rate of loss of Cr(III) from Tf was investigated, as described in this chapter.

2. Experimental

2.a. Chemicals

Iron-free human serum Tf and bovine serum Tf were obtained from Aldrich (St. Louis, MO). Doubly deionized water was used throughout. All reagents were used as received unless otherwise noted. Cr(III) solutions were prepared by using $Cr(III)Cl_3 \cdot 6H_2O$. ApoTf concentrations were determined by using the extinction coefficient ($\boldsymbol{\varepsilon}$=9.12×10^4 $M^{-1}cm^{-1}$) at 280 nm [22].

2.b. Tf Solution Preparation

Dichromic transferrin solutions were prepared by dissolving lyophilized human serum apo-Tf in a 7.4 pH 0.1 M HEPES/25 mM HCO_3^- buffer. Concentration of the apo-Tf was measured with UV-Vis using $\boldsymbol{\varepsilon}$=9.12×10^4 $M^{-1}cm^{-1}$. A solution of $Cr(Cl)_3$ was prepared in 0.1 M HEPES/25 mM HCO_3^- buffer, and an aliquot added to the apo-Tf solution to achieve a ratio of 1.9 Cr:1 Tf. Full 2:1 Cr:Tf loading was avoided to minimize amount of free aqueous $[Cr(H_2O)_6]^{+3}$ in solution. The solution was allowed to incubate for 48 hours to ensure full loading of the Cr(III) into Tf.

2.c. sTfR Isolation

In the preparation of sTfR, 10 mM potassium phosphate (KPi)/150 mM NaCl pH 7.5 buffer was used throughout unless otherwise noted. Buffer also contained 0.5 mM phenylmethylsulfonyl fluoride (PMSF) (dissolved in a minimum of ethanol), 0.1 mM dithiothreitol (DTT), and 0.02 % (w/v) NaN_3 unless otherwise noted. Adjustments to pH of solution were achieved using HCl or NaOH. The purification method was adapted from the previously reported method of Schwartz [2]. Bovine marrow was obtained from local commercial vendors. Bulk marrow tissue was harvested from marrow bones and homogenized in a blender in KPi/NaCl buffer. The homogenate was spun down at 17,700 x *g* for 90 min; the supernatant was discarded, and the pellets were suspended in KPi/NaCl buffer. The resulting solution was made 1% in Triton X-100, a surfactant, and the product was stirred for 30 min. The lysate solution was spun at 17,700 x *g* for 35 min. The supernatant was collected andfiltered over glass wool and the pellets were discarded. The supernatant was then adjusted to pH 5.0 using 1 M HCl, and desferrioxamine added to achieve a concentration of 0.2 mM. This solution was allowed to sit for 15 min with gently swirling as iron from cellular components was released and chelated. The solution was then adjusted to pH 8.0, allowed to sit for 15 min, made 40 % (w/v) using ammonium sulfate, and then centrifuged at 17,700 x *g* for 20 min. This solution was then allowed to sit overnight. The precipitate of the ammonium sulfate solution was then collected and dissolved in 300 mL of KPi/NaCl buffer over a 3 hr period. The resulting solution was dialyzed in KPi/NaCl solution overnight. Dialysates were pooled and centrifuged at 17,700 x *g* for 40 min. The pH slightly adjusted to pH 7.50. The TfR- containing solution was applied to a 2 mL CNBr column loaded with Fe_2-Tf and washed with 500 mL of KPi/NaCl 0.2% Triton X-100 buffer. The CNBr column was prepared using CNBr-activated Sepharose and loaded with bovine

Fe_2-Tf (8.5 mg/mL) according to manufacturer's instructions with the final acidic wash omitted (to avoid removing Fe(III) from the Tf immobilized on the column). CNBr-activated Sepharose was obtained from GE Healthcare. The column was washed with 500 mL of KPi/NaCl and then 50 mL KPi/NaCl with CHAPS (10 mM) before the Fe(III) was removed using 10 mL of pH 4.9 acidic wash containing: citric acid (50 mM), NaCl (100 mM), CHAPS (10 mM), and 1 mM desferrioxamine. An elution buffer of pH 7.5 KCl (2 M), HEPES (50 mM), and CHAPS (10 mM) was then applied and fractions of the elute were collected. Fractions containing appreciable absorbance at 280 nm were pooled and frozen for later proteolysis. The solution of TfR1 was thawed, and trypsin was added to achieved a 1:1 molar ratio of TfR1:Trypsin (ultraviolet-visible (UV-Vis) spectroscopy was used to determine protein concentration to establish the amount of trypsin required). The solution was allowed to incubate in an ice bath for 30 min after which 100 molar excess of PMSF (dissolved in a minimum of ethanol) was added to stop proteolysis. The solution was immediately applied to a Sephacryl S-200 High Resolution column and washed with 200 mL of in KPi/NaCl buffer. Fractions were collected for UV-Vis analysis. Fractions with notable absorbance at 280nm were pooled and concentrated using Amicon ultrafiltration.

2.d. EPR Spectroscopy

CW-EPR spectra were measured on a Bruker (Billerica, MA) ELEXSYS E540 X-band spectrometer with an ER 4102 ST resonator. CW spectra were measured at 9.44 GHz with a microwave power of 21.1 mW by using a magnetic field modulation frequency of 100 kHz with an amplitude of 30 gauss. Spectra were taken at liquid nitrogen temperatures with a quartz insertion dewar. All results are presented as the average of at least triplicate experiments. Error bars in figures represent standard deviation.

2.e. Data Analysis

Data analysis, calculation of averages and standard deviations, and fitting of curves to the appropriate equations were performed using SigmaPlot 11 (SPSS, Inc., Chicago, IL). The iterative curve fitting algorithm of SigmaPlot 11 uses the Marquardt-Levenberg algorithm to find the parameters of the independent variables that provide the best fit between the data and the equation.

CW EPR spectrum processing and simulations were performed using the EasySpin package in MATLAB (Mathworks, R2017b). Polynomial fitting of the spectral baseline corrections was performed using Xepr software of the ELEXSYS. The g-values, g-strain, and weight of the simulated spectrum were fit using the "pepper" function in EasySpin.

3. Results and Discussion

Recently, holo-Tf binding to TfR1 has been demonstrated to be species selective [6, 23, 24]. Bovine Fe_2-Tf showed lower binding affinity compared with that of human Fe_2-Tf toward TfR1 at pH 7.4 such that the any of bovine Fe_2-Tf left at acid pH below detection limits. This emphasized the need for bovine Tf experiments to utilize bovine TfR (or experiments with human Tf to use human TfR) to accurately model behaviors between the proteins. Due to the more convenient nature of acquiring bovine tissue for purification of TfR (compared to human tissue), several experiments utilizing bovine Tf and Cr(III) were repeated in a similar manner to those previously reported utilizing human Cr_2-Tf. A representative set of EPR spectra is provided in Figure 3.1. Bovine Cr_2-Tf has a somewhat different EPR signature from that of human Cr_2-Tf; the EPR peaks for the C and N lobe bound Cr(III) are indistinguishable, having the same g-value (g~5.4). In human Cr_2-Tf, the Cr(III) bound in the different lobes of Tf can be distinguished due to dissimilar EPR features despite the two site possessing the same ligands. A difference in the

second coordination sphere about the Cr(III) centers is speculated to cause this dissimilarity; presumably bovine Cr_2-Tf lacks these differences as the EPR features of Cr(III) bound at the two sites are indistinguishable. The appearance of a single Cr_2-Tf EPR feature for both sites has previously been observed in human Cr_2-Tf that has been glycated and Cr_2-Tf heat-treated 24 hr after binding of the Cr(III) [22]. The conversion of these signals was ascribed to conformation issues associated with Cr(III) binding and warrant further investigation. Otherwise, following acidification to pH 5.5, bovine Cr_2-Tf displays a loss of this EPR signal at a rate of $0.0196 \pm 0.0033\ min^{-1}$ (slower then C-lobe Cr(III) loss from human Tf, but faster than N-lobe Cr(III) loss, 0.12 ± 0.01 and $0.0012 \pm 0.0001\ min^{-1}$, respectively).

The effects of binding of Fe(III)-Tf to TfR on the release of Fe(III) have been studied in detail [25]. Fe_2-Tf when bound to TfR accelerates the release of the metal from the C-lobe and decreases the rate of loss from the N-lobe, reversing the order that Fe(III) is released from non-receptor bound Tf. Soluble TfR (sTfR) has been shown to have the same effect, accelerating the release of Fe(III) from the C-lobe of Tf by nearly ten-fold. While Fe(III) is present in the N-lobe, release of Fe(III) from the C-lobe is slowed, and when Fe(III) is present in the C-lobe, the rate of loss of Fe(III) is increased from N-lobe [4]. The magnitude of this effect is diminished with lowered pH [26]. This suggests for Fe(III) that a degree of cooperativity exists between the lobes for Fe(III) loss from Tf; if this effect persists for other metals or if Fe(III) in one lobe would have a similar effect on a different metal are unclear.

The effects of binding of Cr_2-Tf to TfR have not been investigated in great detail. The only previous research on the topic concluded that Cr_2-Tf would bind to TfR but did not investigate the effect the receptor binding had on the release of Cr(III) during acidification [9]. In the current study, the effects of receptor binding on Cr(III) loss were probed using sTfR isolated

from bovine marrow. Given that the sTfR was from a bovine source, bovine serum Tf was used as it has been shown that human Tf binding to bovine receptor is poor. Lowering the pH from 7.4 to 5.5 results in the rapid loss of the EPR signal from the Cr_2-Tf/sTfR complex (Figure 3.2). The EPR signal from the nonspecific bound Cr(III) appears after the loss of the Cr_2-Tf/sTfR signal. Cr(III) loss occurs with a half-life of 0.242 min (corresponding to a rate constant of $2.86 \pm 0.50\ \text{min}^{-1}$) such that virtually all Cr(III) is lost from the Tf-TfR complex within an endosomal cycle (~15 min). Unlike for Fe(III), loss is accelerated for Cr(III) in both binding sites of bovine Cr_2-Tf. A comparison of the rate of Cr(III) loss from bovine Cr_2-Tf alone and bovine Cr_2-Tf in the presence sTfR is given in Figure 3.3.

The conformation effects induced by TfR in the release of Cr(III) from Tf also points out the importance of the Cr_2-Tf conformation. Preparation of the protein using physiological bicarbonate concentrations in the incubation buffer result in rapid binding of Cr(III) to Tf (essentially complete within 25 min), but 24-48 hr of incubation is typically used to prepare Cr_2-Tf to ensure complete saturation of the protein [17]. The half-life of Cr(III)-Tf in circulation after Cr(III) is bound by Tf is much shorter than the incubation time used in these preparations (e.g. Fe(III) after first binding with Tf will circulate on average 75 min before undergoing endocytosis in a healthy adult male [27]); thus, studies need to investigate what conformational changes, if any, Cr(III) undergoes when binding with Tf and what will be the dominant form of Cr-Tf while in circulation.

The nonspecifically bound Cr(III) EPR signal observed in Figure 3.2 matches the EPR signal for nonspecifically bound Cr(III) in experiments without TfR present. Previously, Lay and coworkers postulated that Cr(III) might crosslink Tf and TfR to stop the dissociation of the proteins post endocytosis and stopping Cr(III)'s accumulation into the cell [28]. The lack of line

width broadening, shifting, or other distortion to the EPR features one would expect if the nonspecific Cr(III) were bound to new ligands when crosslinking with the receptor protein indicate that this is likely not happening. Cr(III) release from Tf-Tfr complex is rapid under endosomal conditions.

4. Conclusion

The EPR features arising from Cr(III) bound to bovine Tf differ from that of Cr(III) bound to human serum Tf. The rate of Cr(III) loss from bovine Tf after acidification also differs from that human serum Tf being faster than N-lobe bound Cr(III) loss but slower than C-lobe bound Cr(III) loss. The release Cr(III) release from bovine serum Tf after acidification occurs at a rate of approximately $0.0196 \pm 0.0033\ \text{min}^{-1}$ ($t_{½}$=35 min), which is sufficient for only partial delivery of Cr(III) to an endosome. The rate of loss of Cr(III) from the Cr_2-Tf-sTfR complex is very rapid compared to Cr_2-Tf alone. The rate at which Cr(III) is loss from Tf-sTfR complex is sufficiently rapid for ~100% Cr(III) loss to occur during the time for endocytosis. The rate of loss of Cr(III) from Tf in an endosome cannot be used to explain its inability to enter a cell via endocytosis as recently postulated [28].

After the release of Cr(III) from the Tf-sTfR complex, non-specific binding of Cr(III) to the surface of Tf is observed indicating that additional steps in the endocytosis process are still to be elucidated. A biological chelating ligand(s) that has yet to be identified would be needed to bind the Cr(III) after it is released. The ligand would then assist in the transport from the endosome to the rest of the cell. Knowing the identity of the ligand is critical to design further experiments to investigate how Cr(III) is transported from the endosome to the rest of the cell. The divalent metal transporters that transport Fe(II) are not viable for Cr(III) transport, as they do not transport the trivalent ions and Cr(III) will not reduce easily under biological conditions. To

date, only monocarboxalyte transporters have been investigated as potential Cr(III) transporters; inhibition of said transporters had no effect on Cr(III) accumulation in cells [29]. Ligands (ascorbate and citrate, for example) that have been examined as potential chelators do not bind Cr(III) at pH 5.5 in a time consistent with endocytosis. The Cr(III) not only must be bound in this narrow time frame (~15 min), but the resulting complex must also be transported out of the endosome before it refuses with cellular membrane.

REFERENCES

1. Kleven, M. D.; Jue, S.; Enns, C. A. Transferrin receptors TfR1 and TfR2 bind transferrin through differing mechanisms *Biochemistry* 2018, *57*, 1552

2. Turkewitz, A.P.; Amatruda, J. F.; Borhani, D.; Harrison, S. C.; Schwartz, A. L. A High yield purification of the human transferrin receptor and properties of its major extracellular fragment. *J. Biol. Chem.,* 1988, *263*, 8318

3. Agthoven, A.; Goridis, C.; Naquet, P.; Pierres, A.; Pierres, M. Structural characteristics of the mouse transferrin receptor. *Euro. J. Biochem.* 1984, *140*, 433

4. Bali, P. K.; Aisen, P. Receptor-modulated iron release from transferrin: differential effects on N- and C-terminal sites *Biochemistry* 1991, *30*, 9947

5. Harms, K.; Kaiser, T. Beyond Soluble transferrin receptor: old challenges and new horizons *Best. Pract. Res. Cl. En.* 2015, *29*, 799

6. Leverence, R.; Mason, A. B.; Kaltashov, I. A. Noncanonical interactions between serum transferrin and transferrin receptor evaluated with electrospray ionization mass spectrometry *Proc. Natl. Acad. Sci.* 2010, *107*, 8123

7. Bali, P. K.; Zak, O.; Aisen, P. A new role for the transferrin receptor in the release of iron from transferrin *Biochemistry* 1991, *30*, 324

8. El Hage Chahine, J.-M.; Hémadi, M.; Ha-Duong, N.-T. Uptake and release of metal ions by transferrin and interaction with receptor 1 *Biochim. Biophys. Acta* 2012, *1820*, 334

9. Kornfeld, S. The effect of metal attachment to human apotransferrin on its binding to reticulocytes *Biochim. Biophys. Acta* 1969, *194*, 25

10. Harris, W. R.; Stenback, J. Z. The bicarbonate-dependence of zinc(II)-transferrin binding *J. Inorg. Biochem* 1988, *33*, 211

11. Eckenroth, B. E.; Steere, A. N.; Chasteen, N. D.; Everse, S. J.; Mason, A. B. How the binding of human transferrin primes the transferrin receptor potentiating iron release at endosomal pH *Proc. Natl. Acad. Sci.* 2011, *108*, 13089

12. Vincent, J.B.; Love, S.; *Biochim. Biophys. Acta* 2012, *1820*, 361

13. Harris, W. R. Anion binding properties of the transferrins. Implications for function *Biochim. Biophys. Acta* 2012, *1820* , 348

14. Halbrooks, P. J.; Mason, A. B.; Adams, T. E.; Briggs, S. K.; Everse, S. J. the oxalate effect on release of iron from human serum transferrin explained *J. Mol. Biol* 2004, *339* , 217

15. Cazzola, M.; Huebers, H. A.; Sayers, M. H.; MacPhail, A. P.; Eng, M.; Finch, C. A. Transferrin saturation, plasma iron turnover, and transferrin uptake in normal humans. *Blood* 1985, 66 , 935

16. Benjamín, J. A.; Cardona, A. E.; Vázquez, Á. L.; Dones, C. Y.; Pabón, H. L.; Rodríguez, H. M.; Rodríguez, I.; González, J. C.; Pazol, J.; Pérez-Ríos, J. D.; Catala, J. F.; Carrasquillo, M.; De Jesus, M. G.; Cordero, N. A.; Cruz, P. M.; González, P.; Hernández, R.; Gaur, K.; Loza, S. A.; Tinoco, A. D. Exploring serum transferrin regulation of nonferric metal therapeutic function and toxicity *Inorganics* 2020, *8*, 48

17. Deng, G.; Wu, K.; Cruce, A. A.; Bowman, M. K.; Vincent, J. B. Binding Of trivalent chromium to serum transferrin is sufficiently rapid to be physiologically relevant *J. Biol. Inorg. Chem.* 2015, *143*, 48

18. Davis, C. M.; Vincent, J. B. Chromium oligopeptide activates insulin receptor tyrosine kinase activity. *Biochemistry* 1997, 36, 4382

19. Wang, H.; Kruszewski, A.; Brautigan, D. L. Cellular chromium enhances activation of insulin receptor kinase. *Biochemistry* 2005, 44, 8167

20. Hua, Y.; Clark, S.; Ren, J.; Sreejayan N., Molecular mechanisms of chromium in alleviating insulin resistance. *J. Nutr. Biochem*. 2012, 23, 313

21. Yin, R. V.; Phung, O. J. Effect of chromium supplementation on glycated hemoglobin and fasting plasma glucose in patients with diabetes mellitus. *Nutr. J.* 2015, 14, 14.242

22. Deng, G.; Dyroff, S. L.; Lockart, M.; Bowman, M. K.; Vincent, J. B. the effects of the glycation of transferrin on chromium binding and the transport and distribution of chromium in vivo *J. Inorg. Biochem.* 2016, *164*, 26

23. Kawabata, H.; Tong, X.; Kawanami, T.; Wano, Y.; Hirose, Y.; Sugai, S.; Phillip Koeffler, H. Analyses for binding of the transferrin family of proteins to the transferrin receptor 2 *Br. J. Haematol.* 2004, *127*, 464

24. Levina, A.; Lay, P. A. Vanadium(V/IV)-transferrin binding disrupts the transferrin cycle and reduces vanadium uptake and antiproliferative activity in human lung cancer cells *Inor.g* 2020, *59*, 16143

25. Steere, A. N.; Byrne, S. L.; Chasteen, N. D.; Mason, A. B. Kinetics of iron release from transferrin bound to the transferrin receptor at endosomal pH *Biochim. Biophys. Acta* 2012, *1820*, 326

26. Hamilton, D. H.; Turcot, I.; Stintzi, A.; Raymond, K. N. Large cooperativity in the removal of iron from transferrin at physiological temperature and chloride ion concentration *J. Inorg. Biochem* 2004, *9*, 936

27. Huff, R. L.; Hennessy, T. G.; Austin, R. E.; Garcia, J. F.; Roberts, B. M.; Lawrence, J. H. Plasma and red cell iron turnover in normal subjects and in patients having various hematopoietic disorders *J. Clin. Invest.* 1950, *29*, 1041

28. Levina, A.; Nguyen Pham, T. H.; Lay, P. A. Binding of Cr(III) to transferrin could be involved in detoxification of dietary chromium(III) rather than transport of an essential trace element. *Angew. Chem. Int. Ed*. 2016, 55, 8104

29. Rhodes, N.; LeBlanc, P. A.; Rasco, J. F.; Vincent, J. B. Monocarboxylate transporters are not responsible for Cr^{3+} transport from endosomes. *Biol. Trace Elem. Res.* 2012, 148, 409

Table 3.1. Dissociation constants and corresponding half-lives for Cr(III) dissociation from the Cr(III) binding site of bovine transferrin in the absence of chelating ligands and in the presence or absence of sTfR at pH 5.5 and 4.5. SD – standard deviation.

Rate Constants for Cr(III) Dissociation at pH 5.5

Sample	k (min^{-1})	SD (min^{-1})	$t_{1/2}$ (min)
Bovine Cr_2-Tf	**0.0196**	**0.0033**	**35.3**
Bovine $(Cr_2\text{-Tf})_2$-sTfR	**2.86**	**0.50**	**0.242**

Figure 3.1. EPR spectra of 0.5 mM bovine Cr2-Tf at 37 °C at pH 7.4 before (time zero) and after acidification to pH 5.5.

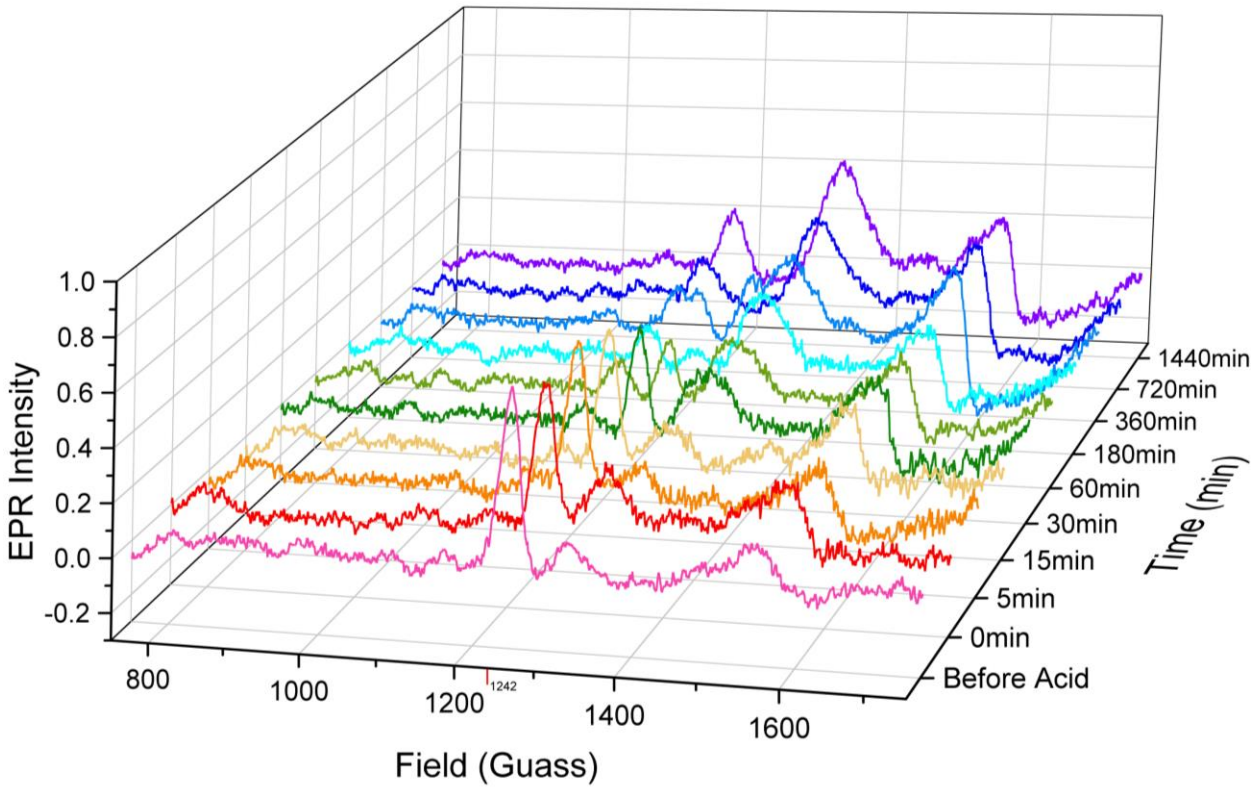

Figure 3.2. EPR spectra of 0.5 mM bovine Cr2-Tf at 37 °C incubated with 0.25 mM bovine sTfR at pH 7.4 before (time zero) and after acidification to pH 5.5.

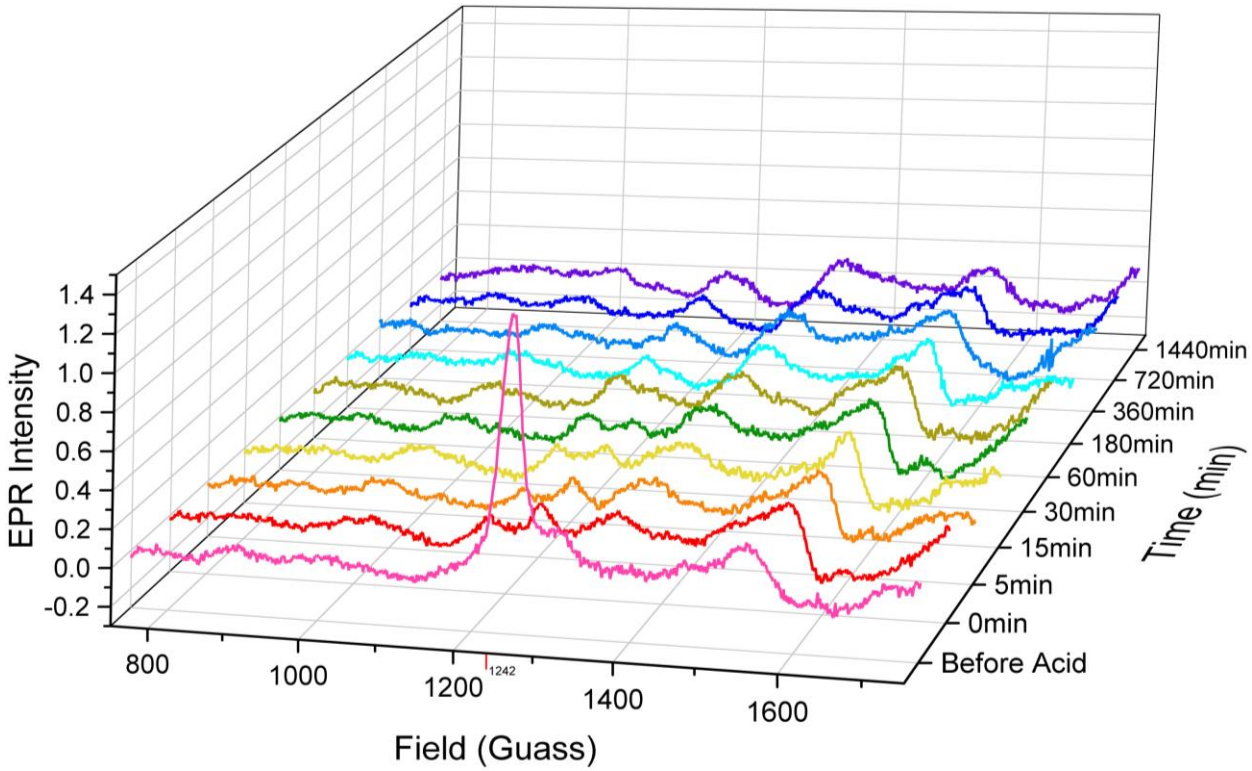

Figure 3.3. Loss of EPR signal from Cr2-Tf in the presence and absence of sTfR at pH 5.5. Black circles, absence of sTfR; black triangles with sTfR

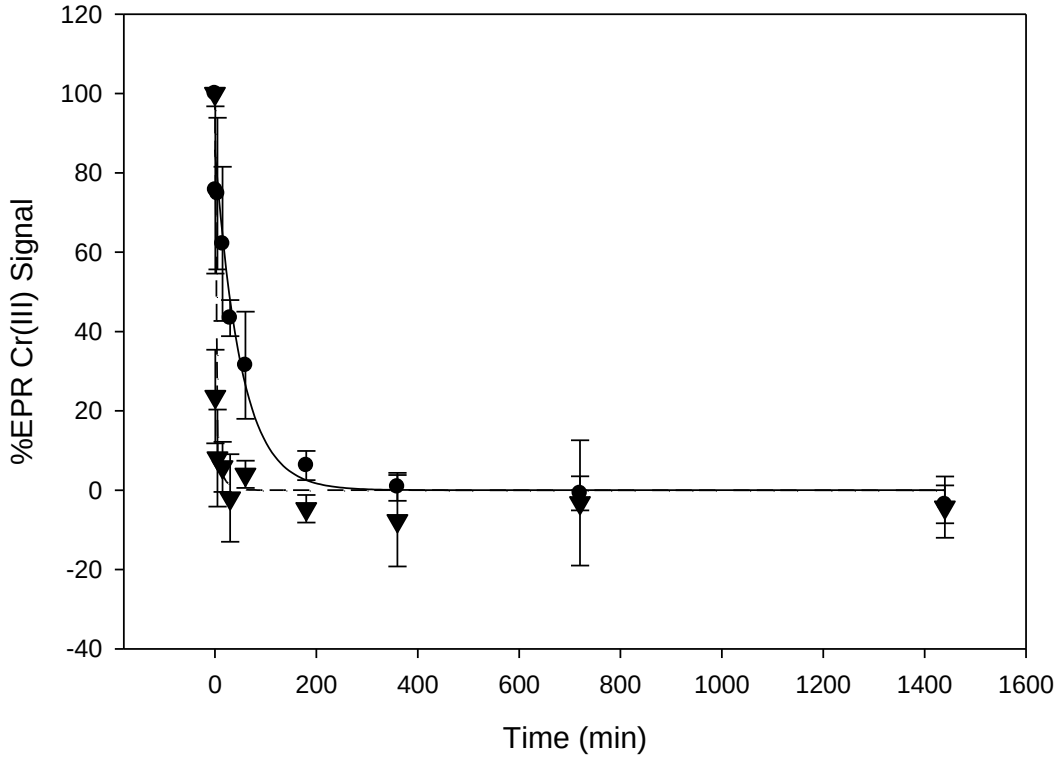

SIGNIFICANCE OF CONFORMATION CHANGES DURING THE BINDING AND RELEASE OF CHROMIUM(III) FROM HUMAN SERUM TRANSFERRIN

1. Introduction

Transferrin (Tf) is a serum protein responsible for transporting Fe(III) in the bloodstream and delivering it to cells via endocytosis. Tf is selective for Fe(III) and is adapted to bind it; however, many ions with similar charge-to-size ratio are also bound by Tf, although none bind as well as Fe(III) [1]. Of these ions, Cr(III) is particularly relevant as Tf has been speculated to serve as the physiological transporter of the metal in the bloodstream. Tf binds the metal ions at one of two binding sites located on either of the two lobes of the Tf, the C lobe or N lobe. The binding sites of Tf are composed of identical metal-binding ligands; two tyrosine residues, an aspartate reside, and a histidine residue with coordination completed by a synergistic anion, typically (bi)carbonate. The lobes share roughly 40% sequence homology [2]. The typical blood saturation level of Tf is 30%, allowing for other metals to occupy a vacant metal binding site in serum[2].

The binding and release of metal ions from Tf are accompanied by significant conformation changes in the Tf molecule. Apo-Tf possess a far more ‘open’ conformation with increased solvent access within the binding cleft were the metal binding sites are located. Fe_2-Tf has a ‘closed’ conformation that lacks this enhanced solvent access and improves the affinity of the protein to bind to its receptor, transferrin receptor (TfR). After being bound by TfR, the entire holo-Tf-TfR complex is internalized in an endosome whose pH is lowered to 5.5-4.5 via H^+ pumps. The acidification prompts the release of the metal, which is removed from the

endosome. The endosome subsequently re-fuses with the cell membrane, recycling the now apo-protein back into the bloodstream.

Tf is believed to be the physiological carrier of Cr(III) from the bloodstream to tissue. Numerous *in vivo* studies have been conducted which support Tf as being the physiological carrier [3, 4, 5, 6], although recent studies have challenged the viability of Tf as the transporter of Cr(III) into the cell [7]. The rate at which Tf binds and release Cr(III) has garnered considerable attention as of late; and while its binding has been demonstrated to be rapid enough for Tf to be the physiological transporter in the bloodstream (under physiological conditions), the rate at which Cr(III) dissociates from the protein is under scrutiny [7, 8]. The binding of Cr(III) to Tf was thought to be very slow on the order of days in the bloodstream, but the binding was shown to be rapid (reaching equilibrium in 15 mins) in the presence of physiological levels of bicarbonate (25 mM) [8]. The dissociation of Cr(III) from Tf has recently been speculated to be too slow to occur during endocytosis, which leads to crosslinking of the Tf and TfR protein through Cr(III) [7]. Studies probing the release of Cr(III) from Tf found when bound to the receptor protein (in its soluble form) the release of the metal is rapid enough to feasibly occur during endocytosis [7]. Additionally, the release of the metal from the different metal binding sites (denoted C-lobe or N-lobe depending where the site is located) occurred at very different rates when not complexed with TfR.

Recent studies have demonstrated that the binding of Cr(III) to Tf is more complicated than previously assumed [8]. The two binding sites on either lobe of Tf can be distinguished by unique EPR signatures in the g = 5.2-5.6 range [8]. The different EPR features between the two sites presumably arises from differences in the secondary coordination sphere about the site as the ligands at both metal binding sites are identical (binding site given in Figure 4.1). The EPR

features in this range were assigned to Cr(III) in a specific lobe of Tf. Features at g ~ 5.6 and 5.2 arises from Cr(III) bound to the N-lobe of Tf; the features at g ~ 5.4 belongs to Cr(III) bound to the C-lobe of Tf. Selectively displacing the Cr(III) in the C-lobe of Tf with another metal resulted in the absence of the g ~ 5.4 feature, confirming these assignments [9]. These EPR features appear after incubation of Tf with Cr(III) for two weeks in ambient bicarbonate concentrations (pH 7.4) or for 2 days in 25 mM bicarbonate. Cr(III) in the N-lobe terminus binding site has EPR features at g = 5.2 and 5.6, and Cr(III) bound in the C-terminal binding site has a feature at 5.4. Again, these EPR features appear after some time (2 days to many days depending on preparation used); yet, Cr(III) is known to bind rapidly on the scale of minutes to Tf [8]; additionally, given that the half-life of Fe-Tf in the bloodstream after binding is ~90 minutes, conformational effects that take place on the order of days would have little relevance in the actual physiological cycle of transferrin. Thus, examining Cr-Tf shortly after the initial binding of Cr(III) is critical to determine if Cr-Tf behaves differently from the traditionally prepared forms utilized in previous studies.

The type of transferrin used is also critical to the metal behavior in the binding site. Lactoferrin has similar features for Cr(III) bound in its metal binding sites; however, the C-terminal lobe Cr(III) corresponds to EPR features at g = 5.15 and 5.62, while the N-lobe bound Cr(III) correspond to a feature g= 5.43 [10], the opposite behavior human serum Tf. Curiously, despite the g-values for the binding sites being reversed compared to human blood serum Tf, the metal affinity behavior is the same for Cr(III) bound lactoferrin or Tf, with the C-terminal lobe having weaker metal affinity compared to Cr(III) bound to the N-lobe. Despite having identical metal-binding ligands and similar structures, the binding sites on these similar proteins (or even

binding sites on the same protein) exhibit significantly different metal binding behavior and EPR features due differing environments about the Cr(III) centers beyond the immediate ligands.

Previously, Cr_2-bovine Tf was observed to produce only one EPR feature at g = 5.4, despite having a similar structure and identical ligands compared with human serum Tf. Heat-treated and glycated human serum Tf have been used in Cr(III) binding studies and has been reported to generate a single g = 5.41 EPR feature one day after addition of Cr(III), despite binding two equivalents of Cr(III) per Tf [11]. The EPR feature at g = 5.41 lost intensity concomitantly with the increase in intensity of EPR features at g = 5.14 and 5.64; yet, a conformation of $Cr(III)_2$-Tf apparently exists such that both metal sites give rise to this single EPR feature. Different conformations of $Fe(III)_2$-Tf have been studied during the uptake and release of the metal when complexed with TfR with noted effects on metal affinity; however, the exact nature and structural differences between these conformation is still disputed [12, 13, 14]. A previous study on Cr(III)-Tf noted that the rate of Cr(III) loss from the C-lobe of Tf, which has a single g = 5.4 feature, was significantly faster than Cr(III) loss from the N-lobe [11]; if a conformation exists in which the N-lobe Cr(III) site is distorted such that its EPR features resemble the C-lobe binding site, it would be unsurprising if the Cr(III) affinity of the site was also effected.

Herein are reported time-dependent spectroscopic studies of the binding and release of Cr(III) from human serum Tf that have been used to identify multiple different conformations of $Cr(III)_2$-Tf and their role in the binding and release of Cr(III) as well as discussion of their physiological relevance and re-interpretation of previous studies based on these findings.

2. Experimental

2.a. Materials

Iron-free human serum Tf was obtained from Aldrich (St. Louis, MO). Doubly deionized water was used throughout. All reagents were used as received unless otherwise noted. Cr(III) solutions were prepared by using $Cr(III)Cl_3 \cdot 6H_2O$. ApoTf concentrations were determined by using the extinction coefficient ($\boldsymbol{\varepsilon} = 9.12 \times 10^4\ M^{-1}\ cm^{-1}$) at 280 nm [8].

2.b. Methods

Dichromic-Tf was prepared as previously described [8, 11]. For binding studies, samples of apo-Tf were prepared immediately beforehand by dissolving the protein (0.5 mM) in a buffered solution (Hepes (4-(2-hydroxyethyl)-1-piperazineethanesulfonic acid), 100 mM, and HCO_3^-, 25 mM), and the pH of the resulting solution was adjusted to 7.5. A stock Cr(III) solution was prepared using $CrCl_3*6H_2O$ in the Hepes/bicarbonate buffer solution but without adjusting the pH to 7.5. An aliquot of the Cr(III) solution was added to the apo-Tf solution to achieve a Cr(III) concentration of 1 mM; addition of the $CrCl_3$ solution lowers the desired pH to 7.4. Addition of Cr(III) in this manner to the Tf solution prevents the formation of Cr(III)-carbonate precipitates. Aliquots of the $Cr(III)_2$-Tf solution were taken at prescribed intervals following the addition of the Cr(III) solution, and the aliquots were rapidly frozen for later EPR analysis.

To model the acidification of the endosome that triggers release of metal ions from Tf, $Cr(III)_2$-Tf in a buffered solution (Hepes, 100 mM) at pH 7.4 containing 25 mM bicarbonate at 37 °C was acidified by the addition of hydrochloric acid to pH 4.5 or 5.5. After time prescribed intervals, aliquots were removed and frozen for analysis by EPR spectroscopy. Similar studies were performed in the presence of chelating ligands that could potentially accelerate Cr(III)

release. Titrations of Cr_2-Tf with HCl were performed beforehand to determine the quantity of HCl to be added to achieve the desired pH. Dr. Molly Lockart provided assistance in acquisition and processing of the 3 pulse ESEEM. All results except ESEEM (Electron Spin Echo Envelope Modulation) measurements are presented as the average of at least triplicate experiments. Error bars in figures represent standard deviation.

2.c.. Instrumentation

Ultraviolet-visible spectra were obtained by using a Cary (Aligent, Santa Clara, CA) 500 or Beckman Coulter (Brea, CA) DU800 UV–visible spectrophotometer. Binding of Cr^{3+} to Tf was monitored at 245 nm. Solutions were continuously stirred at 37 °C using a 6 × 6 Peltier thermostatted multicell holder. Continuous wave (CW) EPR were measured on a Bruker (Billerica, MA) ELEXSYS E540 X-band spectrometer with an ER 4102 ST resonator. CW spectra were measured at 9.44 GHz with a microwave power of 21.1 mW by using a magnetic field modulation frequency of 100 kHz with an amplitude of 30 G. Spectra were taken at liquid nitrogen temperatures with a quartz insertion Dewar. Electron spin echo envelope modulation (ESEEM) spectra were measured using an ELEXSYS E680 EPR spectrometer (Bruker-Biospin, Billerica, MA) equipped with a Bruker Flexline ER 4118 CF cryostat. ESEEM measurements were made at 5 K both at 3375 G (337.5 mT) and at 2020 G (202.0 mT). Data were collected using a three pulse stimulated echo sequence, $\pi/2 - \tau - \pi/2 - T - \pi/2 - \tau + T -$ echo, where $\pi/2$ represents a 16 ns microwave pulse, and T and τ represent delays between the pulses. The pulse sequence was repeated at a rate of 1.25 kHz. The delay time τ was chosen to be 120 ns, a value that was optimal for both echo intensity and nuclear modulation. Spectra were processed in the Xepr software (Bruker Biospin, Billerica MD). Plots were made using Origin2018 (OriginLab, Northhampton MA).

2.d. Data Analysis

Data analysis, calculation of averages and standard deviations, and fitting of curves to the appropriate equations was performed by using SigmaPlot 11 (SPSS, Inc., Chicago, IL). The iterative curve fitting algorithm of SigmaPlot 11 uses the Marquardt-Levenberg algorithm to find the parameters of the independent variables that provide the best fit between the data and the equation.

CW EPR spectra processing and simulations were performed using the EasySpin package in MATLAB (Mathworks, R2017b) [12]. Polynomial fitting of the spectral baseline corrections was performed using Xepr software of the ELEXSYS. The g-values, g-strain, and weight of the simulated spectrum were fit using the "pepper" function in EasySpin [12].

3. **Results and Discussion**

Tf has been observed to undergo three distinct conformation changes during the binding of Cr(III) under physiological conditions, pH 7.4 and 25mM bicarbonate. The resulting phases can be distinguished by EPR and/or UV spectroscopies.

3.a. First phase/Formation of conformer 1

Human serum Tf and other forms of Tf prepared using traditional techniques have been described in detail; human serum Cr_2-Tf is noted to have a faint visible spectrum possessing a blue hue with low intensity visible maxima at 440 and 635 nm. These visible maxima have an intensity and wavelength that are typical of Cr(III) in pseudo-octahedral environments. While some electronic studies have been done with human serum Tf, most electronic studies have used conalbumin when investigating the metal binding behavior of transferrins. When titrating a conalbumin solution with Cr(III), a linear increase in the intensity of 435 and 610 nm maxima is

observed until two equivalents of Cr(III) are added; the increase in visible maxima continues after 2 equivalents of Cr(III) with a decreased linear slope. The behavior of the intensity change with added Cr(III) past 2 eq. of metal is indicative of Cr(III) binding in both metal binding sites until the two equivalents are reached followed by a slow increase due to added Cr(III) in solution or non-specifically adhered to the protein's surface [8]. The visible spectral region is useful in experiments in which the concentration of the protein and metal can be sufficient to get observable levels of absorbance, the low extinction value of the transitions (on the order of ~10 M^{-1} cm^{-1}) is prohibitive for using this region in submillimolar concentrations. However, transitions from the $\pi \rightarrow \pi^*$ band of the two tyrosine ligands in the binding sites of transferrin proteins are perturbed when a metal is bound (such as Cr(III)) [8]. These transitions are intense enough to allow for micromolar concentrations of the protein/metal to be used. During the addition of Cr(III), the intensity of bands at 245 nm and 295 nm increase upon addition of up to 2 equivalents of Cr(III); this behavior is consistent with the metal binding in both metal binding sites and is unaffected by non-specifically bound Cr(III). The intensity change in the bands is very pronounced and is reported by Tan and Woodworth at $\Delta\varepsilon$ to have a 245 nm of 38.7×10^3 ($\pm 2.8 \times 10^3$) M^{-1} cm^{-1} for 2 equivalents of Cr(III) binding to conalbumin at ambient bicarbonate concentration after 48 hours [13]. Electronic studies utilizing human serum Tf yield similar results [8]. An increase in the $\Delta\varepsilon$ at 245 nm is observed upon the addition of Cr(III) to a human serum Tf solution under similar conditions, although the change is less than the 38.7×10^3 ($\pm 2.8 \times 10^3$) M^{-1} cm^{-1} observed with conalbmuin. However, in both titration studies, whether at ambient or 25 mM bicarbonate, the initial slopes of $\Delta\varepsilon$/Cr are well under 19×10^3 M^{-1} cm^{-1} (1/2 the total change for 2 equivalents of Cr(III)). Furthermore, curves for the binding of chromic ions to Tf/conalbumin under 2 hours or as a function bicarbonate concentration do not reach a $\Delta\varepsilon$ of

$38.7 \times 10^3\ M^{-1}\ cm^{-1}$, yet the chromic ions have been shown to be tightly bound within this time frame [8]. These results indicate that the binding of the Cr(III) to Tf/conalbumin results in an initial change in $\Delta\varepsilon$ under $38.7 \times 10^3\ M^{-1}\ cm^{-1}$, followed by some slow processes that accounts for the remaining increase in the $\Delta\varepsilon$ until it reaches its maxima. Tan and Woodworth proposed that the deprotonation of a tyrosine residue is accompanied by a $\Delta\varepsilon$ at 245 nm of $\sim 10 \times 10^3\ M^{-1}\ cm^{-1}$ such that the staggered slopes in the binding curves could be explained by the initial rapid deprotonation/binding of a tyrosinate followed by a slow deprotonation/binding of a second tyrosinate [13].

The initial phase of binding of Cr(III) to Tf is complete in circa 15 min and gives rise to conformer **1** of the Cr(III)/Tf structure. This phase of Cr(III) binding is accompanied by the largest increase of $\Delta\varepsilon$ at 245nm of the three phases and is ascribed to the binding of Cr(III) to tyrosine residues of the binding pocket. This binding phase has previously been studied when exploring the synergistic effects of the bicarbonate anion [8]. The binding of the Cr(III) to Tf is first order with bicarbonate concentration; and at a bicarbonate concentration of 25 mM (the bicarbonate concentration in the human bloodstream) [14], the rate constants are 3.16 ± 0.13 and $0.189 \pm 0.003\ min^{-1}$ for the binding of Cr(III). This first phase is also accompanied by an increase of the $\Delta\varepsilon$ at 245nm which reaches a maxima of $\sim 24 \times 10^3\ M^{-1}\ cm^{-1}$.

EPR spectroscopy can also be used to observe the conversion of aqueous Cr(III) (added as an aliquot of solution of $CrCl_3$) to Cr(III) bound to conformer 1 of Tf. Upon dissolution of H_2O, $CrCl_3$ is first converted into its hydrolysis products; the aqueous mixture of products which has a symmetric feature at g~2 (Figure 4.2). As the EPR signal of aqueous Cr(III) diminishes, another feature at g~2 appears and is ascribed to the short-lived intermediate, conformation 1. The new feature peaks in intensity ~10 mins after the addition of $CrCl_3$ to the Tf

solution. The rate of growth of this feature matches the average rate of Cr(III) binding to Tf in physiological bicarbonate measured using ultraviolet spectroscopy within this time regime. The binding of Cr(III) to Tf has been shown to be stoichiometric 2:1 with Tf within this time regime [8]. These results indicate that after ~10 min the majority of Tf is present as this transient species with two bound Cr(III) and a prominent g~2 EPR feature.

A crystal structure of Fe(III)-Tf has been reported with Fe(III) bound in the N-lobe binding site with the protein still in the 'iron-free' open configuration [15]. The Fe(III) is bound to the two tyrosine ligands of the binding site, but the rest of the coordination sphere is completed by a nitrilotriacetate ligand, present due to the Fe(III) being added as a Fe^{3+}·NTA complex. The nitrilotriacetate anion is stabilized by H-bonds with nearby protein ligands, but not residues present in the anion binding pocket (i.e. the ligand is non-physiological and its size and shape likely contribute to the open conformation). This study presents two unique observations. First Fe(III) likely binds first to the two tyrosine ligands in the binding pocket (this is as supported by measuring H^+ release during Fe(III) binding to Tf in which two protons are detected to be released from the protein early in metal binding [16]). Second, a metal can bind in the active site with the protein retaining the open conformation. ESEEM studies were conducted on Cr(III) Tf at various times (5, 60, and 1440 mins after the addition of Cr(III)) Apo-Tf solutions that had been incubated with Cr(III) for 5, 60, and 1440 min were rapidly frozen for ESSEM analysis; and at each time point, ^{14}N coupling between the Cr(III) and the protein is present. This coupling presumably arises from the interaction between the Cr(III) and the imidazole ring of the histidine ligand. At 5 min of Cr(III) incubation with Tf the primary conformer will be conformer 1; the ^{14}N coupling indicates for conformer 1 the metal is bound to histidine residues of the metal binding site of the protein (Figure 4.3). As previous studies have

demonstrated, the first step in metal binding should be the binding of the tyrosine ligands followed by the binding of the Asp and His ligands [17]; thus, if the His ligand is already bound, the Tyr ligands should be bound as well. These results demonstrate that conformer 1 does not arise from incomplete binding of the metal in the binding site (as the histidine residue is present at all points), rather that conformation 1 likely differs from other confirmations in much longer range structural differences.

Recent efforts to crystallize Cr(III)-containing Tf have been successful; the X-ray structure of human serum Tf with Cr(III) bound in the C-lobe of Tf has been reported [18]. The protein was prepared as Cr_2-Tf and crystallized in a solution containing malonate using the hanging drop method. The malonate anion displaced the synergistic bicarbonate in the anion binding pocket. The N-lobe lacking a metal center was in the open conformation as expected of a metal free Tf lobe. While not an accurate physiological analogue due to the presence of malonate in the anion binding pockets, the Cr(III) containing Tf structure does give some insights into its binding and behavior of the metal. Fe(III)- and Ti(IV)-containing Tf have also been crystallized under similar conditions yielding nearly identical structures [19, 20]. The binding sites of Tf with Cr(III) or Fe(III) are virtually superimposable demonstrating that the binding of Cr(III) does not differ significantly from that of Fe(III). Furthermore, the bond distances between Cr(III) and the ligands are typical for O/N-Cr(III) bonds (with the exception of one tyrosine at 2.27 Å, which is only slightly longer than typical) demonstrating no significant distortions within the binding site that might explain the faster rate of loss during acidification of Fe(III) compared to that of Cr(III) in the N-lobe.

3.b. Second Phase/Formation of Conformer 2

As the feature at g~2 of conformer 1 disappears, a new EPR feature at g = 5.42 appears. The g = 5.42 feature reaches a maximum at ~120 min after the initial addition of Cr(III), and the growth of this EPR feature coincides with an increase of $8 \times 10^3\ M^{-1}\ cm^{-1}$ in the ultraviolet absorption at 245 nm (Figure 4.6). The EPR features and changes in $\Delta\varepsilon_{245nm}$ are ascribed to conformational changes within the protein's structure that perturb at least one tyrosine residue that gives rise to a new product, conformer 2. These changes are suspected to be from the local environment around the binding pocket or otherwise nearby the Cr(III) centers due to both spectroscopies being sensitive towards the binding sites. These changes are likely movement of the protein to accommodate the metal in the binding site and it is unlikely that they are due to large global protein changes on the magnitude of open to closed conformational shifts.

Previous studies have attributed the EPR feature at g ~ 5.42 exclusively to the weaker C-terminal metal binding site of Tf [9, 11, 21]. This is accurate only for the final conformation of Cr_2-Tf that exists after adequate incubation in sufficient bicarbonate concentration. In early stages of incubation of Cr(III) with Tf, the EPR feature at g ~5.42 belongs to both Cr(III) centers at both metal binding sites; the feature decays with time corresponding with an increase in features corresponding to conformer 3 (Figure 4.4 and 4.5). Conformer 2's unique feature of possessing two Cr(III) ions with only one EPR feature at g~5.42 explains previously reported results. Heat-treated and glycated human serum Tf 24 hours after the addition of Cr(III) display only one EPR feature at g=5.41; after 48 hours the 'typical' Cr_2-Tf EPR spectrum with features at g=5.14 and g=5.64 were observed [11]. Bovine serum Tf prepared in the presence of two equivalents of Cr(III) in 25 mM HCO_3^- generates only one sharp feature at g ~5.4 after 48 hrs of incubation unlike human serum Tf which displays three features at g ~ 5.08, 5.42, and 5.66

despite all Cr(III) centers possessing identical ligands [22]. ESSEM studies on Tf incubated with Cr(III) at varying time points shows nitrogen coupling with the Cr(III) center (presumably with the imidazole group from the histidine residue in the binding pockets) indicating that conformer 2 is in the 'closed' state of the protein (Figure 4.3).

3.c. Third Phase/Formation of Conformer 3

The EPR feature at g~ 5.4 reaches a maxima ~12 hours after Cr(III) addition to Tf, after which the feature decays with a rate of loss of the g~5.4 feature that matches the rate of appearance of two new EPR features at g ~5.6 and g~5.1 which correspond to the formation of a new conformer of Cr_2-Tf, conformer 3. After sufficient time, conformer 3's EPR features match those of the 'typical' EPR spectra of $Cr(III)_2$-Tf incubated for 48 hours in 25 mM HCO_3^- or that of Cr_2-Tf incubated for two weeks under ambient bicarbonate. The decay in the g~5.42 feature and growth of the g~5.1 and 5.6 features also coincides with a decrease in the ultraviolet extinction coefficient at 245 nm, suggesting movement about at least one of the binding sites that perturbs a tyrosine ligand.

$Cr(III)_2$-Tf has been generated previously in ambient bicarbonate concentrations by allowing the Cr(III) and apo-Tf to incubate for two weeks [21]. While this process takes significantly longer, the end result is Cr_2-Tf that has an identical CW-EPR spectrum to that Cr_2-Tf prepared in 25 mM HCO_3^- over 24 hrs, i.e. conformer 3. A difference exists between the electronic spectra of human serum Tf with Cr(III) in 25 mM HCO_3^- buffer and conalbumin with Cr(III) in which the observed a maximum molar absorptivity at 245 nm of 24×10^3 M^{-1} cm^{-1} for conformer 3 (24 hours following the addition of Cr(III)) and the reported values for Cr(III) added to conalbumin at [38.7×10^3 ($\pm 2.8 \times 10^3$) M^{-1} cm^{-1}]. While the structure of the two proteins are similar, the sequence of the proteins are not identical which may explain some of the absorptivity

differences. Molar absorptivity values varied depending on what metal type was binding ranging from [38.7×10^3 ($\pm 2.8 \times 10^3$) M^{-1} cm^{-1}] to [19.2×10^3 ($\pm 2.2 \times 10^3$) M^{-1} cm^{-1}] for the study with conalbumin such that the absorptivity reported for human serum Tf bound with Cr(III) is similar to other metals bound with conalbumin [13].

The ligands binding the Cr(III) center of conformer 3 are speculated to be identical to those from conformers 1 and 2. ESEEM studies reveal for three distinct time points in which conformer 1, 2, or 3 are the dominate species that prominent nitrogen coupling to the Cr(III) center can be observed. Unless Cr(III) binding to Tf differs drastically from Fe(III), binding to tyrosine ligands precedes the binding of the HIS/ASP residues such that if nitrogen coupling can be observed, the sites should be in a closed state with the four protein-provided ligands in place [16]. In the case of Fe(III), stop flow fluorescence studies have been used to identify four distinct species involved in Fe(III) binding [23]. The first rapid step is the binding of Fe(III) simultaneously with bicarbonate in the C-terminal binding site of Tf and occurs ~ 0.1 second after the addition of Fe(III). The second step occurs with the loss of two protons, which is ascribed to the to the binding of the phenolate groups of the two tyrosines; this step occurs in the course of 1 second. The third change is a conformational shift involving a single proton loss and is complete in ~ 400 seconds, this third change triggers rapid Fe(III) binding by the N-terminal site due to improved cooperativity between the lobes due to the structural shifts. The last, slowest, step occurs over 3,000 seconds and is a global conformation change resulting in the typical ‘closed’ conformation Fe_2-Tf. These process when compared with Cr(III) binding studies suggest that large inital extinction coefficient growth observed in the Cr(III)-Tf UV spectra encompasses the first several phases observed in Fe(III) binding. This is also supported by a previous study which demonstrated the first order dependence on bicarbonate concentration for

the initial phase of Cr(III) binding to Tf [8]. The final slow step for $Cr(III)_2$-Tf in which the protein assumes its final conformation appear to occur two distinct phases both of which are slower than observed for $Fe(III)_2$-Tf.

Other metals have been observed to bind to Tf in ways distinct from Fe(III), but they are useful to compare with Cr(III) binding to Tf. Co(III) has been demonstrated to bind very rapidly (~3 milliseconds) to Tf (when pre-assembled with a carbonate as a Co(III)-carbonate complex), which is followed by three slower processes comparable to those observed for $Cr(III)_2$-Tf [24]. The second process is relatively rapid (~50 s) and corresponds to the binding of the two tyrosinates; however, the final third and fourth process are slow, occurring over 48 hrs. The third process takes over 3,000 seconds with the final fourth process taking significantly longer. These process are suspected to encompass the binding of a second Co(III) to the N-site, proton loss accompanying the binding, and conformational changes throughout the protein; however, these two phases are resolved poorly and with only a single technique, fluorescence emissions spectroscopy [24]. The rates of the final two process appear independent of Tf concentration (within the uncertainty of the experiment) and the slower time frames resemble those observed for Cr(III)-Tf binding.

3.d. Release of Cr(III) from Transferrin

Cr(III) has been shown to be released from $Cr(III)_2$-Tf at pH 4.5 and 5.5, simulated endosomal conditions [11]. The release of Cr(III) proceeds rapidly from the C-terminal metal binding site, while the release of Cr(III) from the N-terminal site proceeds much more slowly. The release from the N-terminal site was observed to be accelerated with the addition of various chelating ligands; however, the rate of Cr(III) loss appeared independent of the identity of the ligand within experimental error, suggesting the ligands may be displacing the synergistic

bicarbonate rather than coordinating with the Cr(III) center. When $Cr(III)_2$-Tf was bound to Tf receptor, the rate of Cr(III) loss was greatly accelerated to fit within the time for the frame of endocytosis cycle. Besides the loss of $Cr(III)_2$-Tf features, new EPR features appear from the non-specific binding of Cr(III) to Tf. These EPR features are also generated after the addition of Cr(III) to apoTf at pH 5.5, indicating they are Cr(III) nonspecifically bound to Tf rather than at a metal binding site. The current binding study begs the question if conformation changes occur during Cr(III) release from Tf similar to those of its binding. If the release could occur at neutral pH, one would expect the reverse of the binding process to resemble the release process; however, the release of Cr(III) from Tf at acidic pH clearly differs from the binding process.

While the half-life of human serum Tf in the blood stream is 7.6 days, the turnover half-life of $Fe(III)_2$-Tf is only 1.7 hours (the turnover corresponds to $Fe(III)_2$-Tf being internalized and the apo-Tf recycled back into the bloodstream). Given the turnover rate of metal bound Tf, 1.7 hr, the conformer with greatest biological relevance would be conformer 2 ; conformer 3 (with EPR features at g~ 5.2, 5.4, and 5.6) forms too slowly for it to be of significance *in vivo*. This is important as conformer 3 is the product after 24 or more hours of incubation and thus possesses limited physiological relevance given holo-Tf turnover rate despite being the species traditionally utilized in Cr_2-Tf studies [4, 7, 8, 11]. Conformer 1 does have potential *in vivo* relevance given its short lifetime; however, the predominate species will be conformer 2. The EPR feature characteristic of conformer 2 is also nearly identical in appearance and g-value to bovine $Cr(III)_2$-Tf bound to TfR [11], which suggests both species could have similar conformations. Both of these two newly identified conformations of $Cr(III)_2$-Tf are of physiological significance given the short half-life of holo-Tf, and previous results utilizing conformer 3 of Cr_2-Tf should be carefully considered in light of these new findings.

Given the potential physiological significance of conformer 2, the loss of Cr(III) from conformer 2 was examined as it has not been studied previously. Loss of Cr(III) from $Cr(III)_2$-Tf has only been studied using conformer 3 [7 11]. The loss of Cr(III) from Tf can readily be followed using both EPR and UV spectroscopies (Figure 4.8), and these techniques were used previously in tandem to investigate loss of Cr(III) from Tf incubated for 1 day (primarily conformer 3). Rapidly (<15 minutes), the C-terminal Cr(III) from Tf is loss, as signified by the loss of the C-terminal Cr(III) EPR feature at g~ 5.4 with the concomitant loss of half the UV absorption intensity at 245 nm. The slower loss of Cr(III) from the N-lobe of Tf follows with the decay of the EPR features at g~5.1/5.6 and continued loss of absorption intensity. The loss of these Cr(III) EPR features coincides with the appearance of new features between g 5-6 corresponding to Cr(III) non-specifically bound to Tf. The loss of Cr(III) from Cr_2-Tf prepared after incubation for only 1 hr (primarily conformer 2 although some conformer 3 is present) was investigated in a similar manner as this preparation should most closely represent the *in vivo* species. Loss of Cr(III) was initiated by addition of HCl to pH 5.5 which resulted in the rapid loss of the Cr(III) EPR feature at g~5.4 (primarily contributed by conformer 2) as well as the eventual loss of Cr(III) EPR features, g~5.4/5.6, associated with conformer 3 which were lost at a similar rate observed in other experiments; eventually the four EPR features associated with Cr(III) non-specifically bound to Tf appear (Figure 4.9). The loss of the EPR features at g~5.4 and g~5.2/5.6 were fit to a monophasic exponential loss equation to obtain the first order rate constants of 0.113 and 0.0044 min^{-1} respectively (Figure 4.10). These rate constants correspond to half-lives of 5.21 and 1.6×10^2 min, which are comparable to rates of features loss from $Cr(III)_2$-Tf prepared by incubating Cr(III) and Tf for 2 d at 37 °C pH 7.4 in 25 mM bicarbonate [11]. The rate of loss upon acidification for both Cr(III) in conformer 2 appears similar to the rate

of loss of Cr(III) from the weak binding site of traditionally prepared Cr_2-Tf. Thus, the conformation about the Cr(III) binding sites of conformer 2 (which generates EPR feature g~5.4) allows for rapid loss of Cr(III) upon acidification than the conformation about the N-site in conformer 3. Neither loss is nearly as rapid as loss of Cr(III) from the $Cr(III)_2$-Tf and TfR complex with a half-life of 0.242 min [11].

The g ~ 2 feature of conformer 1 notably is generated shortly after the addition of Cr(III) to apo-Tf is not observed following the acidification of Cr_2-Tf from any preparation. As mentioned before, the mechanism of Cr(III) loss due to acidification is certainly not the reverse the binding process observed at pH 7.4 such that the absence of conformer 1 is not unexpected. The loss of approximately half of the absorption intensity at 245 nm following the acidification Cr_2-Tf indicates the loss of Cr(III) binding to a tyrosine residue coincides with the loss of EPR feature ~5.4. Thus, in the case of acidification, loss of EPR features arises from loss of Cr(III) from the binding site and does not arise from the interconversion of conformations. Due to the short life span of conformer 1 and the significant amounts of aqueous Cr(III)/conformer 2 species present throughout its life span, no attempts were made to study the release of Cr(III) from conformer 1 upon acidification.

4. Conclusion

The formation of $Cr(III)_2$-Tf is more complicated than originally thought and the various conformers that are generated during Cr(III) binding can be observed by EPR and UV spectroscopy. UV spectroscopy can be used to determine the rate of formation for the first conformer, yet due to the overlapping EPR features and the inability to quantitatively determine the concentration of each species various times, the rate of formation of conformer 2 and conformer 3 were not resolved using these spectroscopic techniques. The distribution of the

various conformers as a function of time was estimated using the integrated rate equation for three consecutive irreversible reactions using $k^1 = 2.4$, $k^2 = 4.3 \times 10^{-2}$, and $k^3 = 1.5 \times 10^{-3}$ min^{-1} (Figure 4.7).

When considering which conformer of Cr(III)-Tf is the most physiologically relevant, how long the Cr(III) will circulate with Tf following the initial binding of the metal to the protein in the bloodstream must be considered. Cr(III)'s fate after being injected into the bloodstream of rats has been followed using radiolabeled Cr(III) [4, 5]. The results show that >50% of Cr(III) accumulates in tissue (primarily liver and skeletal muscle) 30 minutes after injection of Cr(III) in the form $^{51}Cr(III)_2$-Tf. Approximately ~90% of the injected Cr(III) is lost from the bloodstream in a rapid process at a rate of ~0.084 min^{-1} (half-life ~12 minutes) and $^{51}Cr(III)$ isolated from hepatocytes elutes in a band corresponding to the molecular weight of Tf, ~80 kDa [4]. Immunoblotting of the content of those bands also indicates the presence of Tf [4]. When Cr_2-Tf is co injected with insulin the rate of movement of Cr(III) into tissues is enhanced suggesting a Tf-mediated process [5]. Cr_2-Tf stored at elevated temperature or glycated diminishes Cr(III) accumulation in tissues resulting in a greater accumulation in the bloodstream. Co-injection of insulin with the heat treated or glycated Cr_2-Tf enhances Cr(III) accumulation in liver tissue only. This is in contrast with freshly prepared Cr_2-Tf coinjected with insulin which lead to elevated Cr(III) levels in both muscle and liver tissue. Thus, Cr(III) appears to be transported from the bloodstream to the tissues by Cr_2-Tf, and this movement from blood stream to tissue occurs with a lifetime of the Tf-bound Cr(III) that is similar to that of Tf-bound Fe(III); that is to say, on average, the time in which Cr(III)-Tf will circulate is only ~ 60 min such that confirmations that take significantly longer to form are of limited physiological relevance.

Conformer 3 should be considered of limited physiological relevance due to the long incubation times (>720 min) required to form significant amounts of it.

EPR and electronic spectroscopic studies have revealed that the binding of Cr(III) to apo Tf has different phases than the binding of Fe(III) to Tf. The addition of Cr(III) to apo-Tf in the presence of 25 mM HCO_3^- results in a series of conformational changes after the initial binding of Cr(III). These different conformations have distinct spectroscopic features and, vary in the rate of Cr(III) loss from the metal-protein complex once acidified. The rate of formation of these separate conformers is also important given the life time of Cr(III)-Tf in the bloodstream is too short for significant amounts of conformer 3, the equilibrium product and one most commonly utilized in Cr-Tf studies, to form. Additionally, conformer 2 has an enhanced rate of loss of Cr(III) from Tf compared to conformer 3; this is presumably through structural differences about the binding site, which result in the differing spectroscopic features. The differences in metal loss behavior between the different conformations emphasis the importance of knowing which conformation of Tf is being utilized in a study for properly interpreting the results.

REFERENCES

1. Vincent, J. B.; Love, S. The binding and transport of alternative metals by transferrin *Biochim. Biophys. Acta.* 2012, *1820*, 362

2. Baker, E. N. Structure and reactivity of transferrins *Adv. Inorg. Chem.* 1994, 389

3. Hopkins, L. L.; Schwarz, K. Chromium (III) binding to serum proteins, specifically siderophilin *Biochim. Biophys. Acta.* 1964, *90*, 484

4. Clodfelder, B. J.; Vincent, J. B. The time-dependent transport of chromium in adult rats from the bloodstream to the urine *J. Biol. Inorg. Chem.* 2005, *10*, 383

5. Clodfelder, B. J.; Emamaullee, J.; Hepburn, D. D.; Chakov, N. E.; Nettles, H. S.; Vincent, J. B. The trail of chromium(III) in vivo from the blood to the urine: the roles of transferrin and chromodulin *J. Biol. Inorg. Chem.* 2001, *6*, 608

6. Clodfelder, B. J.; Upchurch, R. G.; Vincent, J. B. A comparison of the insulin-sensitive transport of chromium in healthy and model diabetic rats *J. Inorg. Biochem* 2004, *98*, 522

7. Levina, A.; Nguyen Pham, T. H.; Lay, P. A. Binding of Cr(III) to transferrin could be involved in detoxification of dietary chromium(III) rather than transport of an essential trace element. *Angew. Chem. Int. Ed*. 2016, 55, 8104

8. Deng, G.; Wu, K.; Cruce, A. A.; Bowman, M. K.; Vincent, J. B. Binding of trivalent chromium to serum transferrin is sufficiently rapid to be physiologically relevant *J. Biol. Inorg. Chem.* 2015, *143*, 48

9. Harris, D. C. Different metal-binding properties of the two sites of human transferrin *Biochemistry* 1977, *16*, 560

10. Ainscough, E. W.; Brodie, A. M.; Plowman, J. E.; Bloor, S. J.; Loehr, J. S.; Loehr, T. M. Studies on human lactoferrin by electron paramagnetic resonance, fluorescence, and resonance raman spectroscopy *Biochemistry* 1980, *19*, 4072

11. Edwards, K. C.; Kim, H.; Vincent, J. B. Release of trivalent chromium from serum transferrin is sufficiently rapid to be physiologically relevant *J. Inorg. Biochem* 2020, *202*, 110901

12. Stoll, S.; Schweiger, A. EasySpin, a comprehensive software package for spectral simulation and analysis in EPR *J. Magn. Reson.* 2006, *178*, 42

13. Tan, A. T.; Woodworth, R. C. Ultraviolet difference spectral studies of conalbumin complexes with transition metal ions *Biochemistry* 1969, *8*, 3711

14. Vincent, J. B.; Edwards, K. C. The absorption and transport of chromium in the body. *The Nutritional Biochemistry of Chromium(III),* 3rd; Vincent, J. B.; Elsevier, Amsterdam 2019, 129

15. Mizutani, K.; Yamashita, H.; Kurokawa, H.; Mikami, B.; Hirose, M. Alternative structural state of transferrin: the crystallographic analysis of iron-loaded but domain-opened ovotransferrin N-lobe *J. Biol. Inorg. Chem.* 1999, *274*, 10190

16. Thorstensen, K.; Romslo, I. A mechanism for iron uptake by transferrin *Biochem.* 1990, *271*, 1

17. Chahine, J.-M. E.; Fain, D. The mechanism of iron transferrin interactions uptake of the iron nitrilotriacetic acid complex *Dalton Trans.* 1993, 20, 3137

18. Petersen, C. M.; Edwards, K. C.; Gilbert, N. C.; Vincent, J. B.; Thompson, M. K. X-ray structure of chromium(III)-containing transferrin: first structure of a physiological Cr(III)-binding protein *J. Inorg. Biochem* 2020, *210*, 111101

19. Tinoco, A. D.; Saxena, M.; Sharma, S.; Noinaj, N.; Delgado, Y.; Quiñones González, E. P.; Conklin, S. E.; Zambrana, N.; Loza-Rosas, S. A.; Parks, T. B. Unusual synergism of transferrin and citrate in the regulation of Ti(IV) speciation, transport, and toxicity. *J. Am. Chem. Soc.* 2016, *138*, 5659

20. Yang, N.; Zhang, H.; Wang, M.; Hao, Q.; Sun, H. Iron and bismuth bound human serum transferrin reveals a partially-opened conformation in the N-lobe *Sci. Rep.* 2012, *2*

21. Aisen, P.; Aasa, R.; Redfield, A. G. The chromium, manganese, and cobalt complexes of transferrin *J. Biol. Inorg. Chem.* 1969, *244*, 4628

22. Deng, G.; Dyroff, S. L.; Lockart, M.; Bowman, M. K.; Vincent, J. B. The effects of the glycation of transferrin on chromium binding and the transport and distribution of chromium in vivo *J. Inorg. Biochem.* 2016, *164*, 26

23. Harris, W. R. Anion binding properties of the transferrins implications for function *Biochim. Biophys. Acta.* 2012, *1820*, 348

24. Chikh, Z.; Hémadi, M.; Miquel, G.; Ha-Duong, N. T.; El Hage Chahine, J. M. Cobalt and the iron acquisition pathway: competition towards interaction with receptor 1 *J. Mol. Biol.* 2008, *380*, 900

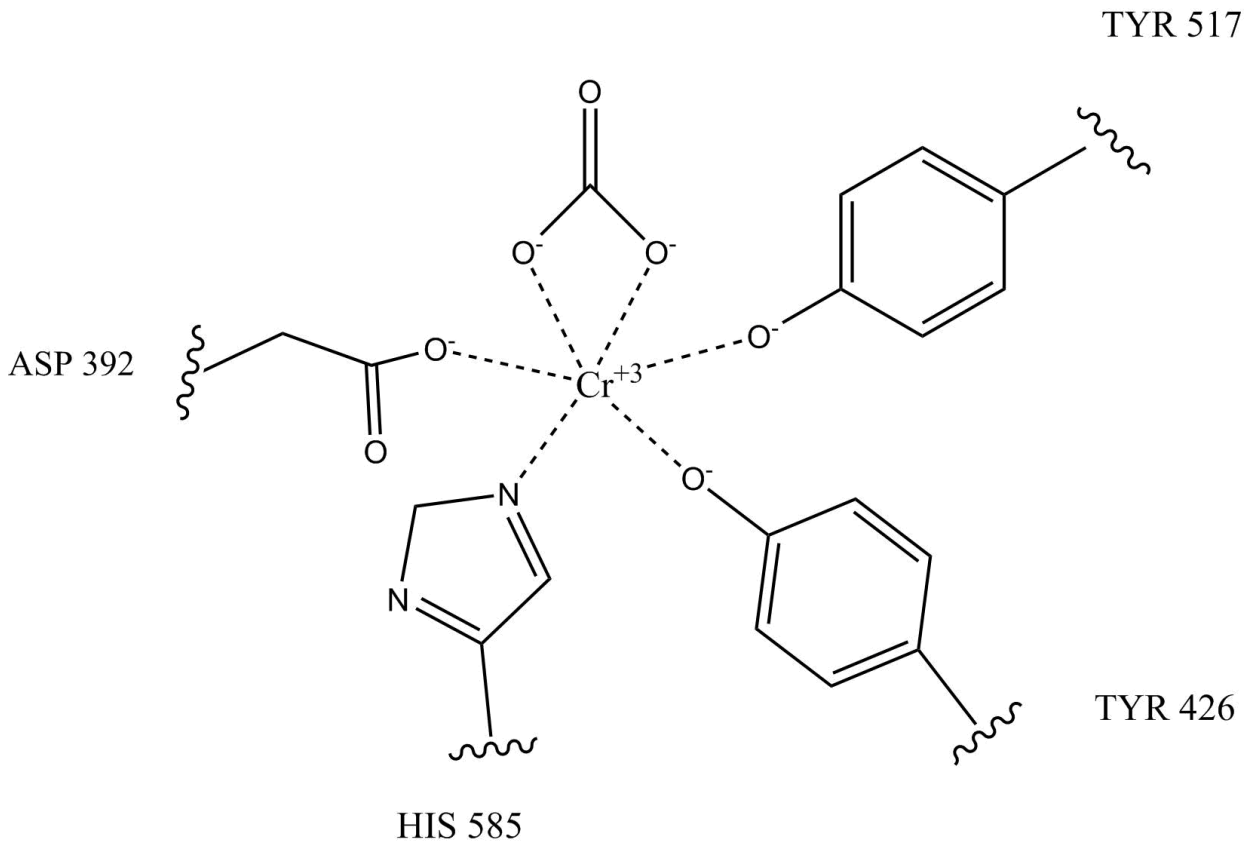

Figure 4.1. Proposed Cr(III) ligation in the C-terminal lobe metal-binding site of Tf. Numbering follows the sequence of human serum Tf.

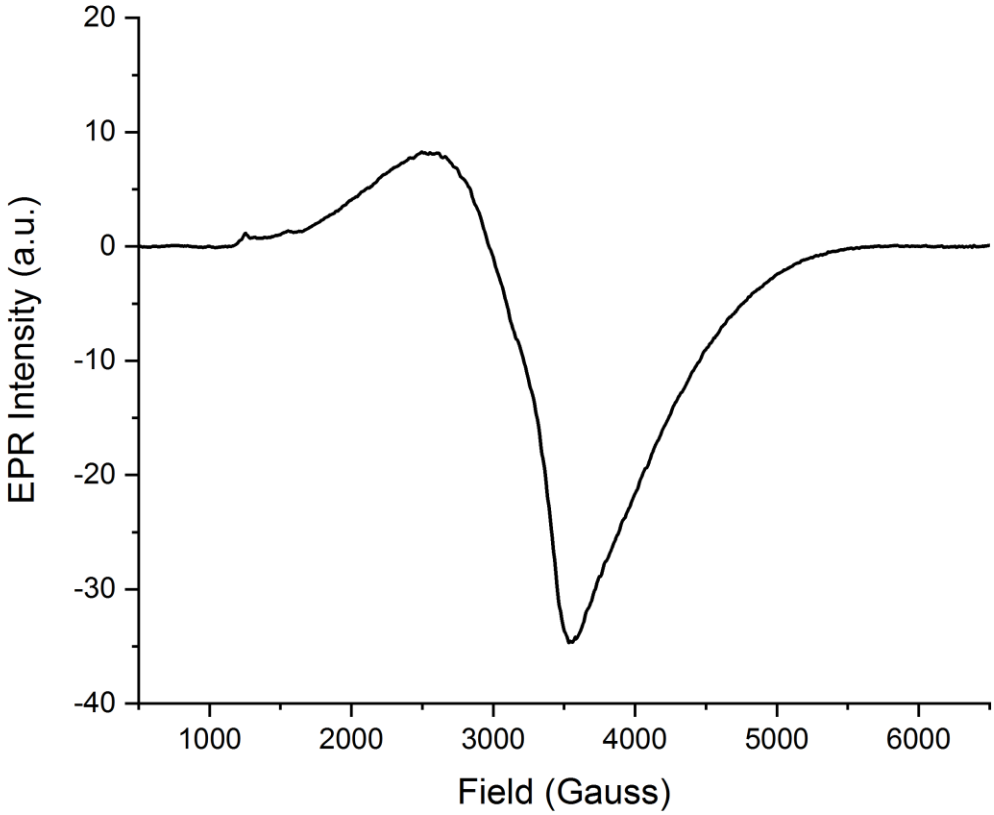

Figure 4.2. EPR spectrum of $Cr(III)_2$-Tf 5 min after addition of Cr(III) to apoTf in 100 mM HEPES with 25 mM HCO^{3-}, pH 7.4, at 37 °C. The major feature at g ~ 2 (~3500 G) corresponds primarily to conformer **1** of $Cr(III)_2$-Tf. A trace of the feature from conformer **2** at g ~ 5.4 (~1200 G) can also be observed.

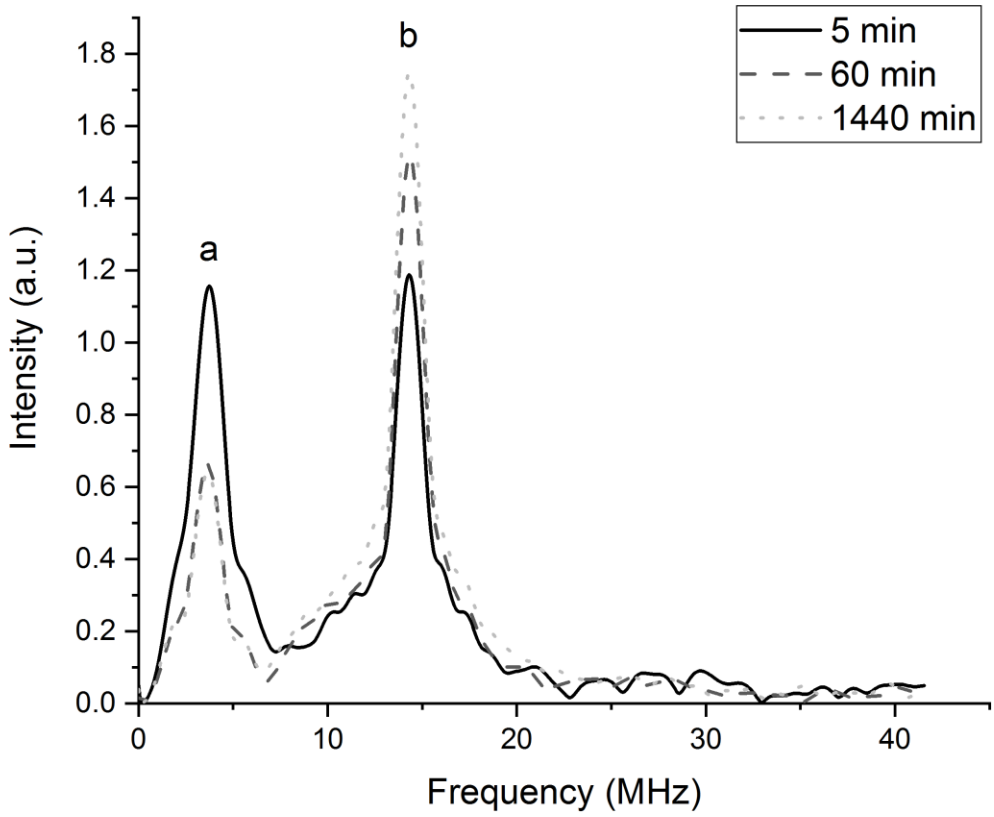

Figure 4.3. Three-pulse ESEEM spectra of apo-Tf incubated with 2.0 equivalents of Cr(III) at 5, 60, and 1440 min following the addition of Cr(III). a - Feature at 4 MHz corresponds to coupling between ^{14}N in the vicinity of the Cr(III). b - Feature at ~15 MHz corresponds to coupling between Cr(III) and nearby ^{1}H's. The intensities of these spectral features depend on the tau used during measurement.

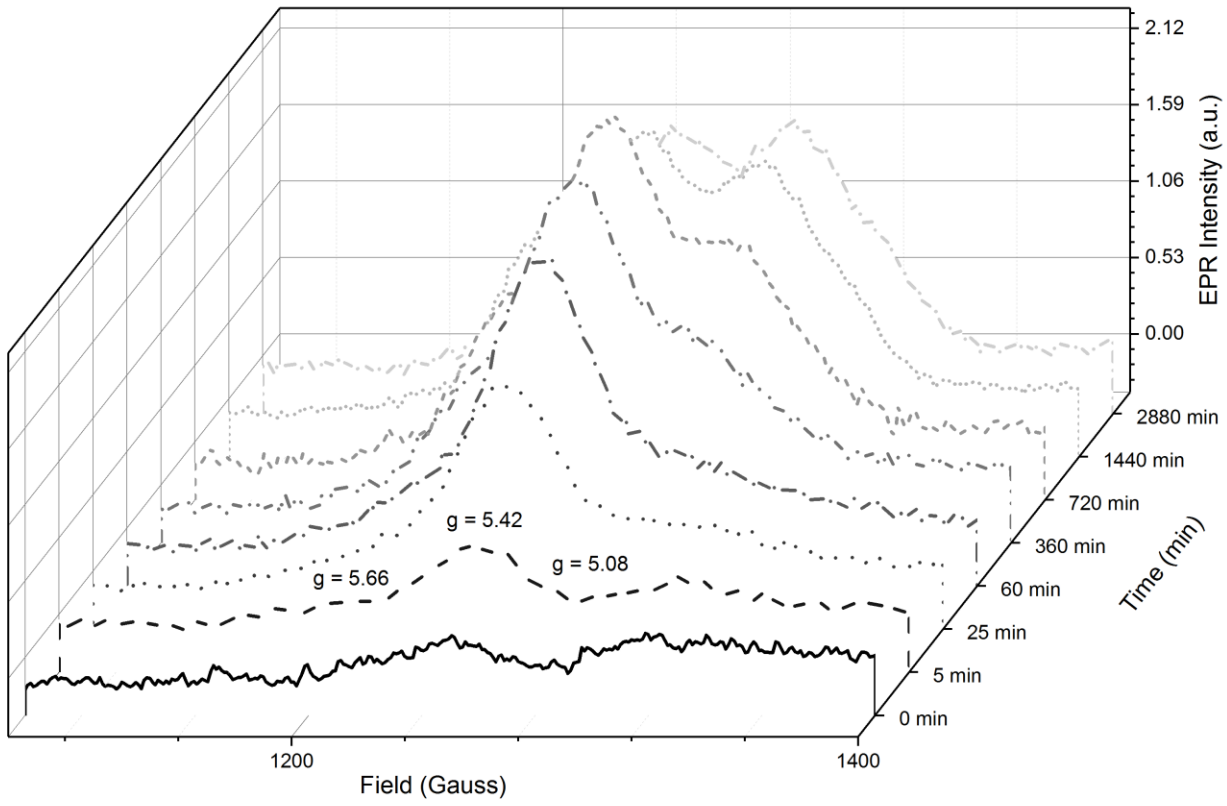

Figure 4.4. EPR spectra at time intervals after the addition of Cr(III) to apoTf in 100 mM HEPES buffer with 25 mM HCO_3^-, pH 7.4, at 37 °C.

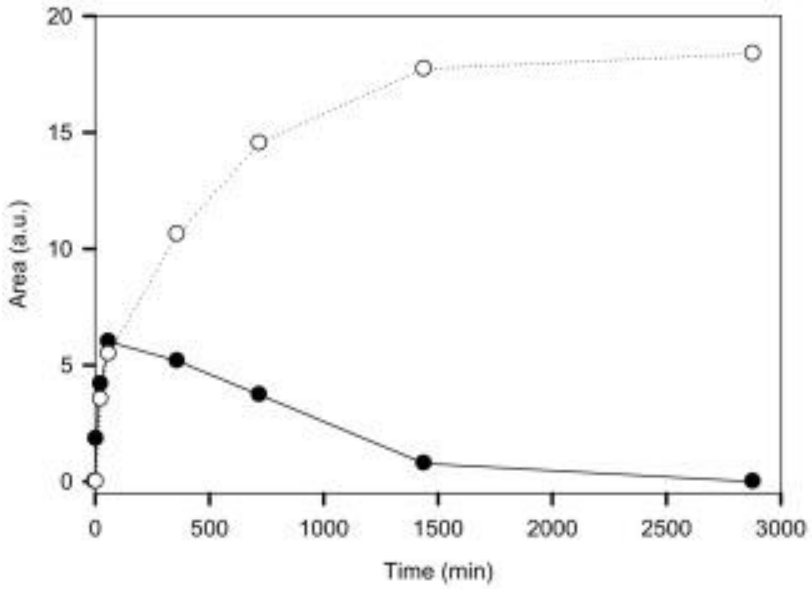

Figure 4.5. Changes in the amplitude of the EPR features from conformer **2** (solid circles and line) and conformer **3** (open circles and dashed line) of $Cr(III)_2$-Tf as a function of time.

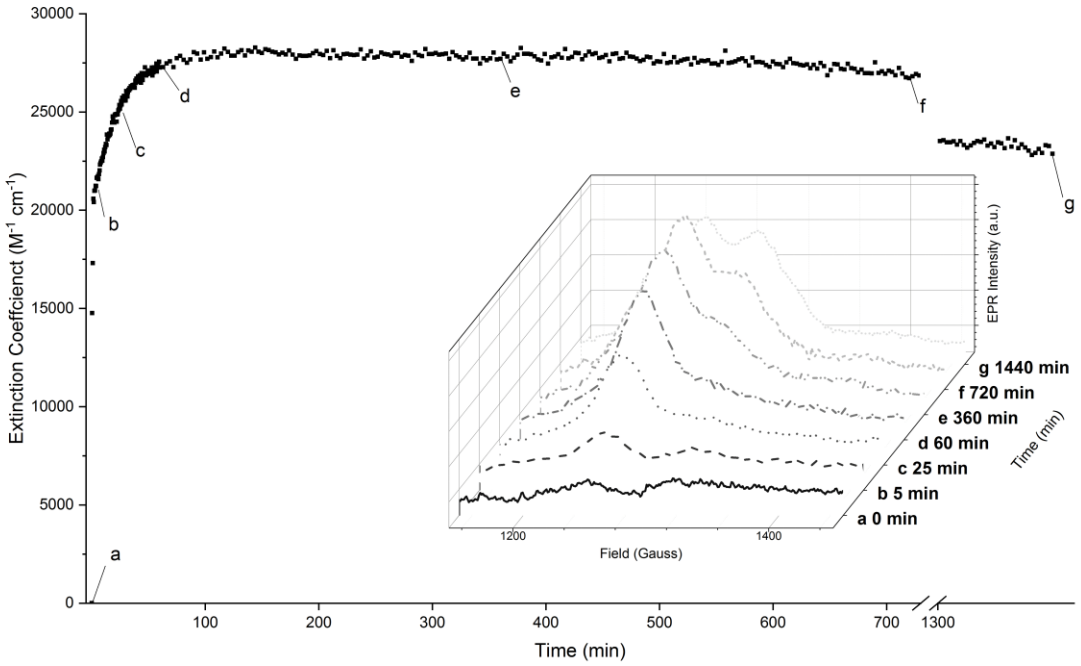

Figure 4.6. Change in extinction coefficient at 245 nm as a function of time corresponding to the formation of conformations of $Cr(III)_2$-Tf following the addition of Cr(III) to apoTf in 100 mM HEPES with 25 mM HCO_3^-, pH 7.4, at 37 °C. Inset: EPR spectra of aliquots were taken at prescribed intervals concurrent with the UV measurements.

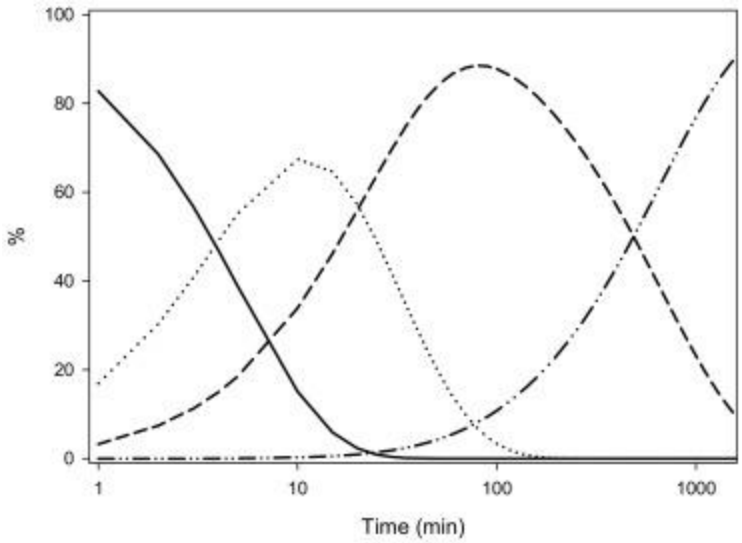

Figure 4.7. Simulated distribution with time of apoTf and conformations of $Cr(III)_2$-Tf species following the addition of Cr(III) to apoTf. Solid line – apoTf; dotted line – conformer **1**; dashed line – conformer **2**; and dotted and dashed line – conformer **3**.

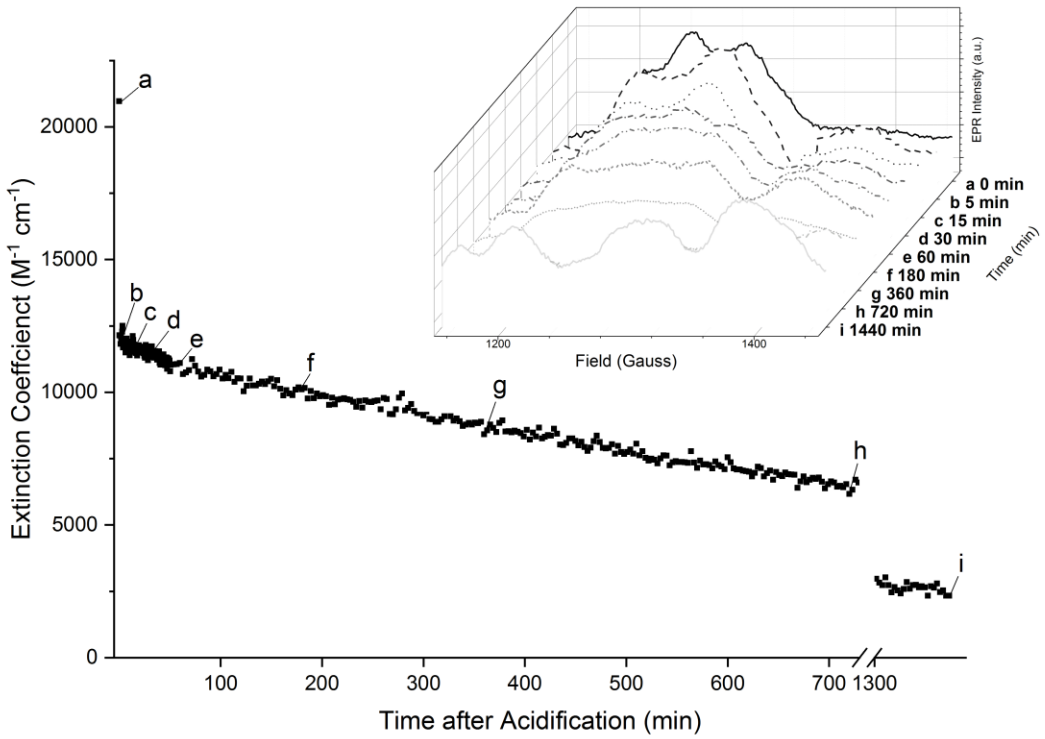

Figure 4.8. Decrease of the extinction coefficient at 245 nm of Cr_2-Tf blanked against apo-Tf following lowering of pH to pH 5.5. Acidification initiated after 24 h of Cr(III) incubation with Tf (2 Cr(III):1Tf) at pH 7.4, 37 °C. Inset: EPR spectra of aliquots were taken at prescribed intervals concurrent with the UV measurements.

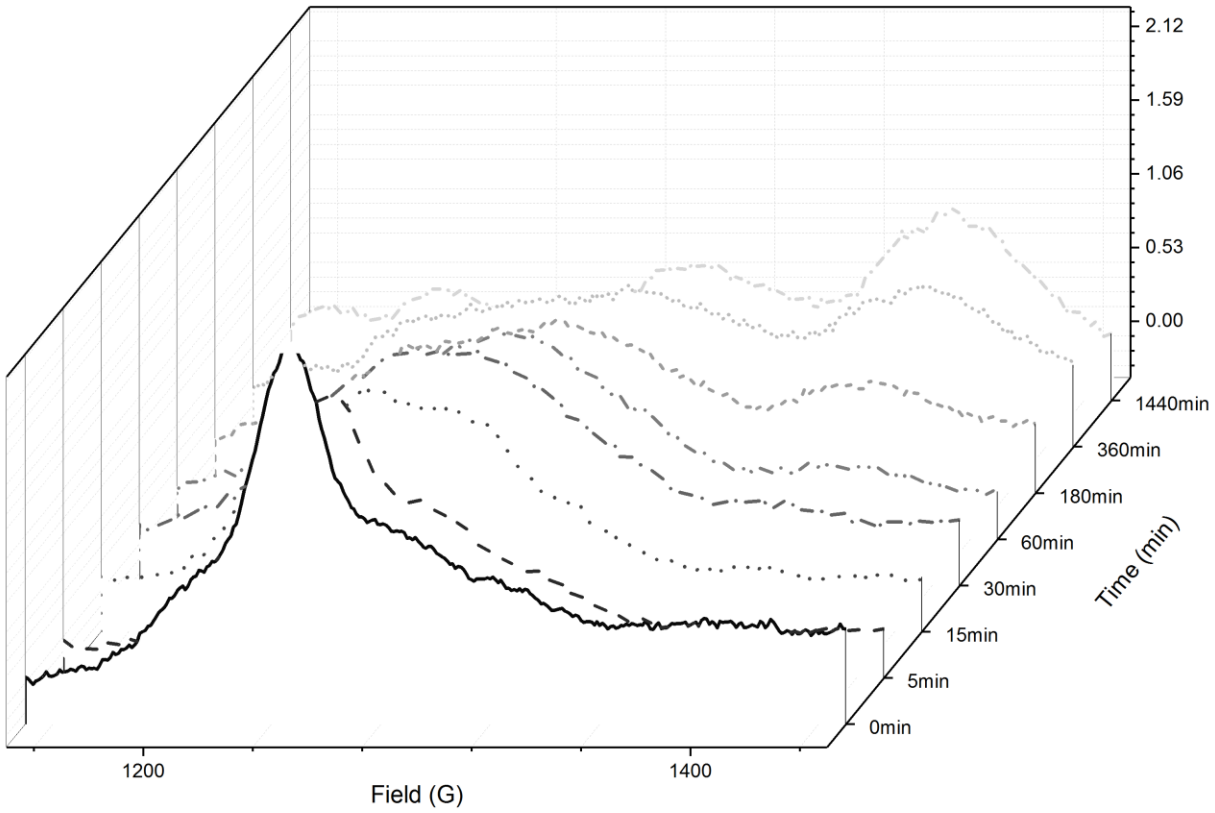

Figure 4.9. EPR spectra of $Cr(III)_2$-Tf (formed by incubation of Cr(III) and Tf for 60 min) in 100 mM HEPES with 25 mM HCO_3^-, pH 7.4, at 37 °C at time intervals following the lowering of pH to 5.5.

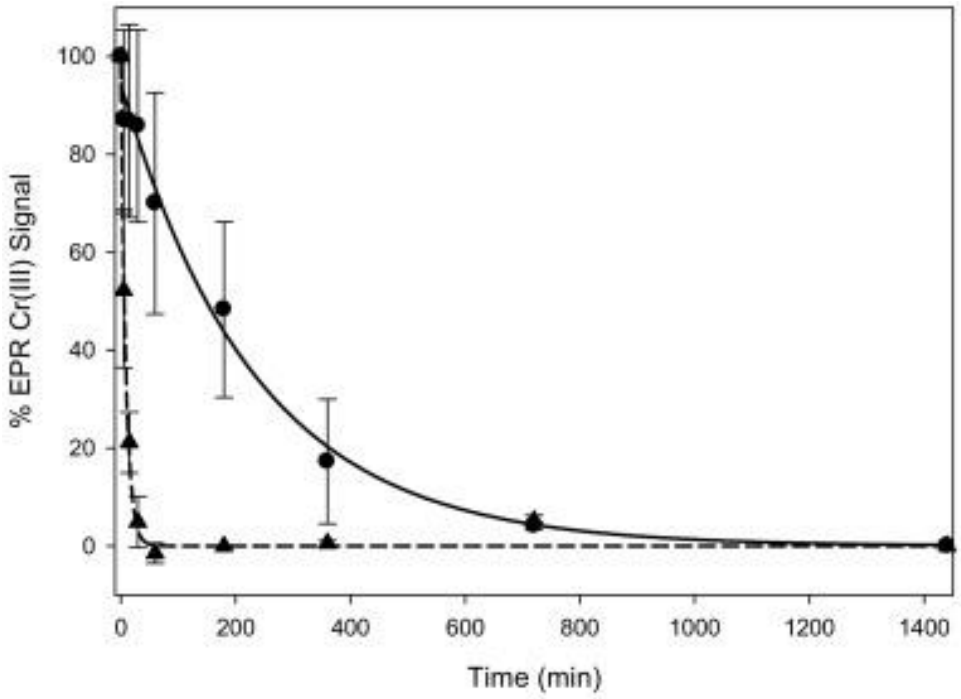

Figure 4.10. Percentage loss of Cr(III) from $Cr(III)_2$-Tf's after acidification to pH 5.5. Black triangles - loss of Cr(III) from primarily conformer **2** (g ~ 5.4 feature) of $Cr(III)_2$-Tf (formed 1 h after the addition of $CrCl_3$ to apoTf in 100 mM HEPES with 25 mM HCO_3^-, pH 7.4, at 37 °C). Black circles - loss of the Cr(III) from the N-lobe site (g ~ 5.2 and 5.6 features) of conformer **3** (formed 48 h after the addition of $CrCl_3$ to apoTf in 100 mM HEPES with 25 mM HCO_3^-, pH 7.4, at 37 °C).

LOW-MOLECULAR-WEIGHT CHROMIUM-BINDING SUBSTANCE MAY BIND AND CARRY CR(III) FROM THE ENDOSOME

1. Introduction

Fe(III) has poor availability in aerobic conditions due to the insoluble nature of Fe_2O_3, yet Fe(III) is required for virtually all life, necessitating a transport system for the nutrient. The protein transferrin, Tf, is responsible for transporting iron in its trivalent state from the bloodstream to tissues in mammals. Tf possesses two binding sites that are adapted to be selective for Fe(III) and other ions of similar charge-to-size ratios. Of the many various metals Tf can bind, only the transport of Fe(III) and potentially Cr(III) are biologically relevant [1-4]. Cr(III) has long been proposed to be carried by Tf in the bloodstream, yet the Cr-Tf interaction has been tenuous since its proposal in 1960s with several challenges and revisions to it's interaction. When radiolabeled ^{51}Cr is injected into the blood stream, immunoprecipitation of the serum results in ~80% of Cr(III) complexed with Tf [5]. When $^{51}Cr(III)$ is injected into rats as $^{51}Cr(III)_2$-Tf, $^{51}Cr(III)$ accumulates in the tissues within thirty minutes [1]. Cr_2-Tf has been shown to bind with its receptor protein, transferrin receptor (TfR), by native electrospray ionization mass spectrometry and bio-layer interferometry [6, 7].

Despite macro level studies showing Cr(III)'s accumulation into tissue when injected as Cr_2-Tf, studies investigating the molecular interactions between Cr(III) and Tf have had mixed results. The ability for Tf to deliver Cr(III) to a cell has been challenged. Experiments with HepG2 cells have shown that Cr(III) did not accumulate into cells when loaded into Tf. Follow-up BLI experiments suggested that the Cr_2-Tf did bind to its receptor protein, transferrin receptor

(TfR), as expected; however, the data were interpreted as the Cr-Tf-TfR complex failing to dissociate after being returned to pH 7.4. This result was taken as evidence to support a 'detoxification' mechanism by which Tf 'ties up' Cr(III) and sequesters it in the bloodstream. Recent experiments have shown that Cr(III) is capable of being released from the binding site of Tf under mimicked endosomal conditions at a rate consistent with endocytosis [8-9]. However, this is not the complete picture. For Cr(III) to be transported by Tf it must not only be released at a rate consistent with endocytosis, but the Cr(III) must also be removed from the endosome. The reduction potential of Cr(III) makes it unlikely to be reduced by physiological oxidoreductases and a trivalent metal ion transporter is not known. Instead, if Cr(III) is to be removed from the endosome it is likely removed complexed with a chelating ligand.

Some efforts have already been made to test potential chelating ligand candidates for binding Cr(III) under endosomal conditions. In an early experiment measuring the rate of Cr(III) loss from Tf, the presence of a chelating ligand accelerated the loss of Cr(III), but the prospective ligands did not bind the Cr(III) under those conditions [9]. Instead, Cr(III) appeared to accumulate in a nonspecific binding site(s) of Tf. EDTA was tested along with biologically relevant ligands and, despite its large affinity for Cr(III), Cr(III) still accumulated in the non-specific site(s) at acidic pH [9]. Thus, a potential chelating ligand will require very high affinity for Cr(III) even under acidic conditions.

A clue about the identity of the ligand is suggested in the discrepancy between two cell culture studies looking at the uptake of Cr(III) from Cr_2-Tf [6, 10]. C2C12 mouse muscle myoblast cells grown in supplemented Dulbecco's modified minimal essential media (DMEM) containing 10 % fetal bovine serum incorporated Cr(III) from $Cr(III)_2$-Tf at levels 33% of that for Fe(III) from $Fe(III)_2$-Tf [6, 10]. Cr(III) primarily appeared in microsomal factions (possibly

reflecting Cr(III) in endosomes) 15 min after the addition of Cr(III) as $Cr(III)_2$-Tf. Then, Cr(III) primarily appeared in the cytosol 30-60 min after addition of $Cr(III)_2$-Tf. In contrast, the previously discussed HepG2 human liver carcinoma cells were in serum-free DMEM and reported to not uptake Cr(III) from $Cr(III)_2$-Tf [7]; however, a separate study using those same cells in serum-supplemented DMEM have reported Cr(III) accumulation within cells [11]. Thus, a component of serum could be responsible for binding Cr(III) in the endosome and could be responsible for Cr(III) transport from the endosome to the cell. An oligopeptide low-molecular-weight chromium-binding substance, LMWCr, is a component of serum, is known to bind Cr(III) with high affinity, and is bound with Cr(III) expelled in the urine, making it potential candidate for Cr(III) binding in the endosome.

LMWCr was first discovered by the Wada group in 1981 when isolated from cytosolic hepatocyte fractions of rats after an injection of $K_2Cr_2O_7$ [12]. Since then LMWCr has been isolated from numerous sources including rabbits, porcine, dogs, cows, humans, alligator, and chickens [12-16]. LMWCr is known to be involved with Cr(III) transport as it is the form Cr(III) expelled in urine. Virtually all Cr(III) expelled in urine is found complexed with LMWCr [17]. Cr(III) complexed with LMWCr has also been found at lower levels in plasma [17]. LMWCr is capable of binding 4 Cr(III) ions tightly; the Cr(III)s are in an octahedral coordination geometry primarily with oxygen based ligands. The oligopeptide is composed of the amino acids glycine, glutamic acid, aspartic acid, and cysteine; however, the exact sequence and structure proves elusive. Tandem mass spectrometry (MS/MS) revealed the partial sequence EEEEGDD [18]. A synthetic model peptide EEEEGDD was found to bind 4 Cr(III) ions per peptide with similar cooperativity ($n = 3.82$ vs $n = 3.47$) and binding constants (1.10×10^{21} M^{-4} vs 1.54×10^{21} M^{-4}) as those of LMWCr [19]. Injection of Cr_2-Tf in rats causes levels of Cr_4-LMWCr to begin to

increase in the urine of rats within 30 min of injection; given the turnover rate of Fe_2-Tf in rats (9-30 min depending on the demand for Fe by the rats), it is possible for the Cr(III) bound to the $Cr(III)_2$-Tf to be released in the endosome and then bound by apo-LMWCr and for the LMWCr to be removed from the cell to return to the bloodstream before it is lost in urine [8].

Herein are described studies to examine the feasibility of LMWCr to bind Cr(III) from $Cr(III)_2$-Tf under endosomal conditions.

2. Materials and methods

2.a. Materials

Iron-free human serum Tf and bovine serum Tf were obtained from Aldrich (St. Louis, MO). Doubly deionized water was used throughout. All reagents were used as received unless otherwise noted. Cr(III) solutions were prepared by using $Cr(III)Cl_3 \cdot 6H_2O$ unless otherwise noted. ApoTf concentrations were determined by using the extinction coefficient ($\varepsilon = 9.12 \times 10^4$ M^{-1} cm^{-1}) at 280 nm [20].

2.b. Methods

Dichromic-Tf was prepared as previously described [21]. Apo-LMWCr was isolated using a previously reported procedure with the absence of the catalytic amount of sodium cyanoborohydride [22]. The concentration of the apo-oligopeptide was determined using the method of Udenfriend [23]; glycine was used as a standard. Tf receptor was isolated from bovine bone marrow using transferrin affinity chromatography as previously described [8]; soluble Tf receptor, sTfR, was prepared from Tf receptor using the literature procedure [24]. Bovine bone marrow was obtained from a local commercial grocery and was stored at -80 ^oC until use.

To model the acidification of the endosome that triggers release of metal ions from Tf, $Cr(III)_2$-Tf in a buffered solution (Hepes, 100 mM) at pH 7.4 containing 25 mM bicarbonate at 37 ^oC was acidified by the addition of hydrochloric acid to pH 5.5. After time prescribed intervals, aliquots were removed and frozen for analysis by EPR spectroscopy. Titrations of $Cr(III)_2$-Tf with HCl were performed beforehand to determine the quantity of HCl to be added to achieve desired pH.

$Cr(III)_2$-Tf/sTfR solution were prepared in a 2:1 mole ratio of Tf to sTfR in the presence of 0.8 apoLMWCr per $Cr(III)_2$-Tf. The Cr_2-Tf/sTfR solution was allowed to incubate 1 h at 37 ^oC before acidification.

The reaction of Cr(III) and ATP was performed by adding ATP (3 mM) to a solution of $Cr(NO_3)_3 \cdot 9H_2O$ at 37 ^oC. The temperature was maintained using a 37 ^oC water bath. Aliquots were removed at time intervals for analysis by electronic spectroscopy.

All results are presented as the average of at least triplicate experiments. Error bars in figures represent standard deviation.

2.c. Instrumentation

Ultraviolet-visible spectra were obtained by using a Cary (Aligent, Santa Clara, CA) 500 or Beckman Coulter (Brea, CA) DU800 UV-visible spectrophotometer. Binding of Cr^{3+} to transferrin was monitored at 245 nm. Solutions were continuously stirred at 37 ^oC using a 6 x 6 Peltier thermostated multicell holder. Fluorescence measurements were collected on a BioTek Synergy™ 2 Multi-Mode Microplate Reader multicell fluorescence spectrophotometer using an excitation wavelength of 385 nm and analyzing the wavelength of 495 nm. Continuous wave (CW) EPR were measured on a Bruker (Billerica, MA) ELEXSYS E540 X-band spectrometer with an ER 4102 ST resonator or an ELEXSYS E680 EPR spectrometer (Bruker-Biospin,

Billerica, MA) equipped with a Bruker Flexline ER 4118 CF cryostat. For the E549 spectrometer, CW spectra were measured at 9.44 GHz with a microwave power of 21.1 mW by using a magnetic field modulation frequency of 100 kHz with an amplitude of 30 gauss. For the E680 spectrometer, the parameters used were a frequency of 9.71 GHz with a microwave power of 21.1 mW using a magnetic field modulation frequency of 100 kHz with a modulation amplitude of 15 gauss. Peak positions are reported as g-values. Spectra were taken at liquid nitrogen temperatures (77-85 K) with a quartz insertion Dewar.

2.d. Electrostatic Surface Potentials and Docking

For the comparison of the electrostatic surface of the protein, the (protein data base) PDB file 1SUV [25], a human transferrin receptor-transferrin complex in which Fe(III) is loaded into all binding sites and each lobe is in the closed conformation, was utilized. In addition, each PDB file was split by chain designator and multiple files were generated containing the individual chain monomers of the Tf lobes. The DelPhi webserver [26, 27] was run on each of these files to solve the Poisson-Boltzmann equation and calculate the electrostatic energies at pH 7.4 and pH 5.5; from the output the positive and negative charges along the surface of the monomers were determined. These runs were conducted using Clemson University's High Performance Computing cluster, Palmetto (http://compbio.clemson.edu/sapp/delphi_webserver/) using Amber as the force field parameter for protonation. The following parameters were used for the DelPhi runs: percent of protein filling the cube – 70%; scale – 1.0 grids/Å; a dielectric constant of 4.0 for the protein and 80.0 for the solvent; the water probe radius 1.4 Å; and a convergence criteria (maxc=0.0001). The energies calculated were coulombic, solvation, and grid energy and visualized as a potential map.

Docking of LMWCr to the individual lobes of Tf was accomplished with AUTODOCK Tools and AUTODOCK VINA [28,29]. The tools utility was used to assign Gasteiger atomic charge to the ligand and define the grid of interest (x,y,z). The input files for autodock Vina were taken from pdb entry 1SUV in an identical manner described above. The parameters used in Vina included an exhaustiveness parameter at 10, an Energy range of 1 kcal/mol, with other parameters left at the default values.

2.e. Data Analysis

Data analysis, calculation of averages and standard deviations, and fitting of curves to the appropriate equations was performed by using SigmaPlot 11 (SPSS, Inc., Chicago, IL). The iterative curve fitting algorithm of SigmaPlot 11 uses the Marquardt-Levenberg algorithm to find the parameters of the independent variables that provide the best fit between the data and the equation.

CW EPR spectrum processing and simulations were performed using the EasySpin package in MATLAB (Mathworks, R2017b). Polynomial fitting of the spectral baseline corrections was performed using Xepr software of the ELEXSYS. The g-values, g-strain, and weight of the simulated spectrum were fit using the "pepper" function in EasySpin.

Kinetic data was simulated by Dr. Patrick Frantom (The University of Alabama) using KinTek Explorer (version 6.2).

3. Results and Discussion

LMWCr was first reported in 1981 by the toxicology group of Osamu Wada [12, 13]. They identified a low-molecular-weight chromium compound by size exclusion chromatography of the cytosol of liver cells of male mice injected with a single dose of potassium chromate. A similar low-molecular-weight compound was found in the feces and urine and 2 hours after

injection in the plasma. These researchers suggested that LMWCr was formed in the liver and participates in retention and excretion of chromium in the body. The material from the livers of rabbits treated similarly with chromate was partially purified and found to apparently be an anionic organic-chromium complex containing amino acids [30]. Subsequently, LMWCr was found to occur in urine normally, although the amounts were greatly increased after rats were injected with chromate [31]. LMWCr from human and rat urine was found not be saturated with chromium. The urine LMWCr was believed to be like that of the liver and other organs of rabbits and dogs and to be involved in removing excess chromium from the body. LMWCr has been shown to be an oligopeptide of 10 or 11 amino acids consisting of glycine, cysteine, aspartate, and glutamate [22, 30]. From mammalian, avian, and reptilian liver and human urine, the peptide contains a seven amino acid long segment of the sequence EEEEGDD [18, 19]. The peptide binds four Cr(III) in an anion-bridged assembly [32].

ApoLMWCr binds Cr(III) tightly (K_f ~10^{21}) and cooperatively (Hill constant, n, = 3.47) and can remove Cr(III) from $Cr(III)_2$-Tf at pH 7.4, although achieving equilibrium takes over 2 weeks [33]. The binding of Cr(III) to apoLMWCr or the ability of LMWCr to remove Cr(III) from $Cr(III)_2$Tf has not been investigated at endosomal pH.

3.a. Removal of Cr(III) from $Cr(III)_2$Tf in the Presence of ApoLMWCr

To model the acidification of endosomes during endocytosis, the pH of solutions of human $Cr(III)_2$-Tf were acidified to pH 5.5, and aliquots of the resulting solutions were taken after time intervals and frozen in liquid nitrogen for analysis by EPR. The two metal-binding sites of Tf can be distinguished by EPR spectroscopy (frozen solutions, 77 K) [34]. Cr(III) in the N-lobe site generates EPR features at g ~ 5.08 and 5.66, while Cr(III) in the C-lobe site generates a feature at 5.42 (and a feature at g ~ 2). Lowering the pH of a solution of $Cr(III)_2$-Tf results in

the loss of both Cr(III) from transferrin with the loss of the EPR feature(s) from the Cr(III) in the metal-binding sites [8]. As noted previously, the loss of the EPR feature from C-lobe Cr(III) is rapid with a slower loss of the features from the N-lobe Cr(III) [8]. In the presence of apoLMWCr, the effect of acidification is qualitatively similar to that in the absence of apoLMWCr (Figure 5.1) as EPR features corresponding to both Cr(III) disappear with the C-lobe feature vanishing more rapidly.

However, apoLMWCr has a quantitative effect on rate the loss of Cr(III) from both lobes of Tf at pH 5.5 (Figure 5.2 and Table 5.1). Previously reported in Chapter 2, the addition of potential chelating ligands (EDTA, citrate, and ascorbate) to $Cr(III)_2$-Tf before acidification to pH 5.5 was shown to result in an increase in the rate of Cr(III) loss from the N-lobe by about a factor of 2 with the increase being identical within error for all three ligands [8]. No significant effect from the presence of the chelating ligands was observed for loss of Cr(III) from the C-lobe. In contrast, the presence of apoLMWCr, which is also a potential chelating ligand, results in an appreciable increase in the rate of Cr(III) loss from of both lobes of Tf. For the N-lobe, the increase is significantly greater than for EDTA, citrate, or ascorbate (Table 1); Cr(III) is lost from the N-lobe more than twice as fast in the presence of LMWCr as in the presence of the other chelating ligands. The rate of Cr(III) loss from the C-lobe is more than twice as fast in the presence of LMWCr than in the absence of any added chelating ligand. As Cr(III) binds slowly to EDTA, citrate, or ascorbate and the effect on the rate of Cr(III) loss from the N-lobe was similar for all three ligands, the ligands were proposed to potentially have a role in displacing the carbonate or binding to a synergistic anion-binding site [8], rather than chelating the Cr(III) to assist its removal from Tf. The presence of anions is known to accelerate the loss of Fe(III) from $Fe(III)_2$-Tf [35]; a variety of anions are known to affect Fe(III) binding and loss by a number of

mechanisms including competition with Tf for Fe(III), replacement of the synergistic carbonate, and allosteric effects [36]. For example, Fe(III) from $Fe(III)_2$-Tf at pH 5.5 is not released within the lifetime of an endosome without the addition of anions, even if they have no chelating ability [35]. The greater effect of apoLMWCr on Cr(III) loss from the N-lobe and the significant effect on Cr(III) loss from the C-lobe could suggest that apoLMWCr is having an effect beyond just assisting the loss of carbonate or binding to a synergistic anion-binding site. In fact, the use of an appropriate chelating ligand may be crucial for certain studies examining the loss of binding of $Cr(III)_2$-Tf to the Tf receptor (*vide infra*).

With time after acidification of $Cr(III)_2$-Tf in the absence of apoLMWCr, four new EPR features appear from Cr(III) adhering to the outside of the apoTf [8]. These features appear considerably slower than the EPR features from Cr(III) in the C- and N-lobes are lost, reflecting the slow rates at which "substitutionally inert" Cr(III) generally binds ligands. The time lapse between the loss of the EPR features from the Cr(III) in the metal-binding sites and the appearance of the four features has been taken as evidence that the latter EPR features are not from Cr(III) still in the metal-binding site but with changed ligation from the lowering of the pH. These EPR signals are also generated if Cr(III) is added to Tf at pH 5.5 where Cr(III) does not bind in the metal-binding sites [8,9]. Aisen et al. showed that the addition of Co(III) or Fe(III) to $Cr(III)_2$-Tf displace the Cr(III) from the metal-binding sites [34]; with time, the EPR signals from the weakly adhering Cr(III) non-specifically bound to the surface of Tf appear. This conclusively demonstrates that the four EPR features arise from Cr(III) adhering to the surface of the protein rather than Cr(III) in altered environments in the metal-binding sites.

The addition of apoLMWCr to a solution of $Cr(III)_2$-Tf greatly reduces the formation upon acidification to pH 5.5 of the four EPR features from the adhering Cr(III) centers. Upon

acidification, EPR features from the formation of LMWCr appear (Figure 5.1). (LMWCr has a distinct, very broad EPR signal arising from its antiferromagnetically coupled assembly of four chromic ions [32]. The EPR spectrum of isolated LMWCr at ~77 K and pH 5.5 and the EPR spectrum at 77 K of LMWCr reconstituted from apoLMWCr at pH 5.5 are shown in Figure 5.2. Thus, apoLMWCr binds the Cr(III) released from the $Cr(III)_2$-Tf, preventing the Cr(III) from adhering to the surface of apoTf. The features from LMWCr appear more rapidly than the appearance of the features from the adhering Cr(III) in the absence of LMWCr. In fact, the formation of LMWCr is also significantly faster than the binding of Cr(III) to chelating ligands such as EDTA under these conditions. If EDTA is present in addition to LMWCr, EPR signals from the formation of a Cr(III)-EDTA complex appear after the features for the formation of LMWCr (data not shown). However, the formation of LMWCr from apoLMWCr and the Cr(III) released from Tf is not rapid compared to length of a cycle of endocytosis; the half time for the appearance of LMWCr was 6.9×10^2 min ($k = 0.0010 \pm 0.0005$ min^{-1}). These results suggest a unique ability of LMWCr to bind Cr(III) released from Cr_2-Tf at pH 5.5 compared to simple chelate ligands.

3.b. Loss of Cr(III) from Tf-TfR Complex in Presence of LMWCr

While the current research was underway, Benjamin-Rivera, et al. suggested that "the finding by Lay et al. by bio-layer interferometry (BLI) might be an artifact of insufficient time allowed to observe metal release and not using physiologically relevant anions in their bio-layer interferometry approach" [37]. Previously, the formation of the $Cr(III)_2$-Tf/Tf receptor complex has been shown to have a dramatic effect on the release of Cr(III) from $Cr(III)_2$-Tf upon acidification [8,9], resulting in release of both Cr(III) from $Cr(III)_2$-Tf to be sufficiently fast to be physiologically relevant. Given this and that the interpretation of the BLI studies of $Cr(III)_2$-Tf

and TfR has been questioned, the release of Cr(III) following the acidification of the $Cr(III)_2$-Tf/Tf receptor complex was examined in the presence of apoLMWCr.

The EPR spectrum of the bovine $Cr(III)_2$-Tf/Tf receptor complex has only the feature at g~5.42, similar to the conformation of human serum $Cr(III)_2$-Tf that appears the first two h after the addition of Cr(III) to Tf and slowly over 2 d converts to the conformation with EPR feature at g~5.06, 5.42, and 5.66 [8,9]. After acidification of the $Cr(III)_2$-Tf/Tf receptor complex in the presence of apoLMWCr, the EPR feature at g~5.42 disappears rapidly, similar to the behavior in the absence of apoLMWCr (Figure 5.3). Fitting the loss of this signal to an exponential decay gives a rate constant of 0.736 ($\pm$0.063) min^{-1}, corresponding to a $t_{1/2}$ of 1.1 min (Figure 5.4). This is ~4-fold slower than the loss of Cr from the $Cr(III)_2$-Tf/Tf receptor complex in the absence of LMWCr [8]; however, it is still greatly enhanced compared to loss of Cr from $Cr(III)_2$-Tf in the presence or absence of apoLMWCr. The rate constants of Fe(III) loss from the $Fe(III)_2$-Tf/Tf receptor complex have been reported to be 2.8 min^{-1} for loss of the first Fe from the N-terminal binding site and 7.8 min^{-1} for the subsequent loss from the C-terminal site and 5.5 min^{-1} for Fe in C-terminal site if lost first and 1.4 min^{-1} for the subsequent loss from the N-terminal site [38]. These values are similar to the rate constant for the loss of Cr(III) from the Cr(III)-Tf/Tf receptor in the absence of apoLMWCr ($k = 2.86\ min^{-1}$ ($t_{1/2} = 0.235$ min)) but indicate Fe(III) loss is faster than Cr(III) loss in the presence of apoLMWCr. However, the overall similarity in the rate constants indicates that the rate of Cr(III) loss from Cr_2(III)-Tf/Tf receptor complex is biologically relevant [8,9].

Most importantly, a striking change in the rate at which apoLMWCr binds Cr(III) from $Cr(III)_2$-Tf is observed when the $Cr(III)_2$-Tf/Tf receptor complex is utilized. For the $Cr(III)_2$-Tf/Tf receptor complex, the released Cr(III) binds to apoLMWCr in a biphasic manner (Figure

5.4-5). About 78 % of the Cr(III) is bound with a $t_{1/2}$ of 2.7 min ($k = 0.253 \pm 0.052$ min^{-1}), a dramatic reduction from the 6.9×10^2 min when using just $Cr(III)_2$-Tf in the presence of apoLMWCr. This approximately 250-fold reduction in the time required for LMWCr to scavenge the released Cr(III) suggests that apoLMWCr must interact with the $Cr(III)_2$-Tf/Tf receptor complex to facilitate the movement of Cr(III) into the apopeptide. The half-time suggests Cr(III) could be released from $Cr(III)_2$-Tf and then bind to apoLMWCr, and finally the LMWCr be transported from the endosome during the time of an endomosal cycle, although, as these steps are slower than for Fe(III) release and chelation, not all the Cr(III) might be removed from the endosome before it fused back with the cell membrane. The second phase corresponds to Cr(III) released from Tf, weakly adhering to the protein, and then binding to apoLMWCr. This accounts for ~20 % of the Cr(III) and has a $t_{1/2}$ of 86 min ($k = 0.0081 \pm 0.0076$ min^{-1}). This rate is in accord with appearance and disappearance of four weak features from the weakly adhering Cr(III) in the EPR spectra. That 80 % of the Cr is bound by apoLMWCr is curious in that a 0.8 apoLMWCr:Tf ratio was used in the study; however, as apoLMWCr cooperatively binds 4 Cr(III) per peptide molecule, sufficient apoLMWCr was present to bind all the Cr(III) released from the $Cr(III)_2$-Tf/Tf receptor complex. Unfortunately, the concentration of apoLMWCr in the blood plasma is not known so that estimating the appropriate ratio of apoLMWCr and Tf/Tf receptor is not possible. Determining the concentrations of apoLMWCr and Cr(III)-containing transferrin in the bloodstream as a function of dietary Cr(III) is an area requiring further exploration. As the EPR spectrum of LMWCr formed after acidification of the $Cr(III)_2$-Tf/Tf receptor complex has an identical EPR spectrum to isolated LMWCr at pH 5.5. and LMWCr reconstituted with 4 Cr(III) at pH 5.5, the results suggest that each molecule of apoLMWCr bound to the Tf/TF receptor complex binds a single Cr(III) followed by transfer of Cr(III) among

the partially loaded LMWCr molecules to give the fully loaded LMWCr. This should not be surprising given that the binding of Cr(III) to LMWCr is extremely cooperative with n = 3.47 [32].

Interestingly, the slight slowing of the release of Cr(III) from the $Cr(III)_2$-Tf/Tf receptor complex in the presence of apoLMWCr could actually be beneficial. This slowing coupled with the increase in the rate of the released Cr(III) binding to apoLMWCr would result in a decrease in window of time available for the released Cr(III) to escape from the complex of Tf, Tf receptor, and apoLMWCr and minimize Cr(III) not trapped by binding to apoLMWCr.

As apoLMWCr has four glutamate residues, two aspartate residues, and a carboxy terminus that can provide negative charges while only the amino terminus may be positively charged at near neutral pH or pH 5.5, apoLMWCr should bear a considerable negative charge before and after the acidification of the endosome. As the rapid transfer of Cr(III) from the $Cr(III)_2$-Tf/Tf receptor complex presumably must involve binding of the LMWCr to the Tf/Tf receptor complex, near the metal binding sites of the Tf, the surface electrostatic potential of a molecule of $Fe(III)_2$-Tf with both lobes closed was calculated. This was done using the structure of human serum $Fe(III)_2$-Tf bound to its receptor (1SUV) [25] with the assumption that replacement of Fe(III) with Cr(III) would have little effect on the surface electrostatic potential. For the only X-ray crystal structure of a transferrin containing Cr(III), human serum transferrin containing malonate as the synergistic anion [39], the structure is virtually superimposable on the structure of the corresponding Fe(III) analog [40]. At pH 7.4, the greatest accumulation of positive charge on the surface of receptor bound $Fe(III)_2$-Tf (Figure 5.6) rests in a cleft located at the hinge where the open conformation of a lobe of Tf folds to form the closed lobe, directly around the coordinated metal atom. When the protein is acidified to pH 5.5, the positive charge

of this region is particularly enhanced. Thus, a cleft of positive charge residues directly above the metal-binding site in this hinge region of both lobes of Tf. This cleft should readily accommodate most of the apoLMWCr molecule.

Starting from the amino terminus of apoLMWCr, six of the first seven amino acids in the primary sequence are aspartate or glutamate residues. This part of apoLMWCr bearing most of the negative charge and metal-binding ligands should readily reside in this cleft, providing a ready pathway for Cr(III) to travel from the metal-binding site in Tf to the concentration of carboxylate groups on apoLMWCr. To test this, the docking of apoLMWCr to both lobes of human serum $Fe(III)_2$-Tf in the closed conformation found in $(Fe(III)_2\text{-Tf})_2$/sTfR (1SUV) was examined. For apoLMWCr, whose amino acid composition but not entire sequence is known, the peptide EEEEGDDCCG was utilized. Including three more nonpolar amino acids at the C-terminus (although their order in the primary sequence is uncertain) is necessary to be certain that the orientation of the peptide is correct. As anticipated, all the lowest energy structures docked apoLMWCr in the positively charged cleft in both the C- and N-terminal lobes of the Tf (for the lowest energy structures, see Figure 5.7). Thus, anionic apoLMWCr fits well into the cationic surface of the cleft along the hinge of thee closed conformations of both lobes of $Fe(III)_2$-Tf, consistent with apoLMWCr having a role in facilitating Cr(III) removal from $Cr(III)_2$-Tf.

3.c. Relationship to BLI studies

Levina, et al. using BLI examined the effects of acidification on the loss of Tf from the Tf/Tf receptor complex upon acidification to pH 5.5. In the case of $Fe(III)_2$-Tf , the loss appeared to be biphasic. The two processes were interpreted as conformational changes associated with the loss of Fe from the $Fe(III)_2$-Tf/Tf receptor complex after acidification and the

subsequent slower dissociation of the newly generated apoTf from the apoTf/Tf receptor complex [6]. Strangely, when using apoTf rather than $Fe(III)_2$-Tf, the data required the same biphasic fit despite no Fe(III) present to be lost. For $Cr(III)_2$-Tf, the rate of change in the wavelength of the BLI experiment for the acidification of the Tf/TF receptor complex was interpreted as the rate conformational changes associated with loss of $Cr(III)_2$-Tf , not apoTf from the Tf/Tf receptor complex after acidification of the complex to pH 5.5, as the data did not require being fit to a biphasic function [6]. Subsequently, the fast process assigned to Fe(III) loss was found by Levina et al. to be an artifact from EDTA interacting with another component of the experiment [41]. The rate constant for loss of apoTf from the $Cr(III)_2$-Tf/Tf receptor complex after acidification of the complex to pH 5.5 appears to be 0.28 min^{-1} ($t_{1/2}$ = 2.5 min) [6]. If this is correct, then Cr(III) loss from $Cr(III)_2$-Tf/Tf receptor complex is appreciably faster than loss of the generated apoTf from the apoTf/Tf receptor complex at pH 5.5, whether or not apoLMWCr is present. Thus, the rates of Cr(III) release from the $Cr(III)_2$-Tf/Tf receptor complex upon acidification of the complex to pH 5.5 (measured in the present work) fall between the rate of Fe(III) release from the $Fe(III)_2$-Tf/Tf receptor complex upon acidification of the complex to pH 5.5 and the rate of loss of the generated apoTf from the apoTf/Tf receptor complex at pH 5.5.

Unfortunately, the association of the slow rate constant measured by BLI with the loss of apoTf from the acidified Tf/Tf receptor complex must also be questioned. As Cr(III) is released faster the proposed rate of $Cr(III)_2$-Tf loss from the Tf/Tf receptor complex, the assignment of BLI change to $Cr(III)_2$-Tf loss from the Tf/Tf receptor complex is incorrect. The lack of need for the biphasic fit for Cr(III)-Tf data is confusing as the side effect from the EDTA should not have been affected by using $Cr(III)_2$-Tf, $Fe(III)_2$-Tf, or apoTf. Additionally, the corresponding rate

constants associated with the loss of apoTf from the acidified Tf/Tf receptor when using $Fe(III)_2$-Tf or apoTf were reported to be 0.012 min^{-1} and 0.078 min^{-1}, giving $t_{1/2}$ values of 58 and 8.8 minutes [6]. However, as for $Cr(III)_2$-Tf and $Fe(III)_2$-Tf, the metals must be lost before the apoTf is lost, the rate of release of apoTf should be slower than for apoTf itself from the receptor complex. Also, since Fe(III) is lost more rapidly than Cr(III), one would expect apoTf loss starting from $Fe(III)_2$-Tf to be faster than from $Cr(III)_2$-Tf, rather than the reverse as postulated [6]. Thus, the BLI results from acidification of the Tf/Tf receptor complexes must be used with caution, and interpretation must await further investigation.

Raising the pH of the Tf/Tf receptor complex from pH 5.5 to pH 7.4 should result in the dissociation of apoTf from the apoTf/Tf receptor complex. For Tf that initially contained Fe(III) or a mixture of Fe(III) and V(IV) or V(V), bio-layer interferometry (BLI) experiments observe wavelength shift with time consistent with this dissociation [41,42]. However, when Cr(III) is initially present in the Tf, the BLI experiments revealed shifts consistent with both loss of apoTf with concurrent rebinding of Cr(III)-containing Tf [6]. This was interrupted in terms of released Cr(III) binding to the Tf/Tf receptor complex on a site(s) other than the tight metal-binding sites that hold the Tf/Tf receptor complex together. However, binding of Cr(III) to weak binding sites of Tf and Tf receptor requires far too much time as shown by the current studies and those described in previous chapters. The difference between the iron and vanadium results and the chromium results probably stems from the use of EDTA to bind the metal ions released from Tf [6, 41, 42]. For iron and vanadium this binding is quick so that the metal ions cannot be rebound by the free apoTf or any apoTf still bound to Tf receptor. However, binding and Cr to EDTA is far too slow at either pH 5.5 or 7.4 for significant binding to occur in the time frames of the BLI experiments, 200 s. The 200 s window corresponds to more than 10 half-lives for the

loss of Cr(III) from the $Cr(III)_2$-Tf/Tf receptor complex at pH 5.5. Thus, aquated Cr(III) ions are present in the solution at pH 5.5 before the pH is raised back to 7.4. Raising the pH to 7.4 should then result in binding of Cr(III) back to Tf followed at this pH by the binding of Cr(III)-containing Tf to the Tf receptor. In the presence of 25 mM bicarbonate (as used in the pH 7.4 portions of the BLI study), Cr(III) binds to Tf with rate constants of 3.16 and 0.189 min^{-1} [21]; thus, Cr(III) can bind rapidly to Tf under the BLI conditions with subsequent binding of Cr(III)-containing Tf to its receptor.

Thus, recently measured rate constants for the binding of Cr(III) to Tf and release of Cr(III) from the Tf/Tf receptor complex are consistent with Tf serving a role in Cr(III) transport from the blood to cells via endocytosis. BLI experiments have also recently been used to propose citrate is the physiological chelate for Fe(III) released from the Tf/Tf receptor complex during endocytosis [40]. However, for Cr(III), this seems unlikely. Citrate has little effect on Cr(III) release from $Cr(III)_2$-Tf and binds Cr(III) slowly[8], and cell culture studies indicate that $[Cr(citrate)_2]^{2-}$ is not transported out of endosomes at least by monocarboxylate transporters [10]. However, these studies raise the question of whether apoLMWCr might be the unknown Fe(III) chelating agent that assists removal of Fe(III) from transferrin before the ferric ions are reduced to ferrous ions for transport across the endosomal membrane by divalent metal ion transporters. Given the similar charge to size ratios of chromic ions and ferric ions, apoLMWCr should readily bind both in a similar fashion. Also, given that Tf is ~30 % loaded with Fe(III) and the low Cr(III) concentrations in the bloodstream, Cr(III) is probably transported as Fe(III)Cr(III)-Tf. Studies in the current laboratory have shown Cr(III) and Fe(III) in mixed Fe(III)-Cr(III)-Tf's, regardless of which lobe the Cr(III) or Fe(III) reside, are lost from Tf in similar fashions with similar rates to Cr(III) in the appropriate lobe from $Cr(III)_2$-Tf and Fe(III) in the appropriate

lobe from $Fe(III)_2$-Tf (J.B. Vincent, K.C. Edwards, D.R. Graham, M.W. Gannon, and S.D. Reith, unpublished results). Studies in this area including the role of apoLMWCr are proceeding.

3.4. In Vivo Relevance

These results of the current study of the release of Cr(III) from the $Cr(III)_2$-Tf/Tf receptor complex in the presence of apoLMWCr have important implications for the interpretation of *in vivo* studies of the transport of Cr(III) from $Cr(III)_2$-Tf and allow for a more sophisticated model for the transport and distribution in the body and urine of Cr(III) from injected $Cr(III)_2$-Tf (Figures 5.8). A kinetics mechanism was developed to explain the in vivo distribution of Cr(III) from $Cr(III)_2$-Tf injected into rats. KinTek Explorer was used to simulate various models of Cr(III) transport with respect to the previously reported *in vivo* data. This software uses fast-numerical integration of rate equations to create real-time simulation curves from schematic kinetic mechanisms. The overall approach was initiated by creation of various reasonable models for Cr(III) transport followed by assignment of experimentally measured rates for any step that was available. The rates for steps with no known rates were manually shifted to optimize agreement between the simulation and experimental data. The simplest model that is consistent with the data is show in Figure 5.9A. The basis of the model stems from two suggestions from the current study: 1) LMWCr formed rapidly enough to be available to carry Cr(III) into the cell and 2) some LMWCr could remain in the endosome when it fuses back with the cell membrane. This allows for some discrepancies in a prior kinetics model [1] to be addressed.

The first step in the current model is the disappearance of Cr(III)-containing Tf from the bloodstream as it taken up by tissue via endocytosis (shown by the red line in Figure 5.9B). The uptake of $Cr(III)_2$-Tf is biphasic. For $Cr(III)_2$-Tf injected via the tail vein into healthy male Sprague-Dawley rats, the fast phase takes place with a $t_{1/2}$ of ~6 minutes ($k = 0.09\ min^{-1}$) [1].

This is appreciably faster than $Fe(III)_2$-Tf disappears from the bloodstream when injected into a tail or leg vein of healthy Sprague-Dawley rats, $t_{1/2}$ = 33 minutes and is surprisingly similar to the rate of disappearance for iron deficient rats, $t_{1/2}$=10 minutes [43]. $Cr(III)_2$-Tf, while not binding as tightly to Tf receptor as $Fe(III)_2$-Tf, appears to bind to the receptor and undergo subsequent endocytosis faster. In the *in vivo* rat studies after an initial rapid decrease, the amount of Cr(III) in $Cr(III)_2$-Tf did not approach zero over time after injection into the tail vein of rats; instead, a small percentage of the Cr(III) remained associated with $Cr(III)_2$-Tf and only slowly diminished over time [1]. The movement of this small percentage of $Cr(III)_2$-Tf represents the slow phase. This phase could also exist for $Fe(III)_2$-Tf; however, a previous study examining the fate of injected $Fe(III)_2$-Tf for a long enough period to observe the slower phase could not be identified. The slow phase should not represent a saturation of Tf/Tf receptor system as the injected $Cr(III)_2$-Tf represents an increase in the rats' serum transferrin of only about 2 %. The exact nature of this slow-moving pool of Cr-containing Tf is uncertain; however, its behavior could be readily modeled. This pool of Cr-containing Tf does not represent Cr that has entered the endocytic pathway and then reentered the bloodstream. All attempts to allow Cr-transferrin to reenter or be regenerated after $Cr(III)_2$-Tf had entered the endosome would not allow the other data to be properly simulated. The most likely origin for the slow phase is commercial transferrin damaged during its isolation, storage, and shipment or during the process of loading the transferrin with Cr(III) so that it is unable to undergo endocytosis. Degradation of this protein resulting in release of Cr(III) in the blood resulting in rapid binding to apotransferrin would result in the Cr(III) being able to enter the endocytic pathway after an appreciable time delay. The steps in the model required for the fit then represent steps in the degradation before the rapid (<2 min) binding of free Cr(III) to apotransferrin. During the 3-day course of the *in*

vivo experiments, some degradation of transferrin is expected, given the short lifetime of the protein in the body (*vide infra*).

A time delay exists between the disappearance of Cr from $Cr(III)_2$-Tf to the appearance of Cr(III) in the blood and subsequently the urine as LMWCr, indicating intermediate steps are present. (After LMWCr appears in the bloodstream, it is lost relatively rapidly in the urine; the mean tubular reabsorption rate of LMWCr has been reported to be 23.5 % in contrast to rates of 85.7 and 92.5 % for chromate and chromium chloride, respectively [15].) Steps in the disappearance of Cr(III) from $Cr(III)_2$-Tf to the appearance of LMWCr in the bloodstream must include the removal of Cr(III) from $Cr(III)_2$-Tf and the transfer to LMWCr.

The appearance of LMWCr in the bloodstream and urine is biphasic. The halftime for the endocytic cycle of transferrin receptor in hepatocytes (at least HepG2 hepatocarcinoma cells) of 16.9 min [44] is similar to the halftime for the rapid phase appearance of Cr(III) in the urine from $Cr(III)_2$-Tf injected intravenously into rats, 14.3 min [1]. Liver is the primary tissue Cr(III) is transported to from Tf in the bloodstream, followed closely by skeletal muscle [1]. This suggests the endocytic cycle could be the rate determining step in the rapid phase appearance of Cr(III) (from serum $Cr(III)_2$-Tf) in LMWCr in the urine. This would suggest a significant pool of urine LMWCr results from Cr(III) released from the $Cr(III)_2$-Tf/Tf receptor complex in inside of endosomes but released into the bloodstream endosomes. The rapid appearance of LMWCr in the bloodstream was fit by using the rate corresponding to the $t_{1/2}$ of hepatocyte endocytosis as the rate determining step.

The second phase of Cr movement from $Cr(III)_2$-Tf in the endosomes to LMWCr in the urine requires the movement of LMWCr into the cell from the endosome followed by the movement of LMWCr from the cell into the bloodstream. The rate of movement of cellular

LMWCr to the bloodstream was measured in the previous *in vivo* study [1]. This allows for the simulation to estimate the rate constant for movement of LMWCr from the endosome to the rest of the cell; the result being 0.055 min^{-1} ($t_{1/2}$ = 12 min). This relatively slow step requires a time not too much shorter than that of an endosomal cycle and is what prevents all the LMWCr formed in the endosome from being transferred to the rest of the cell before the endosome refuses with the cell membrane. The time window is probably more consistent with apoLMWCr acting as an ionophore rather active transport. The current kinetics model and simulation suggests a very significant change from the previous model, which assumed that transport of LMWCr from the cell to the bloodstream was rapid and, thus, required an active transporter. However, the direct movement of LMWCr from the endosome no longer requires the rapid transfer of LMWCr. The slow movement of LMWCr from the tissue cells into the bloodstream becomes the rate limiting step of the movement of Cr(III) from the Cr(III)2-Tf in the bloodstream until Cr(III) is lost as LMWCr in the urine. Significantly, this is consistent with the Cr content of tissues increasing linearly with oral Cr(III) intake [45].

The model was further tested by estimating the concentration of Cr(III)-containing Tf and LMWCr in the endosomes and LMWCr in the rest of the hepatocytes at a series of times from subcellular differentiation and size exclusion chromatography experiments described in the *in vivo* rat study. [1]. Assuming the time-dependent concentration of these species in hepatocytes is a fair representation of the that in other cells, the concentration of Cr(III)-containing Tf and LMWCr in the endosomes and LMWCr in the rest of the hepatocytes at these times was estimated and included in the model (Figure 5.9B). The model does a reasonable job of reproducing the low levels of the endosomal species over time and a good job of simulating the cellular levels of LMWCr.

After injection of $Cr(III)_2$-Tf into the bloodstream, some degradation products of transferrin that contain Cr(III) are detected [1]. A larger fragment appears slower and is maximal after 30 min; its loss is accompanied by the appearance of a smaller fragment. These species after 1 day account for less than 10 % of injected Cr(III) [1]; these Cr(III)-containing fragments of Tf have not been observed in studies where $CrCl_3$ is injected in rats [13], suggesting that they may arise from the sudden increase of serum Tf. However, glycated transferrin has a half-life of 8-10 days; using 10 days as the half-life, about 19% of Tf would be expected to be degraded in three days so that the degradation in the study of injected $Cr(III)_2$-Tf is not unexpected or unreasonable. These degradation products are not included in the new kinetics model to keep the model as simple as reasonably possible, but this could be added as a direct path from $Cr(III)_2$-Tf in the bloodstream to the larger fragment of Tf to the smaller fragment.

In summary, the fate of oral Cr(III) can now be elucidated much further (Figure 5.7). About 1 % of an oral dose of Cr(III) is absorbed via passive diffusion and enters the bloodstream. In the bloodstream, it binds rapidly to Tf. The binding is too rapid for Cr(III) to bind to apoLMWCr; similarly, while Tf can give up its Cr(III) to apoLMWCr, this is far too slow compared to the lifetime of Cr(III)-Tf in the bloodstream. Cr(III)-Tf binds to the Tf receptor and undergoes endocytosis. After acidification of the endosome, Cr(III) is lost rapidly from the Tf/Tf receptor complex and binds to apoLMWCr. About half of the LMWCr enters the bloodstream directly when the endosomes refuse with the cell membrane. The remaining LMWCr enters the cell from the endosome via an unknown mechanism, but which could be as simple as LMWCr acting as an ionophore. This cellular LMWCr is retained for an appreciable period before ending up in the bloodstream. Once in the bloodstream the LMWCr is readily removed by the kidneys and lost in the urine.

This has implications for the bioactive form of Cr(III), at least for rats, mice, and rabbits where supra-nutritional doses of Cr(III) lead to increased GLUT-4 migration, increased insulin sensitivity, and possibly also lowered LDL cholesterol and triglyceride levels [46]. LMWCr, the form that enters and leaves cells, would appear to be the most obvious candidate of the elusive form of Cr(III), as essentially all Cr(III) in the body is otherwise accounted.

3.e. ATP as Ionophore for Cr(III)

Recently, ATP has been proposed as a possible ionophore for the transport of Cr(III) from the endosome based on previous proposals for transport of Ti(IV) released from Tf in the endosome [37]. The products of the binding of Cr(III) to ATP have been elucidated previously, although at more acidic pH's [47]. At pH 3 at 80 ^{o}C, a monodentate complex of Cr(III) and ATP forms rapidly and converts rapidly to bidentate Cr(III) ATP complexes; the reaction reaches equilibrium in about 15 minutes with an approximately 70 % yield of the bidentate complexes [48]. If the pH of solution of Cr(III) and ATP is raised to 5.7 at 4 ^{o}C, the reaction yields the bidentate complexes in 65-75 % yield, although the time course under these conditions was not reported. Consequently, the binding of Cr(III) to ATP at pH 5.5 and 37 ^{o}C was examined. The binding of ATP to Cr(III) is to quite slow under these conditions (Figure 5.10) The reaction appears to contain primarily the bidentate complexes of Cr(III) and ATP, given the maximum absorbance occurs at a wavelength of 602 nm and that the monodentate complex converts to the bidentate complex at pH 5.7. The formation of the bidentate complex was fit to an exponential rise to a maximum, yielding a rate constant of 0.0063 ± 0.0008 min^{-1} and corresponding half-life of 1.1×10^{2} min. The half-life is several times the circa 15 min time for a cycle of endocytosis. Given that simple chelating ligands have little effect on the rate of loss of Cr(III) from $Cr(III)_2$-Tf and the formation of Cr(III)-ATP is much longer than 15 min, this makes a role for ATP as a

carrier for Cr(III) extremely unlikely. To further test the possibility of ATP having a potential role in the transport of Cr(III) from the endosome, the release of Cr(III) upon acidification of the Cr(III)-Tf/Tf receptor complex in the presence of ATP (0.5 mM) was examined. ATP had no effect on the rate of release of Cr(III) from the complex upon acidification, and over time the EPR features from Cr(III) adhering to the outside of Tf appear as in the absence of ATP (Figure 5.11). Hence, in stark contrast to apoLMWCr, the presence of ATP had no observable effect on Cr(III) release or subsequent binding, pointing to the uniqueness of the effect of the presence of apoLMWCr. Whether LMWCr can serve as an ionophore for Cr(III) transport from the endosome requires future investigation. This behavior for Cr(III) is in stark contrast to Tf-bound Ti(IV) where the addition of ATP results in a substantial increase in the rate of Ti(IV) release upon acidification [49].

4. Conclusion

The apopeptide LMWCr can accelerate the loss of Cr(III) from $Cr(III)_2$-Tf when acidified to pH 5.5, modelling the acidification of endosomes during endocytosis. This acceleration is much greater than that from simple chelating ligands such as EDTA. However, the binding of Cr(III) to apoLMWCr is slow under these conditions. With the more biologically relevant $Cr(III)_2$-Tf/TF receptor complex, the binding of Cr(III) to apoLMWCr is greatly accelerated. These results suggest that LMWCr may function to bind Cr(III) released in the endosomes for ultimate removal from the body as part of a Cr(III) detoxification process. The results also raise the possibility that apoLMWCr could have a role in Fe(III) release from $Fe(III)_2$-Tf. In contrast, ATP is unlikely to have a role in transport of Cr(III) from endosomes.

REFERENCES

1. Clodfelder, B. J.; Vincent, J. B. The time-dependent transport of chromium in adult rats from the bloodstream to the urine. *J. Biol. Inorg. Chem.* 2005, 10, 383

2. Clodfelder, B. J.; Upchurch, R. G.; Vincent, J. B. A comparison of the insulin-sensitive transport of chromium in healthy and model diabetic rats *J. Inorg. Biochem.* 2004, *98*, 522

3. Vincent, J. B.; Love, S. The binding snd transport of alternative metals by transferrin *Biochim. Biophys. Acta.* 2012, *1820* (3), 362

4. Vincent, J. B.; Edwards, K. C. The absorption and transport of chromium in the body. *The Nutritional Biochemistry of Chromium(III)*, 3rd; Vincent, J. B.; Elsevier, Amsterdam 2019, 129

5. Hopkins, L. L., Jr.; Schwarz, K. Chromium(III) binding to serum proteins, specifically siderophilin. *Biochim. Biophys. Acta* 1964, 90, 484

6. Levina, A.; Nguyen Pham, T. H.; Lay, P. A. Binding of Cr(III) to transferrin could be involved in detoxification of dietary chromium(III) rather than transport of an essential trace element. *Angew. Chem. Int. Ed*. 2016, 55, 8104

7. Bonvin, G.; Bobst, C. E.; Kaltashov, I. A. Interaction of transferrin with non-cognate metals studied by native electrospray ionization mass spectrometry *Int. J. Mass Spectrom.* 2017, *420*, 74

8. Edwards, K. C.; Kim, H.; Vincent, J. B. Release of trivalent chromium from serum transferrin is sufficiently rapid to be physiologically relevant *J. Inorg. Biochem.* 2020, *202*, 110901

9. Edwards, K. C.; Kim, H.; Ferguson, R.; Lockart, M. M.; Vincent, J. B. Significance of conformation changes during the binding and release of chromium(III) from human serum transferrin *J. Inorg. Biochem.* 2020, *206*, 111040

10. Rhodes, N. R.; LeBlanc, P. A.; Rasco, J. F.; Vincent, J. B. Monocarboxylate transporters are not responsible for Cr^{3+} transport from endosomes *Biol. Trace Elem. Res.* 2012, *148*, 409

11. Gullick, B.M. Characterizing the potential therapeutic agent $[Cr_3O(O_2CCH_2CH_3)_6(H_2O)_3]^+$: its uptake and subcellular distribution and the effects of its oral administration on blood variables. Ph.D. dissertation, The University of Alabama, 2005

12. Yamamoto, A.; Wada, O.; Ono T. A low-molecular-weight, chromium-binding substance in mammals. *Toxicol. Appl. Pharmacol.* 1981, 59, 515

13. Yamamoto, A.; Wada, O.; Ono, T. Distribution and chromium-binding capacity of a low-molecular-weight, chromium-binding substance in mice *J. Inorg. Biochem.* 1984, *22*, 91.

14. Viera, M.; Davis-McGibony, C. M. Isolation and characterization of low-molecular-weight chromium-binding substance (LMWCr) from chicken liver *The Protein Journal* 2008, *27*, 371

15. Wada, O.; Wu, G. Y.; Yamamoto, A.; Manabe, S.; Ono, T. Purification and chromium-excretory function of low-molecular-weight, chromium-binding substances from dog liver *Environ.* 1983, *32*, 228

16. Hatfield, M. J.; Gillespie, S.; Chen, Y.; Li, Z.; Cassady, C. J.; Vincent, J. B. Low-molecular-weight chromium-binding substance from chicken liver and american alligator liver *Comp. Biochem. Physiol. B Biochem. Mol. Biol.* 2006, *144*, 423

17. Vincent, J. B. Chromium(III) and low molecular weight peptides *Encyclopedia of Metalloproteins* 2013, 645

18. Chen, Y.; Watson, H. M.; Gao, J.; Sinha, S. H.; Cassady, C. J.; Vincent, J. B. Characterization of the organic component of low-molecular-weight chromium-binding substance and its binding of chromium *J. Nutr.* 2011, *141*, 1225

19. Arakawa, H.; Kandadi, M. R.; Panzhinskiy, E.; Belmore, K.; Deng, G.; Love, E.; Robertson, P. M.; Commodore, J. J.; Cassady, C. J.; Nair, S.; Vincent, J. B. Spectroscopic and biological activity studies of the chromium-binding peptide EEEEGDD *J. Biol. Inorg. Chem.* 2016, *21*, 369

20. Aramini, J. M.; Vogel, H. J. Aluminum-27 and Carbon-13 NMR studies of aluminum(3+) binding to ovotransferrin and its half-molecules *J. Am. Chem. Soc.* 1993, *115*, 245

21. Deng, G.; Wu, K.; Cruce, A. A.; Bowman, M. K.; Vincent, J. B. Binding of trivalent chromium to serum transferrin is sufficiently rapid to be physiologically relevant. *J. Inorg. Biochem.* 2015, 143, 48

22. Davis, C. M.; Vincent, J. B. Isolation and characterization of a biologically active chromium oligopeptide from bovine liver *Arch. Biochem. Biophys.* 1997, *339*, 335

23. De Bernardo, S.; Weigele, M.; Toome, V.; Manhart, K.; Leimgruber, W.; Böhlen, P.; Stein, S.; Udenfriend, S. Studies on the reaction of fluorescamine with primary amines *Arch. Biochem. Biophys.* 1974, *163*, 390

24. Turkewitz, A.P.; Amatruda, J. F.; Borhani, D.; Harrison, S. C.; Schwartz, A. L. A high yield purification of the human transferrin receptor and properties of its major extracellular fragment. *J. Biol. Chem*, 1988, 263, 8318

25. Cheng, Y.; Zak, O.; Aisen, P.; Harrison, S. C.; Walz, T. Structure of the human transferrin receptor-transferrin complex *Cell* 2004, *116*, 565

26. Smith, N.; Witham, S.; Sarkar, S.; Zhang, J.; Li, L.; Li, C.; Alexov, E. DelPhi Web server v2: incorporating atomic-style geometrical figures into the computational protocol *Bioinformatics* 2012, *28*, 1655

27. Sarkar, S.; Witham, S.; Zhang, J.; Zhenirovskyy, M.; Rocchia, W.; Alexov, E. DelPhi web server: a comprehensive online suite for electrostatic calculations of biological macromolecules and their complexes *Commun. Comput. Phys.* 2013, *13*, 269

28. Morris, G. M.; Huey, R.; Lindstrom, W.; Sanner, M. F.; Belew, R. K.; Goodsell, D. S.; Olson, A. J. AutoDock4 and AutoDockTools4: automated docking with selective receptor flexibility *J. Comput. Chem.* 2009, *30*, 2785

29. Trott, O.; Olson A.J. AutoDock Vina: Improving the speed and accuracy of docking with a new scoring function, efficient optimization, and multithreading. *J. Comput. Chem.*, 2010, 31, 455-461

30. Yamamoto, A.; Wada, O.; Ono, T. Isolation of a biologically active low-molecular-mass chromium compound from rabbit liver *Eur. J. Biochem.* 1987, *165*, 627

31. Wu, G.Y.; Wada, O. Studies on a specific chromium binding substance (a low-molecular-weight chromium binding substance) in urine *Jpn. J. Ind. Health* 1981 23 505-512

32. Jacquamet, L.; Sun, Y.; Hatfield, J.; Gu, W.; Cramer, S. P.; Crowder, M. W.; Lorigan, G. A.; Vincent, J. B.; Latour, J.-M. Characterization of chromodulin by X-ray absorption and electron paramagnetic resonance spectroscopies and magnetic susceptibility measurements *J. Am. Chem. Soc.* 2002, *125*, 774

33. Sun, Y.; Ramirez, J.; Woski, S. A.; Vincent, J. B. The binding of trivalent chromium to low-molecular-weight chromium-binding substance (LMWCr) and the transfer of chromium from transferrin and chromium picolinate to LMWCr *J. Biol. Inorg. Chem.* 2000, *5*, 129

34. Aisen, P., Aasa, R., Redfield A. G. Chromium, manganese, and cobalt complexes of transferrin. *J. Biol. Chem.* 1969 *244*, 4628

35. Carver, F. J.; Frieden, E. Factors affecting the adenosine triphosphate induced release of iron from transferrin *Biochemistry* 1978, *17*, 167

36. Harris, W. R. Anion binding properties of the transferrins implications for function *Biochim Biophys Acta Gen Subj* 2012, *1820*, 348

37. Benjamín, J. A.; Cardona, A. E.; Vázquez, Á. L.; Dones, C. Y.; Pabón, H. L.; Rodríguez, H. M.; Rodríguez, I.; González, J. C.; Pazol, J.; Pérez-Ríos, J. D.; Catala, J. F.; Carrasquillo, M.; De Jesus, M. G.; Cordero, N. A.; Cruz, P. M.; González, P.; Hernández, R.; Gaur, K.; Loza, S. A.; Tinoco, A. D. Exploring serum transferrin regulation of nonferric metal therapeutic function and toxicity *Inorganics* 2020, *8*, 48

38. Byrne, S. L.; Chasteen, N. D.; Steere, A. N.; Mason, A. B. The unique kinetics of iron release from transferrin: the role of receptor, lobe–lobe interactions, and salt at endosomal pH *J. Mol. Biol* 2010, *396*, 130

39. Petersen, C. M.; Edwards, K. C.; Gilbert, N. C.; Vincent, J. B.; Thompson, M. K. X-ray structure of chromium(III)-containing transferrin: first structure of a physiological cr(III)-binding protein *J. Inorg. Biochem.* 2020, *210*, 111101

40. Yang, N.; Zhang, H.; Wang, M.; Hao, Q.; Sun, H. Iron and bismuth bound human serum transferrin reveals a partially-opened conformation in the N-lobe *Sci. Rep.* 2012, *2*

41. Levina, A.; Lay, P. A. Transferrin cycle and clinical roles of citrate and ascorbate in improved iron metabolism *ACS Chem. Biol* 2019, *14*, 893

42. Levina, A.; Lay, P. A. Vanadium(V/IV)-transferrin binding disrupts the transferrin cycle and reduces vanadium uptake and antiproliferative activity in human lung cancer cells *Inorg. Chem.* 2020, *59*, 16143

43. Huebers, H.; Bauer, W.; Huebers, E.; Csiba, E.; Finch, C. The behavior of transferrin iron in the rat *Blood* 1981, *57*, 218

44. Foley, A. A.; Bates, G. W. The influence of inorganic anions on the formation and stability of iron(3+)-transferrin-anion complexes *Biochim. Biophys. Acta.* 1988, *965*, 154

45. Anderson, R. A.; Bryden, N. A.; Polansky, M. M. Lack of toxicity of chromium chloride and chromium picolinate in rats *J. Am. Coll. Nutr.* 1997, *16*, 273

46. Fernandez-Real, J. M.; Lopez-Bermejo, A.; Ricart, W. Cross-Talk between iron metabolism and diabetes *Diabetes* 2002, *51*, 2348

47. Ciechanover, A.; Schwartz, A. L.; Dautry-Varsat, A.; Lodish, H. F. Kinetics of internalization and recycling of transferrin and the transferrin receptor in a human hepatoma cell line effect of Lysosomotropic agents *J. Biol. Chem* 1983, *258*, 9681

48. Dunaway-Mariano, D.; Cleland, W. W. Preparation and properties of chromium(III) adenosine 5'-triphosphate, chromium(III) adenosine 5'-diphosphate, and related chromium(III) complexes *Biochemistry* 1980, *19*, 1496

49. Guo, M.; Sun, H.; McArdle, H. J.; Gambling, L.; Sadler, P. J. TiIV uptake and release by human serum transferrin and recognition of Ti(IV)-transferrin by cancer cells: understanding the mechanism of action of the anticancer drug Titanocene Dichloride *Biochemistry* 2000, *39*, 10023

Table 5.1. First-order rate constants for Cr(III) loss from $Cr(III)_2$-Tf at pH 5.5. SD – standard deviation.

Tf lobe	Chelating Ligand	k (min^{-1})	SD (min^{-1})	$t_{1/2}$ (min)	Ref.
N-lobe	none	0.0014	0.0002	5.0×10^2	[9]
N-lobe	EDTA	0.0033	0.0009	2.1×10^2	[9]
N-lobe	citrate	0.0030	0.0004	2.3×10^2	[9]
N-lobe	ascorbate	0.0036	0.0009	1.9×10^2	[9]
N-lobe	apoLMWCr	0.0170	0.0021	4.1×10^1	this work
C-lobe	none	0.12	0.01	5.6	[9]
C-lobe	apoLMWCr	0.38	0.04	1.8	this work

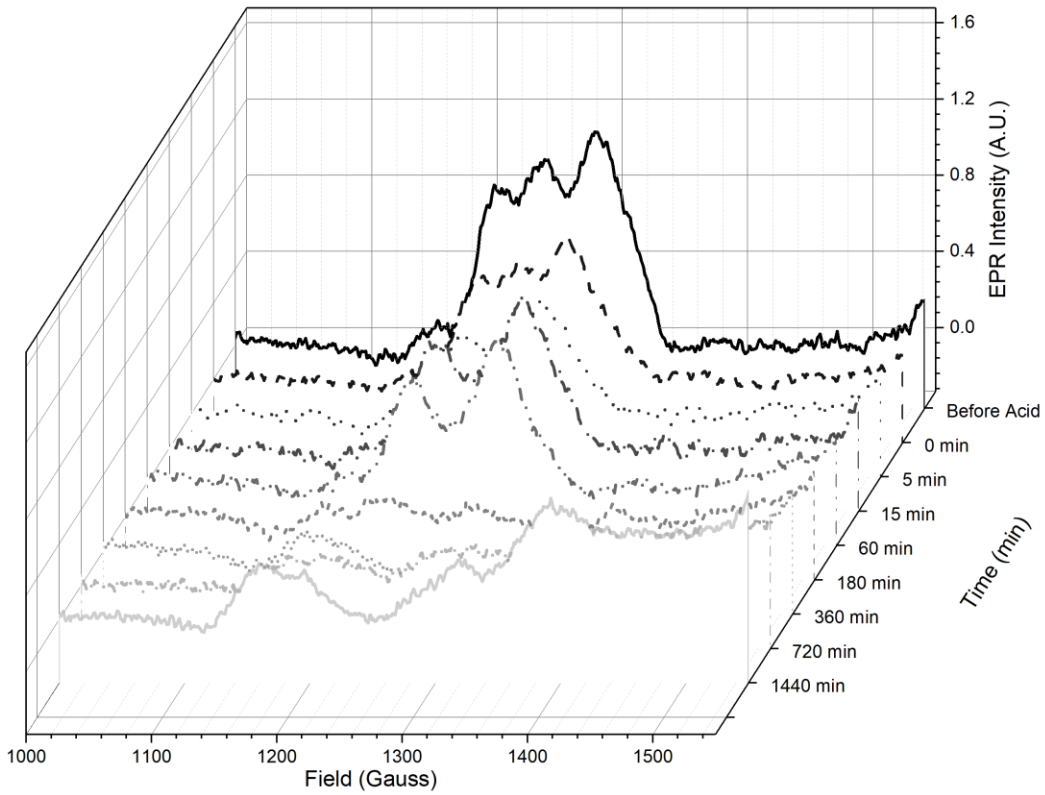

Figure 5.1. EPR spectra of $Cr(III)_2Tf$ in 100 mM HEPES with 25 mM HCO_3^- at 37 ^oC at various times after the addition of acid to change the pH to 5.5 in the presence of 0.48 mM LMWCr. Features at 1210 and 1285 G (g = 5.1 and g = 5.6) correspond to Cr(III) in the N-lobe metal-binding site. The feature at 1245 G (g = 5.4) corresponds to Cr(III) in the C-lobe metal-binding site. The broad feature at centered 1500 G corresponds to LMWCr.

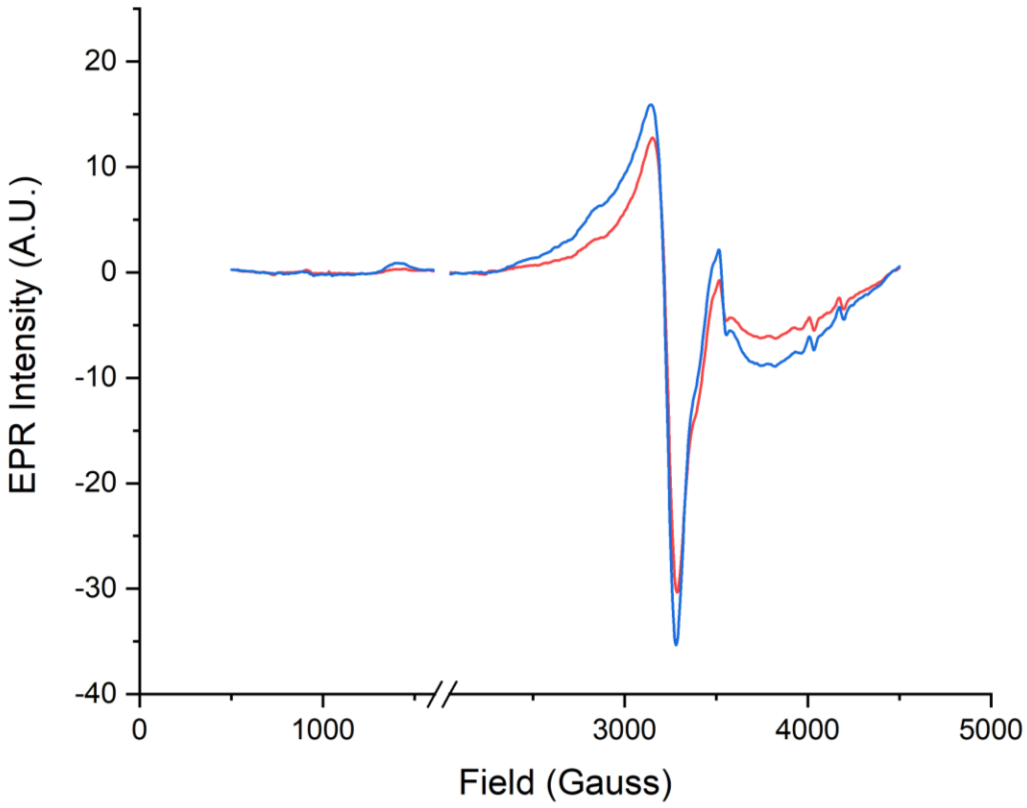

Figure 5.2. EPR spectra of bovine liver LMWCr (blue) (protein concentration 1.55 x 10^{-3} M) and bovine liver apoLMWCr reconstituted with Cr(III) (red) (protein concenctration 4.82 x 10^{-4} M) at pH 5.5 and 77 K.

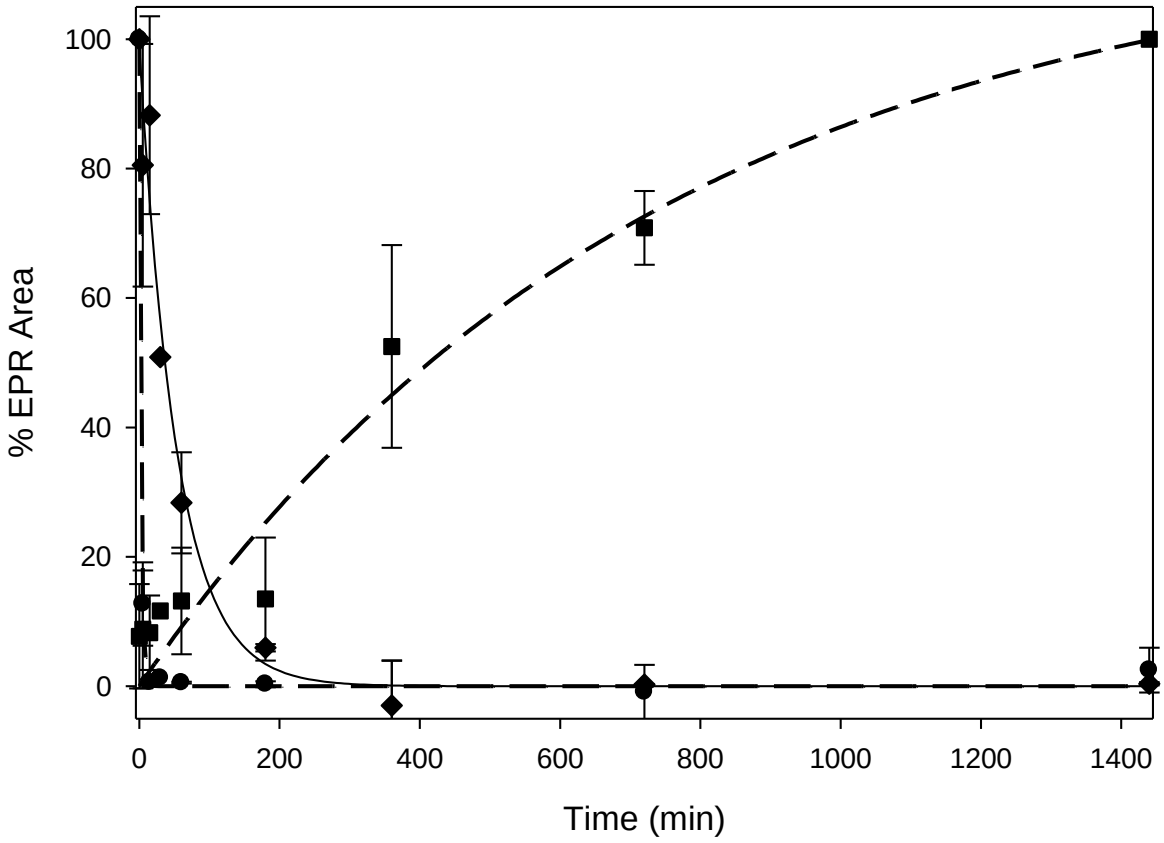

Figure 5.3. Loss of Cr(III) from $Cr(III)_2Tf$ in the presence of apoLMWCr and the appearance of LMWCr at pH 5.5. Black circles represent C-lobe bound Cr(III)-Tf. Black diamonds represent Cr(III) bound N-Lobe of Tf. Black squares represents Cr(III)-LMWCr

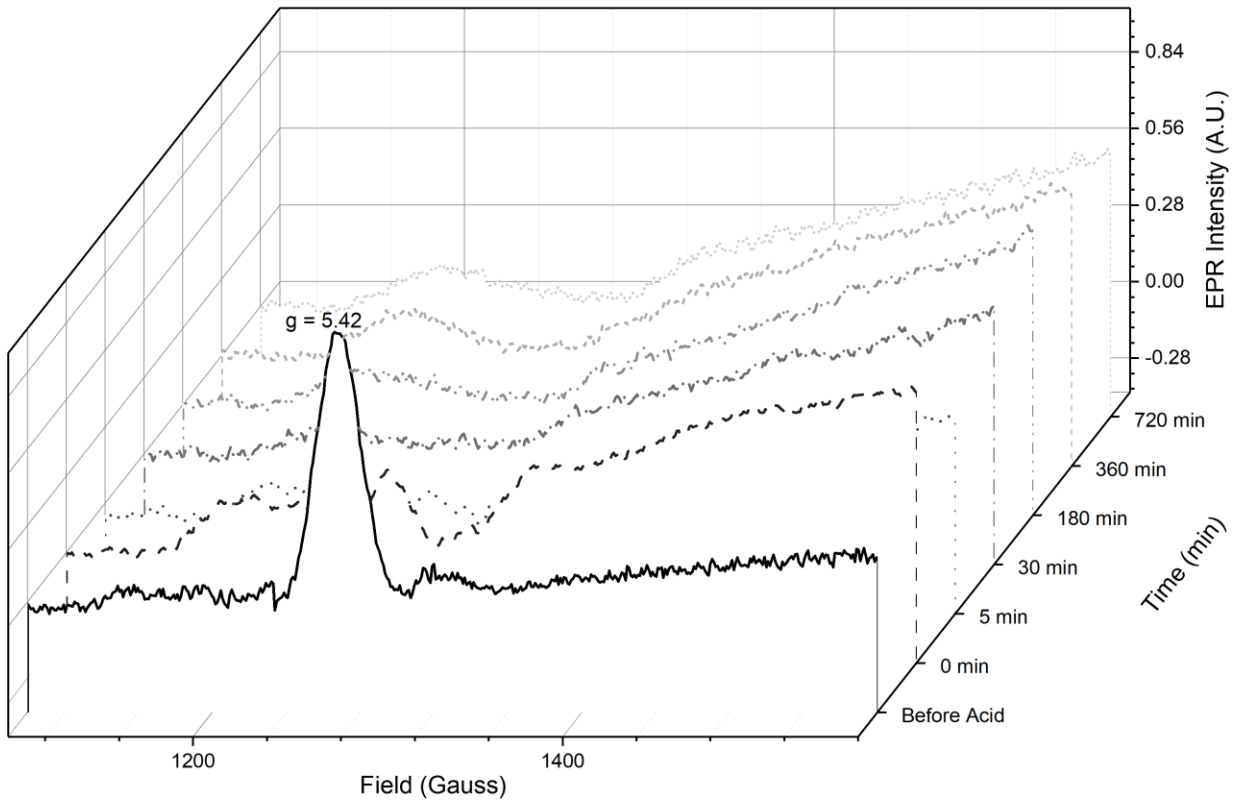

Figure 5.4. EPR spectra of $Cr(III)_2Tf/Tf$ receptor complex in the presence of apoLMWCr in 100 mM HEPES with 25 mM HCO_3^- at 37 ^oC at various times after the addition of acid to change the pH to 5.5 in the presence of 0.48 mM LMWCr. The feature at 1250 G (g = 5.4) corresponds to Cr(III) in the metal-binding sites of Tf. The feature at 1500 G corresponds to LMWCr.

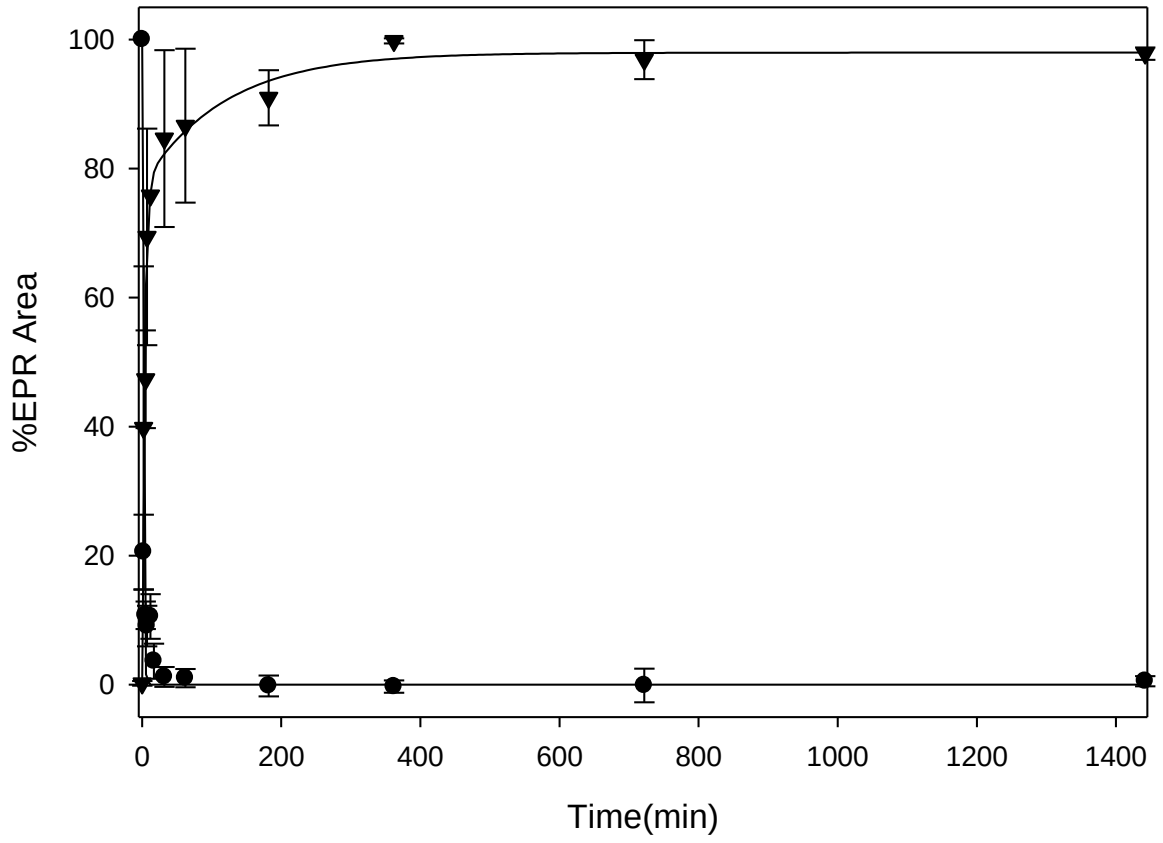

Figure 5.5. Loss of Cr(III) from $Cr(III)_2$Tf/Tf-sTfR complex in the presence of apoLMWCr and the appearance of LMWCr at pH 5.5. Black circles represent Cr(III)-Tf-sTfR. Black triangles represent Cr(III)-LMWCr.

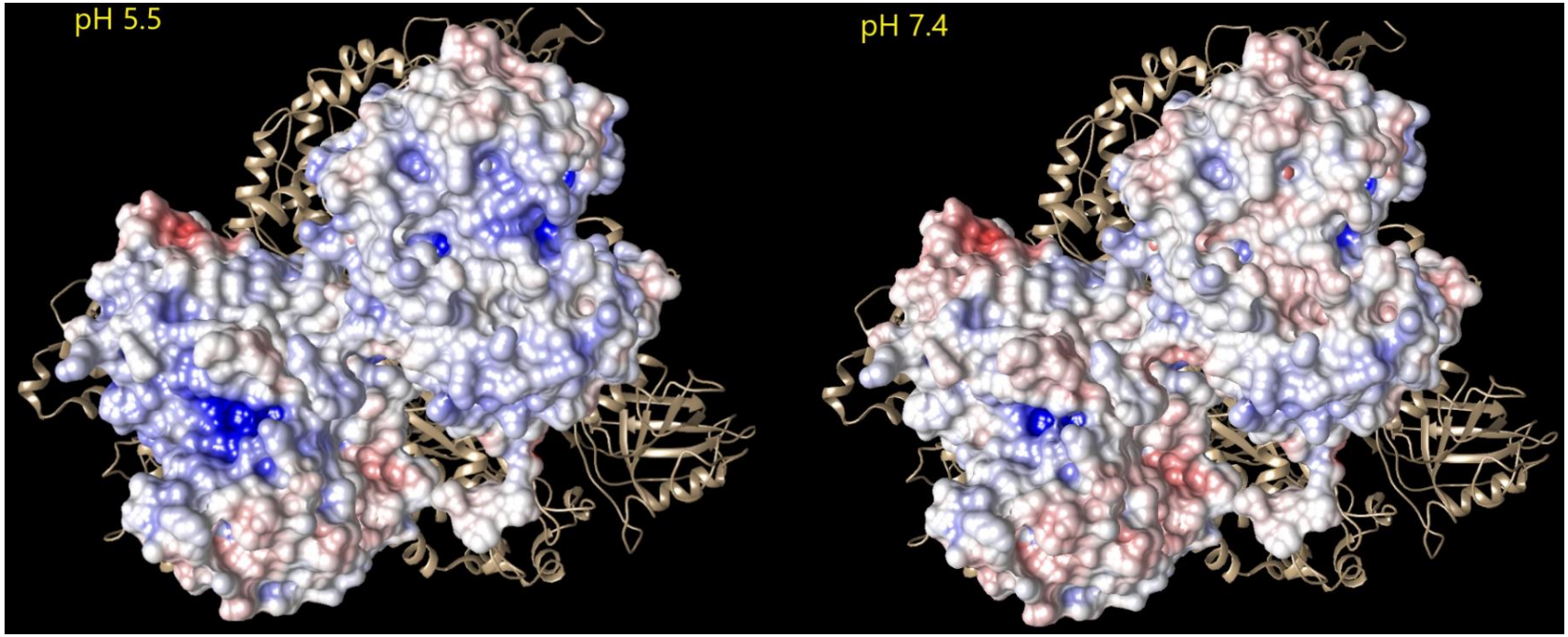

Figure 5.6. Electrostatic potential surface of one Tf molecule of the $(Fe(III)_2\text{-}Tf)_2$/Tf receptor complex at pH 7.4 (right) and pH 5.5 (left).

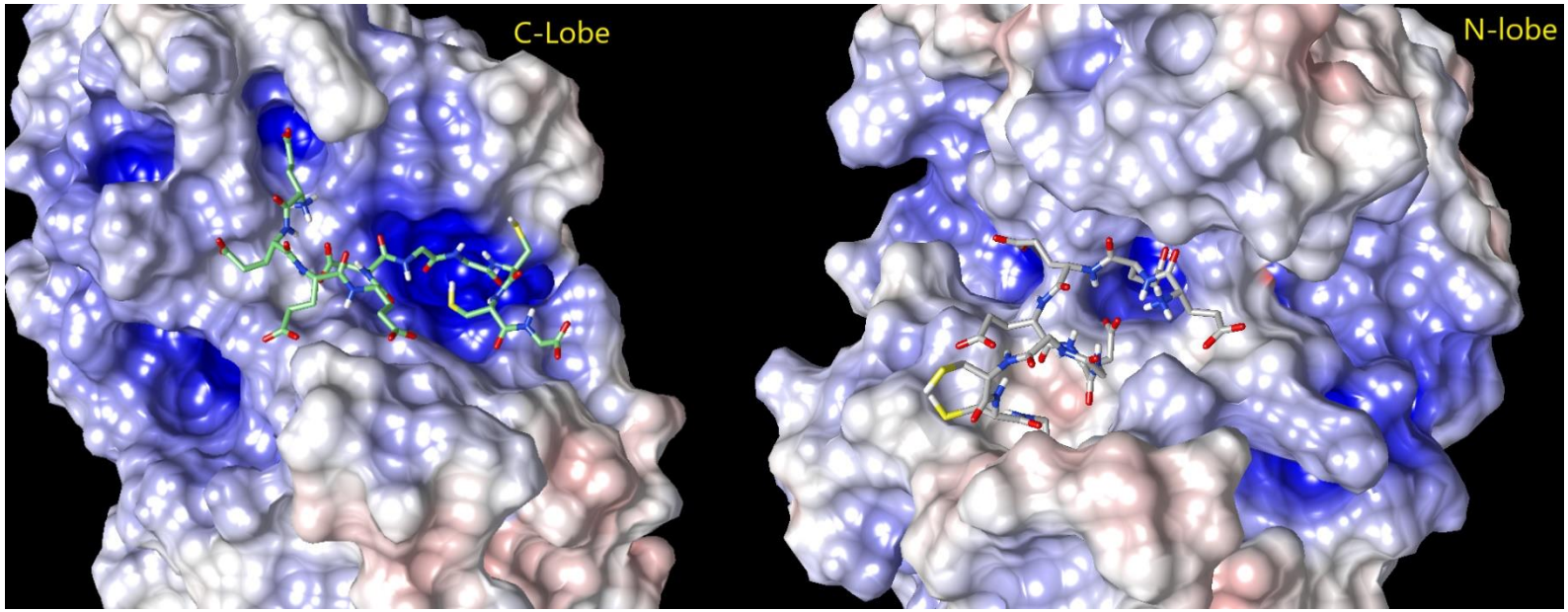

Figure 5.7. Docking LMWCr to $Fe(III)_2$-Tf at pH 5.5.

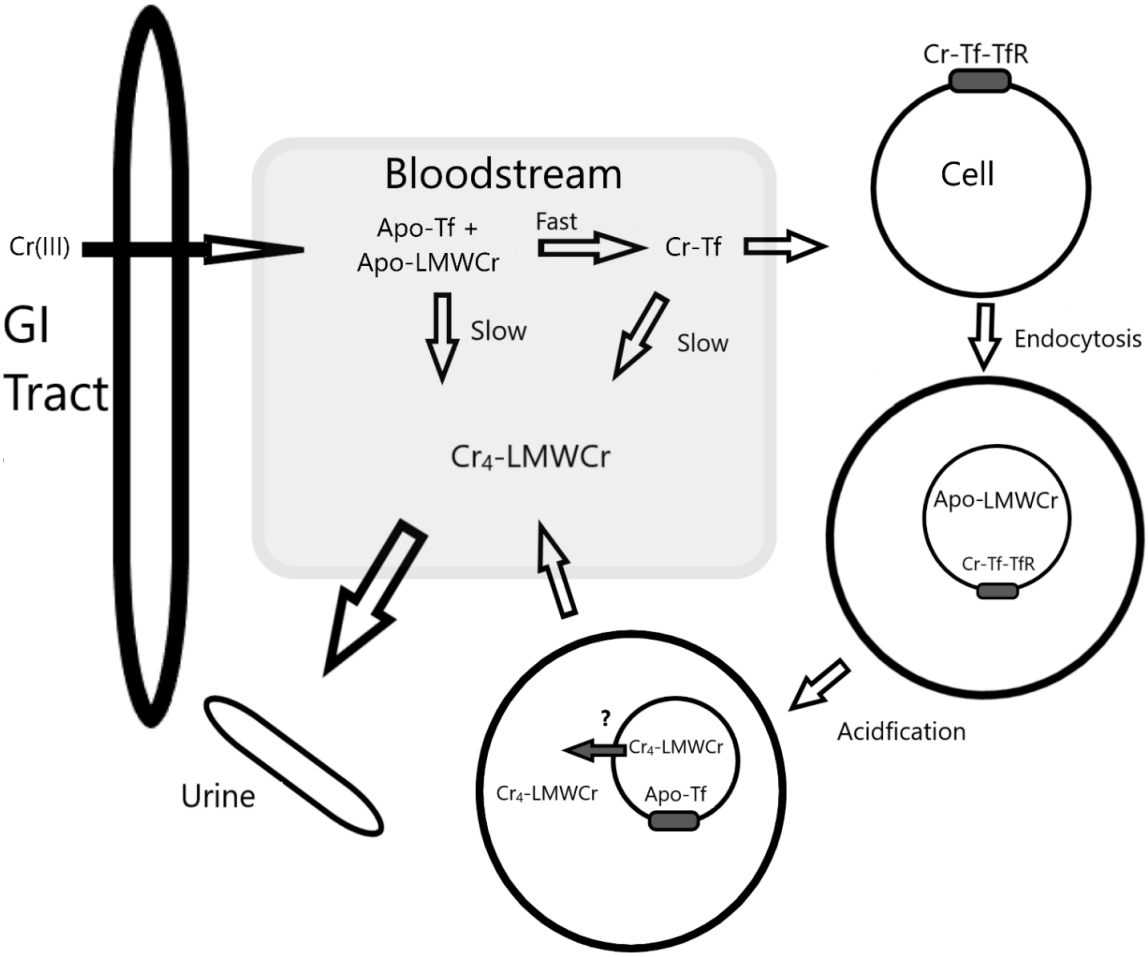

Figure 5.8. Movement of Cr(III) from the gastrointestinal tract to the bloodstream, tissues, and urine. Cr(III) is absorbed by passive diffusion into the bloodstream where it binds rapidly at pH 7.4, ~25 mM HCO_3^- to Tf. Cr(III) binding to apoLMWCr and transfer of Cr(III) from Cr(III)-Tf to apoLMWCr is slow. Cr(III)-Tf binds to the Tf receptor (TfR) and undergoes endocytosis. Acidification of the endosome results in the rapid release of Cr(III) from the Tf/TfR complex with its binding to apoLMWCr. The Cr(III)-loaded LMWCr then either passes through the endosome membrane via an unknown mechanism to deliver Cr(III)-loaded LMWCr to the cell, where the Cr(II)-loaded is subsequently is expelled from the cell into the bloodstream or is delivered to the bloodstream by the fusing of the endosome with the cell membrane. Cr(III)-loaded LMWCr in the bloodstream is removed by the kidneys and the excreted from the body in urine.

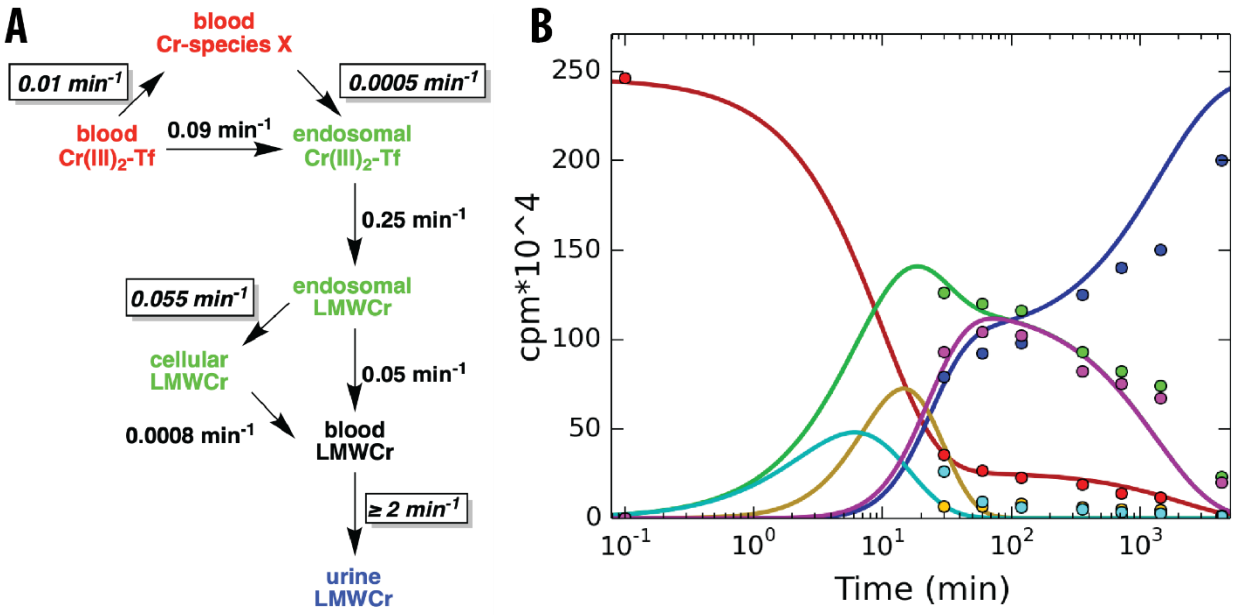

Figure 5.9. Kinetic model and simulation of Cr(III) transport. A) Proposed kinetic mechanism for Cr(III) transport. Text colors correlate with data and simulation traces shown in panel B with total blood transferrin (red) and urine LMWCr (blue). The difference between the blood transferrin and the urine LMWCr data is shown as total tissue (green). The non-boxed rates were fixed based on previously reported measurements. Rate values outlined in boxes were determined manually from the simulation. B) Data for ^{51}Cr(III) measurement in total blood, urine, and tissue are shown as filled red, blue, and green circles. Additional experiments were able to quantify specific Cr(III)-containing species in hepatic cells including endosomal Cr(III)$_2$-Tf (cyan), endosomal LMWCr (yellow), and cellular LMWCr (magenta). The sum of these three species is represented by the green circles. Solid lines represent the simulated totals for each species using the rates listed in panel A.

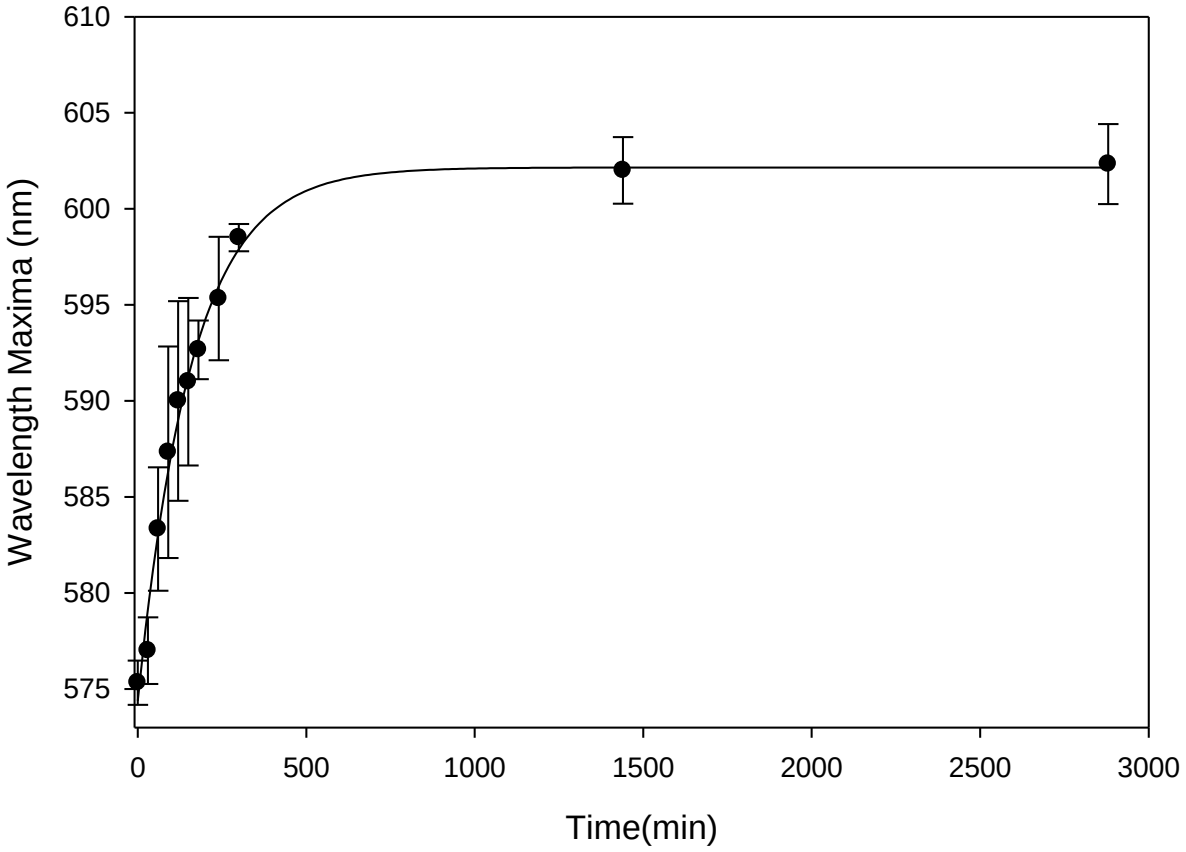

Figure 5.10. Visible maximum as a function of time for the reaction of Cr^{3+} and ATP at pH 5.5 at 37 ^{o}C.

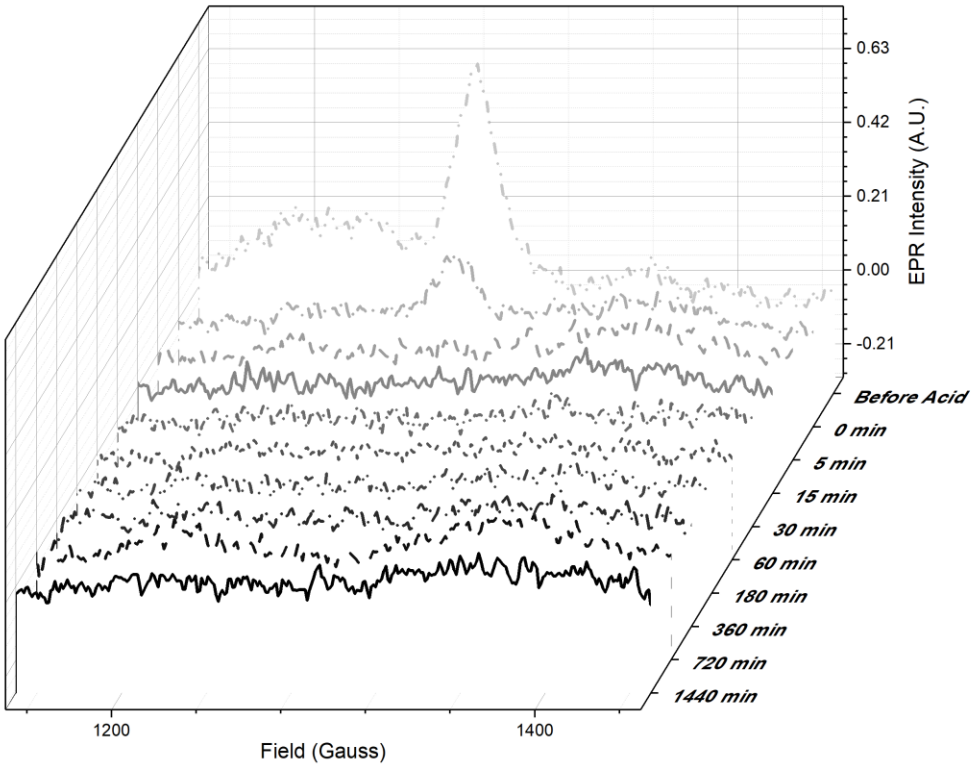

Figure 5.11. EPR spectra of $Cr(III)_2$-Tf/Tf receptor complex in the presence of 0.5 mM ATP in 100 mM HEPES with 25 mM HCO_3^- at 37 ºC at various times after the addition of acid to change the pH to 5.5. The feature at 1250 G (g = 5.4) corresponds to Cr(III) in the metal-binding sites of Tf.

ELECTRON PARAMAGNETIC SPECTRUM OF DIMANGANIC HUMAN SERUM TRANSFERRIN

1. Introduction

Manganese (Mn) is an important biological trace element, being a necessary cofactor in numerous biological reactions and potentially toxic when over accumulated. The transport of manganese to tissues has been studied in great depth in the past thirty years; the predominant pathways by which Mn enters cells is in its divalent state through divalent metal transporter 1 (DMT1), as Mn(II)-citrate complex, and through zinc transport proteins [1-3]. The transport of trivalent Mn has also been studied and appears to be accomplished primarily utilizing transferrin (Tf) mechanism. Transferrins are class of serum protein specialized to bind and transport Fe(III); the proteins consist of two similar lobes (N or C lobe), each possessing a single metal binding site. The binding sites are virtually identical and are composed of 2 ASP, 1 TYR, and 1 HIS (Figure 6.1). Nearby the metal binding site is an anion binding site that is typically occupied by a (bi)carbonate ion, which binds through two carboxylates with the nearby metal. The binding sites are optimized for binding Fe(III) and do so with extremely high affinity at pH 7.4; however, in serum, Tf is typically only ~30% loaded with Fe(III), which leaves numerous open sites on Tf for other metals to bind including Mn(III). Consequently, Mn(III)-Tf could play a physiological role in Mn transport, although the significance, if any, of this transport is poorly understood and appears to be limited [1-3]. The importance of manganese transport by transferrin in healthy individuals has not been established. Because of the toxic effects of Mn bioaccumulation, most research on Mn-transferrin has focused on Mn transport across the blood–brain barrier or Mn

incorporation into neural cells (for example, Refs. [4-28]). The significance of Tf in transport of manganese across the blood–brain barrier is still under investigation.

Serum apotransferrin (apoTf) binds two equivalents of Mn, one in each of the protein's two metal-binding sites in separate lobes of the protein, and the complex possesses an intense visible absorption band (maximum at ~429 nm) with an extinction coefficient of ~9 x 10^3 $M^{-1}cm^{-1}$, giving $Mn(III)_2$-Tf a distinct brown color [28-32]. The presence of the visible charge transfer band suggests Mn was binding as the trivalent ion. Additional spectroscopic and magnetic studies of $Mn(III)_2$-Tf reveal the protein bound the two Mn ions concurrent with 0.93 (bi)carbonate per Mn [31]. $Mn(III)_2$-Tf has no EPR signal (in the conventional perpendicular mode) at 4.2 K, while static magnetic susceptibility measurements are consistent with the presence of two S = 2 centers, confirming that Mn^{3+} is the form bound [31]. $Mn(III)_2$-Tf has ultraviolet/visible maxima at 295, 330, and 430 nm. The development of the intense brown color does not require the addition of hydrogen peroxide and is significantly slower under anaerobic conditions, suggesting air oxidation of Mn(II) to Mn(III) [31]. Slow oxidation of coordinated Mn(II) to Mn(III) has been confirmed by X-ray absorption spectroscopy [33].

Mn(III) exists at much lower levels than Mn(II) in the body (according to X-ray absorption near edge structure spectroscopy) and is stabilized by in low pH and as certain complexes [33]. Tf has been shown to stabilize Mn(III) and would be capable of potentially transporting the ion, analogous to Fe(III) transport. The interaction of Mn(III) with Tf that has primarily studied using visible and infrared spectroscopies; some CW-EPR studies have been performed looking at Mn binding to Tf as Mn(III); however these studies looked at loss of the EPR signal arising from Mn (II) rather than probing the appearance of Mn(III) directly. This is due to Mn(III) possessing an integer spin and thus being silent in traditionally perpendicular EPR

setups. Consequently, tracking the fate of $Mn(III)_2$-Tf under biological conditions previously proved difficult due to the lack of a convenient or robust spectroscopic tool. Parallel mode EPR can potentially be useful in monitoring the Mn(III)-Tf interactions as the integral $S = 2$ center of the Mn(III) is expected to give rise a signal in this mode. This spectroscopic tool is promising as a biological probe in further studies investigating Mn(III)-Tf as EPR has previously been shown to be a powerful tool in analysis of Fe(III)-Tf and Cr(III)-Tf. Thus, the aim of this work is to obtain an EPR spectrum of Mn(III)-Tf

2. Experimental

2.a. Materials

Iron-free human serum Tf was obtained from Aldrich (St. Louis, MO). Doubly deionized water was used throughout. All reagents were used as received unless otherwise notes. Mn(II) solutions were prepared using $MnCl_2 \cdot 4H_2O$ unless otherwise noted. ApoTf concentrations were determined by using the extinction coefficient ($\varepsilon = 9.12 \times 10^4\ M^{-1}cm^{-1}$) at 280 nm [46].

2.b. Preparation of $Mn(III)_2$-transferrin

Dimanganic-Tf was prepared using a variation of the literature procedure [32]. Human serum apo-Tf solution was dissolved in a 100 mM HEPES, 15 mM $NaHCO_3$ buffer at pH 7.4. An aliquot of Mn(II) solution was added to a solution of apo-Tf to give a Mn(II) to Tf ratio of 1.6:1. The electronic spectrum of the solution was monitored over several days, and the concentration of Mn(III) bound to transferrin was determined using the extinction coefficient ($\varepsilon = 8.7 \times 10^3\ M^{-1}cm^{-1}$) at 427 nm [32]; after one week, all added Mn(II) was converted to Tf-bound Mn(III) within experimental error. Prior to EPR analysis, a portion of the $Mn(III)_2$-Tf solution was passed over a G-15 column equilibrated with 100 mM HEPES, 15 mM $NaHCO_3$ buffer to

remove any remaining Mn(II). Samples were frozen for EPR analysis with glycerol added to the solution (20/80 v/v).

2.c. Instrumentation

Ultraviolet-visible spectra were obtained using a Beckman Coulter (Brea, CA) DU800 UV-visible spectrophotometer.

2.d. EPR spectroscopy

Continuous wave (CW) EPR measurements were made on a Bruker (Billerica, MA) ELEXSYS E540 X-band spectrometer equipped with an ER 4116 dual mode resonator, an Oxford ESR900 cryostat, and an Oxford ITC 04 temperature controller for temperature-dependent measurements. Spectra were recorded in both parallel and perpendicular mode at temperatures ranging from 4-60 K. Measurements used a nominal microwave frequency of 9.65 GHz and 9.41 GHz for microwave field polarization transverse and parallel to the applied magnetic field, respectively. Unless otherwise stated, all spectra were collected under non-saturating conditions with a modulation amplitude of 0.9 mT and a modulation frequency of 100 kHz.

2.e. Data analysis

Dr. Brad Pierce (The University of Alabama) performed data analysis and simulations of the various spectra. CW EPR spectra were processed and simulated using SpinCount (version 6.4.7614.18037), which was developed by Professor Michael Hendrich at Carnegie Mellon University [47]. Parallel-mode Mn(III) ($S = 2$) spectra were simulated with the spin Hamiltonian,

Equation 1 $$\widehat{H} = \beta_e \vec{B}_0 \cdot \widetilde{\boldsymbol{g}} \cdot \hat{S} + \boldsymbol{D}\left(\hat{S}_Z^2 - \frac{\hat{S}^2}{3}\right) + \boldsymbol{E}\left(\hat{S}_X^2 + \hat{S}_Y^2\right) + \hat{S} \cdot \widetilde{\boldsymbol{A}} \cdot \hat{I}$$

where D and E describe the zero-field splitting terms, $\tilde{\boldsymbol{g}}$ is the g-tensor, and $\tilde{\boldsymbol{A}}$ is the nuclear hyperfine interaction, which is treated with second-order perturbation theory [48]. Simulations were calculated via diagonalization of Equation 1 and take into consideration all intensity factors, both theoretical and experimental. The concentration of species can be used as a constraint during spectral simulation, which allows quantitative determination of the concentration by comparison of the experimental and simulated signal intensities [47,49]. The only unknown factor relating the spin concentration to signal intensity is an instrumental factor that depends on the microwave detection system. This factor is determined using a Cu(II)EDTA spin standard [50].

3. Results and Discussion

Both the perpendicular and parallel mode CW-EPR spectra of $Mn(III)_2$-Tf were examined (Figure 6.2). In perpendicular mode, a broad resonance can be seen near g=2 with a sharp 6-line hyperfine pattern characteristic of hexaaquaMn(II). This is expected for the S=5/2 ion at X-band frequencies as the microwave quantum (~9 GHz, $h\nu \sim 0.3$ cm^{-1}) exceeds the axial zero field splitting of Mn(II) (D< 0.3 cm^{-1}) resulting in a signal centered at g~2. The signal width indicates that the Mn(II) species is likely not homogenous most likely due to advantageous binding of Mn(II) to nonspecific sites on the surface of Tf (nonspecific binding of Fe(III) and Cr(III) has been observed previously under certain conditions). The hyperfine splitting (~250 MHz) is broad but characteristic of ^{55}Mn(II) (I=5/2). The signal intensity of this Mn(II) from solution is large compared to its parallel mode signal due to the nature of its transitions. Due to the zero field splitting being less than the applied external field (D< $h\nu$), the degeneracy between the doublets is not lifted in the external field, and transitions are observed simultaneously; this results in an increase of intensity ~11.667 fold (i.e. 35/3) compared to a single transition.

Estimation of this Mn(II) signal area corresponds to ~ 40 μM in solution or ~6 % of the total Mn present. This is in good agreement with UV-Vis which found the visible transitions of Mn(III)-Tf to account for ~98% of the managase added using the extinction coefficient 8.7 x 10^3 M^{-1} cm^{-1} reported previously [32]. A trace impurity of $Fe(III)_2$-Tf is also observed in the perpendicular mode spectra at g~4.3, but it accounts for very little of the total protein concentration.

Parallel microwave field polarization allows for a new signal to be observed at g~8.3; this new signal similarly has a 6-line hyperfine pattern characteristic of ^{55}Mn (I = 5/2) nuclear coupling. The signal arising in parallel mode polarization is indicative of an integer spin transition. Furthermore, the effective g-value for an integer spin doublet transitions can be estimated as ~4 times the difference in spin state (i.e. transitions with a $\cdot\Delta m_s$ of | ±1 >, | ±2 >, and | ±3 > would be expected around g~ 4, 8, and 12, respectively). Thus, the observed signal at g~8.3 is attributed to a ±2 transition of Mn(III) (Figure 6.3); the observed decrease in signal intensity with increasing temperature is also consistent with a transition within the ground | ± 2 > doublet (discussed below). The hyperfine splitting (158 MHz) is similarly consistent of ^{55}Mn(III) (I=5/2) from previously reported Mn(III)-bound enzymes, and the narrower spacing is indicative of a homogenous species as expected for Mn(III) in the binding site of Tf [52-56].

Further analysis of the g~ 8.3 signal observed in parallel gave an axial-zero field splitting value of D = -5 ± 1 cm^{-1}. This was determined by fitting the temperature normalized g ~ 8.3 signal observed in parallel mode EPR to a theoretical Boltzmann population distribution for a S = 2 spin system (Equation 2).

Equation 2
$$Intensity \times T \sim n_s = \frac{g_i . e^{-\Delta E_i / k_b T}}{\sum_j g_j \cdot e^{-\Delta E_j / k_b T}} = \frac{(2S_i+1) \cdot e^{-DS_{z,i}^2 / k_b T}}{\sum_j (2S_j+1) \cdot e^{-DS_{z,j}^2 / k_b T}}$$

The axial zero-field splitting was also used in simultaneous simulations of the EPR spectra over the temperature range 4 to 45 K. The *D*-value of -4.7 ± 0.5 cm^{-1} was able to accurately reproduce the relative intensity of the multiline feature at g ~ 8.3 for the temperature range; the two values agreed with each other (Figure 6.4). The simulated spectra shown in Figure 6.4 use the measured *D*-value (*D* = -4.7 ± 0.5 cm^{-1}) with a rhombicity (*E*/*D* = 0.08). The (*E*/*D* = 0.08) is low and near axial with $g_{1,2,3}$ (2.01, 2.01, 2.02) and $A_{1,2,3}$(155, 155, 160) MHz. Figure 6.4 only shows the simulated spectrum for 4.3 K; however, the intensity of the g 8.3 signal of Mn(III) was reproduced across the temperature range 4 to 45 K at prescribed intervals. The Mn(III) concentration predicted by these simulations was approximately 0.9±0.2 mM and agrees with values from the visible electronic spectra. The EPR simulated spectra were best fit with a single set of g-values, A-values, and zero field terms indicating uniformity between the N and C lobe binding sites, i.e. they cannot be distinguished by EPR. Some conformations of the protein allow differentiation of the metals at the binding sites; however, the binding sites of Tf are identical in ligand composition and coordination number and conformations of the protein in which the metals are not distinguishable with EPR have been reported for Cr(III). [44]

4. Discussion

Mn(III) complexes have been characterized through parallel mode EPR and the characteristic splitting pattern of 6 lines with ~158 MHz spacing is also observed for the Mn(III) in other Mn-enzymes, oxalate decarboxylase (OxDC) and manganese dependent superoxide dismutase (Mn-SOD). The EPR signal of Mn(III) OxDc bears remarkable resemblance to the one observed in this experiment; Mn(III)-OxDc is a six coordinate site that exhibits a similar negative axial zero field splitting (*D*=-4.0 cm^{-1}). Presumably, the negative axial zero field splitting observed in both molecules is due to Jahn-Teller distortions for the high spin d^4 ion,

which can result in axial elongation (D<0) of the dz^2 orbital; this distortion breaks the degeneracy of the ^5e_g orbitals such that the energy of the dz^2 orbital is lower than dx^2-y^2 resulting in an unoccupied dx^2-y^2 in both cases (both Mn(III) ions are d^4) [52, 53] (representation given in Figure 6.5). The similarities between the Mn(III) in the sites of both proteins indicates coordination of ligands to the metal centers are the same and share the same axial elongation phenomenon. Thus, the Mn(III) site in $Mn(III)_2$-Tf must possess a (bi)carbonate ligand to complete the six coordination (the other 4 ligands provided by 2 Tyr, 1 Asp, 1 His), which is consistent with results showing $Mn(III)_2$-Tf binding with 0.94 equivalents of (bi)carbonate per Mn(III) [31]. This indicates that Mn(III)-Tf is not significantly different compared to native Fe(III)-Tf in coordination number or active site geometry.

5. Conclusion

A parallel mode EPR signal for the manganic centers in $Mn(III)_2$-Tf has been reported. The signal has been characterized through simulation of its signal and analysis of its hyperfine splitting. The results indcate the manganic centers of $Mn(III)_2$-Tf are similar to those reported in other Mn(III) proteins. Additionally, the coordination and active site geometries about the manganic centers in $Mn(III)_2$-Tf do not differ significantly from those of the native Fe(III) ions in Tf. The parallel mode EPR signal presents as a potential tool for future studies investigating the physiological relevance of $Mn(III)_2$-Tf. As an added benefit, the robustness of the manganic center and ease of preparation of $Mn(III)_2$-Tf suggests the protein could serve as an useful spectroscopic model or analog for other Mn(III)-dependent enzymes.

REFERENCES

1. Bjørklund, G.; Dadar, M.; Peana, M.; Rahaman, M. S.; Aaseth, J. Interactions between iron and manganese in neurotoxicity *Arch. Toxicol.* 2020, *94*, 725

2. Vincent, J. B.; Love, S. The binding and transport of alternative metals by transferrin *Biochim. Biophys. Acta* 2012, *1820*, 362

3. Herrera, C.; Pettiglio, M. A.; Bartnikas, T. B. Investigating the role of transferrin in the distribution of iron, manganese, copper, and zinc *J. Biol. Inorg. Chem.* 2014, *19*, 869

4. Suarez, N.; Walum, E.; Eriksson, H. Cellular neurotoxicity of trivalent manganese bound to transferrin or pyrophosphate studied in human neuroblastoma (SH-SY5Y) cell cultures *Toxicol. In Vitro.* 1995, *9*, 717

5. Chua, A. C.; Morgan, E. H. Manganese metabolism is impaired in the belgrade laboratory rat *J. Comp. Physiol. B, Biochem. Syst. Environ. Physiol.* 1997, *167*, 361

6. Takeda, A.; Devenyi, A.; Connor, J. R. Evidence for non-transferrin-mediated uptake and release of iron and manganese in glial cell cultures from hypotransferrinemic Mice *J. Neurosci. Res.* 1998, *51*, 454

7. Thomson, A. B.; Valberg, L. S. Intestinal uptake of iron, cobalt, and manganese in the iron-deficient rat *Am. J. Physiol.* 1972, *223*, 1327

8. Malecki, E. A.; Cook, B. M.; Devenyi, A. G.; Beard, J. L.; Connor, J. R. Transferrin is required for normal distribution of ^{59}Fe And ^{54}Mn in mouse brain *J. Neurol. Sci.* 1999, *170*, 112

9. Takeda, A.; Ishiwatari, S.; Okada, S. Influence of transferrin on manganese uptake in rat brain *J. Neurosci. Res.* 2000, *59*, 542

10. Malecki, E. A. Limited role of transferrin in manganese transport to the brain *J. Nutr.* 2001, *13*, 1584

11. Yokel, R. A. Brain uptake, retention, and efflux of aluminum and manganese. *Environ. Health Perspect.* 2002, *110*, 699

12. Yokel, R.A.; Crossgrove J. S. *Res. Rep. Health Eff. Inst*. 2004, *119* pp. 7-58

13. Yokel, R. A.; Crossgrove, J. S.; Bukaveckas, B. L. Manganese distribution across the blood–brain barrier: I. Evidence for carrier-mediated influx of manganese citrate as well as manganese and manganese transferrin *NeuroToxicology* 2003, *24*, 15

14. Crossgrove, J. Manganese distribution across the blood-brain barrier III: The divalent metal transporter-1 is not the major mechanism mediating brain manganese uptake *NeuroToxicology* 2004, *25*, 460

15. Li, G.; Zhao, Q.; Zheng, W. Alteration at translational but not transcriptional level of transferrin receptor expression following manganese exposure at the blood–csf barrier in vitro *Toxicol. Appl. Pharmacol.* 2005, *205*, 188

16. Reaney, S.; Smith, D. Manganese Oxidation state mediates toxicity in PC12 cells *Toxicol. Appl. Pharmacol.* 2005, *205*, 271

17. Erikson, K.; Aschner, M. Increased manganese uptake by primary astrocyte cultures with altered iron status is mediated primarily by divalent metal transporter *NeuroToxicology* 2006, *27*, 125

18. Li, G. J.; Choi, B.-S.; Wang, X.; Liu, J.; Waalkes, M. P.; Zheng, W. Molecular mechanism of distorted iron regulation in the blood–csf barrier and regional blood–brain barrier following in vivo subchronic manganese exposure *NeuroToxicology* 2006, *27*, 737

19. Garcia, S. J.; Gellein, K.; Syversen, T.; Aschner, M. A Manganese-enhanced diet alters brain metals and transporters in the developing rat *Toxicol. Sci.* 2006, *92*, 516

20. Reaney, S. H.; Bench, G.; Smith, D. R. Brain accumulation and toxicity of Mn(II) and Mn(III) exposures *Toxicol. Sci.* 2006, *93*, 114

21. Gunter, T. E.; Gavin, C. E.; Aschner, M.; Gunter, K. K. Speciation of manganese in cells and mitochondria: a search for the proximal cause of manganese neurotoxicity *NeuroToxicology* 2006, *27*, 765

22. Garcia, S. J.; Gellein, K.; Syversen, T.; Aschner, M. Iron deficient and manganese supplemented diets alter metals and transporters in the developing rat brain *Toxicol. Sci.* 2006, *95*, 205

23. Michalke, B.; Berthele, A.; Mistriotis, P.; Ochsenkühn-Petropoulou, M.; Halbach, S. Manganese species from human serum, cerebrospinal fluid analyzed by size exclusion chromatography-, capillary electrophoresis coupled to inductively coupled plasma mass spectrometry *J. Trace Elem. Med. Biol.* 2007, *21*, 4

24. Wang, X.; Miller, D. S.; Zheng, W. Intracellular localization and subsequent redistribution of metal transporters in a rat choroid plexus model following exposure to manganese or iron *Toxicol. Appl. Pharmacol.* 2008, *230*, 167

25. Nischwitz, V.; Berthele, A.; Michalke, B. Speciation analysis of selected metals and determination of their total contents in paired serum and cerebrospinal fluid samples: an approach to investigate the permeability of the human blood-cerebrospinal fluid-barrier *Anal. Chim. Acta.* 2008, *627*, 258

26. Wang, X.; Li, G. J.; Zheng, W. Efflux of iron from the cerebrospinal fluid to the blood at the blood-csf barrier: effect of manganese exposure *Exp. Biol. Med.* 2008, *233*, 1561

27. Yokel, R. A. Manganese flux across the blood–brain barrier *Neuromolecular Med.* 2009, *11*, 297

28. Williams, B. B.; Kwakye, G. F.; Wegrzynowicz, M.; Li, D.; Aschner, M.; Erikson, K. M.; Bowman, A. B. Altered manganese homeostasis and manganese toxicity in a huntington's disease striatal cell model are not explained by defects in the iron transport system *Toxicol. Sci.* 2010, *117*, 169

29. Vallee, B. L.; Ulmer, D. D. Optically active metalloprotein chromophores ii transferrin and conalbumin *Biochem. Biophys. Res. Commun.* 1962, *8* (5), 331

30. Ulmer, D. D.; Vallee, B. L. Optically active metalloprotein chromophores. III. heme and nonheme iron proteins *Biochemistry* 1963, *2*, 1335

31. Aisen, P.; Aasa, R.; Redfield, A. G. The chromium, manganese, and cobalt complexes of transferrin *J. Biol. Chem.* 1969, *244*, 4628

32. Tomimatsu, Y.; Kint, S.; Scherer, J. R. Resonance raman spectra of iron(III)-, copper(II)-, cobalt(III)-, and manganese(III)-transferrins and of bis(2,4,6-trichlorophenolato)diimidazolecopper(II) monohydrate, a possible model for copper(II) binding to transferrins *Biochemistry* 1976, *15*, 4918

33. Gunter, T. E.; Gerstner, B.; Gunter, K. K.; Malecki, J.; Gelein, R.; Valentine, W. M.; Aschner, M.; Yule, D. I. Manganese transport via the transferrin mechanism *NeuroToxicology* 2013, *34*, 118

34. Scheuhammer, A. M.; Cherian, M. G. Binding of manganese in human and rat plasma *Biochimica et Biophysica Acta* 1985, *840*, 163

35. Schake, A. R.; Schmitt, E. A.; Conti, A. J.; Streib, W. E.; Huffman, J. C.; Hendrickson, D. N.; Christou, G. Preparation and properties of mononuclear and ferromagnetically coupled dinuclear manganese complexes with 2,2'-biphenoxide *Inorg.* 1991, *30*, 3192

36. O'Hara, P.; Yeh, S. M.; Meares, C. F.; Bersohn, R. Distance between metal-binding sites in transferrin: energy transfer from bound terbium(III) to iron(III) or manganese(III) *Biochemistry* 1981, *20*, 4704

37. Harris, W. R.; Chen, Y. Electron paramagnetic resonance and difference ultraviolet studies of Mn^{2+} binding to serum transferrin *J. Inorg. Biochem.* 1994, *54* , 1

38. Keefer, R. C.; Barak, A. J.; Boyett, J. D. Binding of manganese and transferrin in rat serum *Biochim. Biophys. Acta.* 1970, *221* (2), 390

39. Panić, B. In vitro binding of manganese to serum transferrin in cattle *Scand* 1967, *8*, 228

40. Gibbons, R. A.; Dixon, S. N.; Hallis, K.; Russell, A. M.; Sansom, B. F.; Symonds, H. W. manganese metabolism in cows and goats *Biochim. Biophys. Acta* 1976, *444*, 1

41. Davidsson, L.; Lönnerdal, B.; Sandström, B.; Kunz, C.; Keen, C. L. Identification of transferrin as the major plasma carrier protein for manganese introduced orally or intravenously or after in vitro addition in the rat *J. Nutr.* 1989, *119*, 1461

42. Moutafchiev, D.; Sirakov, L.; Bontchev, P. The competition between transferrins labeled with ^{59}Fe, ^{65}Zn, and ^{54}Mn for the binding sites on lactating mouse mammary gland cells *Biol. Trace Elem. Res.* 1998, *61*, 181

43. Edwards, K. C.; Kim, H.; Vincent, J. B. Release of trivalent chromium from serum transferrin is sufficiently rapid to be physiologically relevant *J. Inorg. Biochem.* 2020, *202*, 110901

44. Edwards, K. C.; Kim, H.; Ferguson, R.; Lockart, M. M.; Vincent, J. B. Significance of conformation changes during the binding and release of chromium(III) from human serum transferrin *J. Inorg. Biochem.*2020, *206*, 111040

45. Deng, G.; Wu, K.; Cruce, A. A.; Bowman, M. K.; Vincent, J. B. Binding of trivalent chromium to serum transferrin is sufficiently rapid to be physiologically relevant *J. Inorg. Biochem.* 2015, *143*, 48

46. Aramini, J. M.; Vogel, H. J. Aluminum-27 and carbon-13 NMR studies of aluminum(3+) binding to ovotransferrin and its half-molecules *J. Am. Chem. Soc.* 1993, *115*, 245

47. Petasis, D. T.; Hendrich, M. P. Quantitative interpretation of multifrequency multimode epr spectra of metal containing proteins, enzymes, and biomimetic complexes *Methods Enzymol.* 2015, 171

48. Abragam, A.; Bleaney, B. *Electron paramagnetic resonance of transition ions*; Clarendon Press: Oxford, 2013

49. Hendrich, M. P.; Debrunner, P. G. Integer-spin electron paramagnetic resonance of iron proteins *Biophys. J.* 1989, *56*, 489

50. Weil, J. A.; Bolton, J. R. *Electron paramagnetic resonance: elementary theory and practical applications*; Wiley: Hoboken, N.J, 2007

51. Folajtar, D. A.; Chasteen, N. D. Measurement of nonsynergistic anion binding to transferrin by epr difference spectroscopy *J. Am. Chem. Soc.* 1982, *104*, 5775

52. Tao, L.; Stich, T. A.; Soldatova, A. V.; Tebo, B. M.; Spiro, T. G.; Casey, W. H.; Britt, R. D. Mn(III) species formed by the multi-copper oxidase MnxG investigated by electron paramagnetic resonance spectroscopy *J. Biol. Inorg. Chem.* 2018, *23*, 1093

53. Pierce, B. S.; Hendrich, M. P. Local and global effects of metal binding within the small subunit of ribonucleotide reductase *J. Am. Chem. Soc.* 2005, *127*, 3613

54. Campbell, K. A.; Force, D. A.; Nixon, P. J.; Dole, F.; Diner, B. A.; Britt, R. D. Dual-mode EPR detects the initial intermediate in photoassembly of the photosystem II Mn cluster: the influence of amino acid residue 170 Of The D1 polypeptide on Mn coordination *J. Am. Chem. Soc.* 2000, *122*, 3754

55. Campbell, K. A.; Yikilmaz, E.; Grant, C. V.; Gregor, W.; Miller, A.-F.; Britt, R. D. Parallel polarization EPR characterization of the Mn(III) center of oxidized manganese superoxide dismutase *J. Am. Chem. Soc.* 1999, *121*, 4714

56. Gupta, R.; Taguchi, T.; Borovik, A. S.; Hendrich, M. P. Characterization of monomeric MnII/III/IV–hydroxo complexes from X- and Q-Band dual mode electron paramagnetic resonance (EPR) spectroscopy *Inorg. Chem.* 2013, *52*, 12568

57. Zheng, M.; Khangulov, S. V.; Dismukes, G. C.; Barynin, V. V. Electronic structure of dimanganese(II,III) and dimanganese(III,IV) Complexes and dimanganese catalase enzyme: a general EPR spectral simulation approach *Inorg. Chem.* 1994, *33*, 382

58. Gerritsen, H. J.; Sabisky, E. S. Paramagnetic resonance of trivalent manganese in rutile (TiO2) *Phys. Rev.* 1963, *132*, 1507

59. Peloquin, J. M.; Campbell, K. A.; Randall, D. W.; Evanchik, M. A.; Pecoraro, V. L.; Armstrong, W. H.; Britt, R. D. ^{55}Mn ENDOR of the S2-state multiline EPR signal of photosystem II: implications on the structure of the tetranuclear Mn cluster *J. Am. Chem. Soc.* 2000, *122*, 10926

60. Krzystek, J.; Telser, J.; Pardi, L. A.; Goldberg, D. P.; Hoffman, B. M.; Brunel, L.-C. High-frequency and field electron paramagnetic resonance of high-spin manganese(III) in porphyrinic complexes *Inorg. Chem.* 1999, *38*, 6121

61. Zhu, W.; Wilcoxen, J.; Britt, R. D.; Richards, N. G. Formation of hexacoordinate Mn(III) in bacillus subtilis oxalate decarboxylase requires catalytic turnover *Biochemistry* 2016, *55*, 429

62. Sheng, Y.; Stich, T. A.; Barnese, K.; Gralla, E. B.; Cascio, D.; Britt, R. D.; Cabelli, D. E.; Valentine, J. S. Comparison of two yeast MnSODs: mitochondrial saccharomyces cerevisiae versus cytosolic candida albicans *J. Am. Chem. Soc.* 2011, *133*, 20878

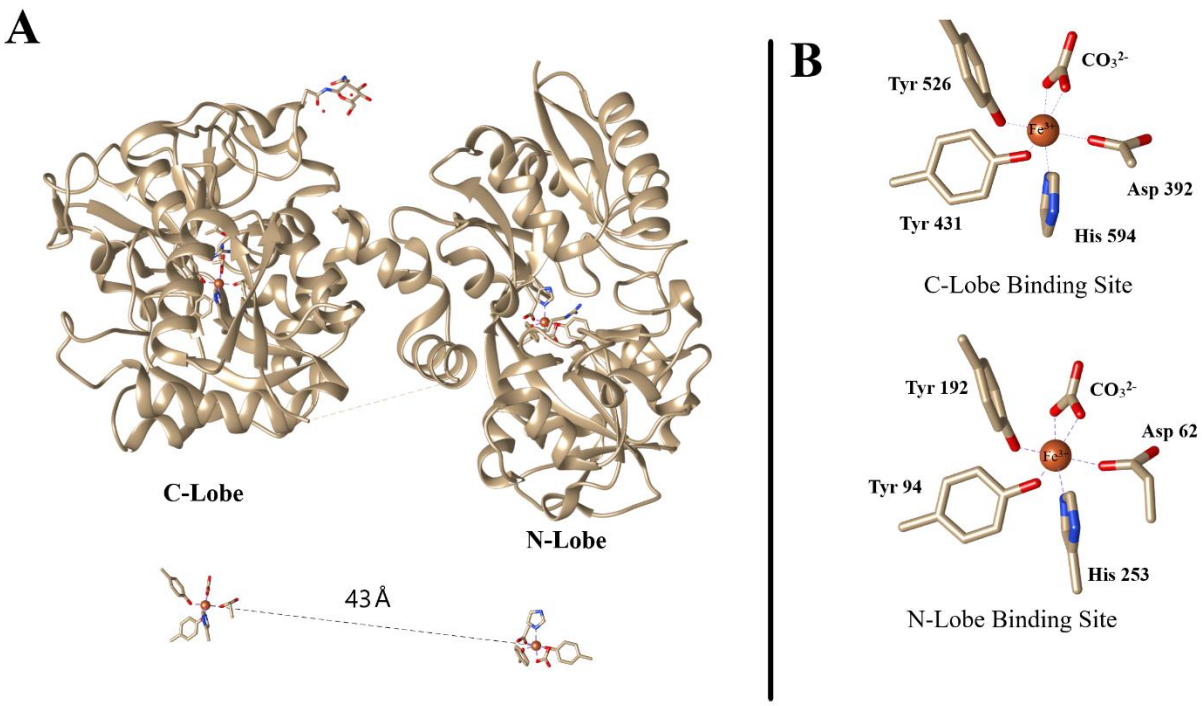

Figure 6.1. A X-ray crystallographic structure for porcine $Fe(III)_2$-Tf (pbd code 1H76) illustrating the distance separating the N-terminal from the C-terminal Fe-binding sites; no structure is yet available for the closed conformation of human $Fe(III)_2$-Tf. However, the porcine protein provided ligands are identical to those in the human protein. B. Comparison of the C-lobe and N-lobe metal binding sites of porcine $Fe(III)_2$-Tf.

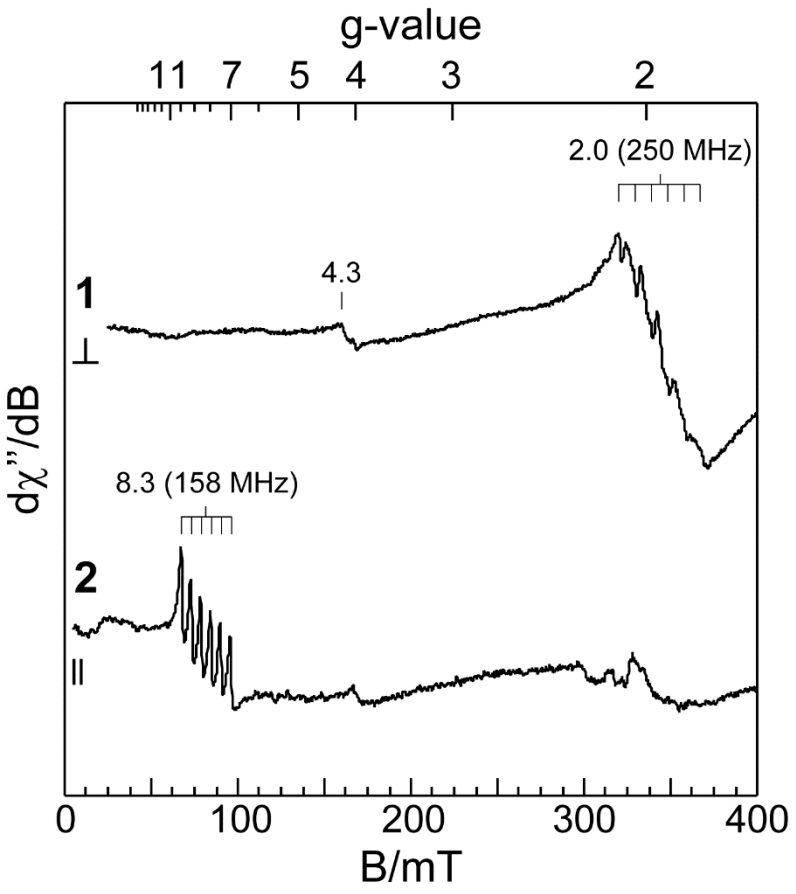

Figure 6.2. Perpendicular and parallel mode X-band (9 GHz) CW EPR spectra of 0.38 mM $Mn(III)_2$-Tf. Instrumental parameters: microwave frequency, 9.64 GHz (perpendicular) and 9.41 GHz (parallel); microwave power, 20 mW; modulation amplitude, 0.9 mT; temperature, 15 K.

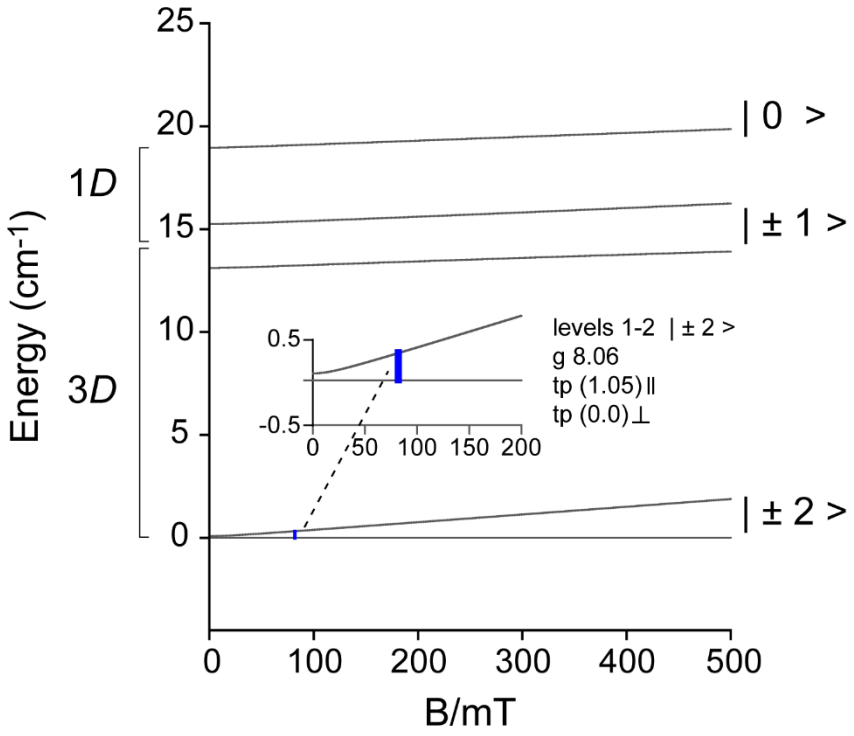

Figure 6.3. Energy level diagram illustrating the splitting of doublets within the Mn(III) $S = 2$ spin system. For clarity, only the splitting along the z-principle axis is shown. The observed transition within the ground, | ± 2> doublet is highlighted and transition probabilities (tp) are shown for both transverse and parallel field polarizations. The energy level was calculated using the same zero field splitting parameters and g-values identified by simulation of the $Mn(III)_2$-Tf EPR spectra (Shown in Figure 6.2). [$S = 2$; $D = -5.0$ cm^{-1}; E/D, 0.08; $g_{1,2,3}$ (2.01, 2.01, 2.02)].

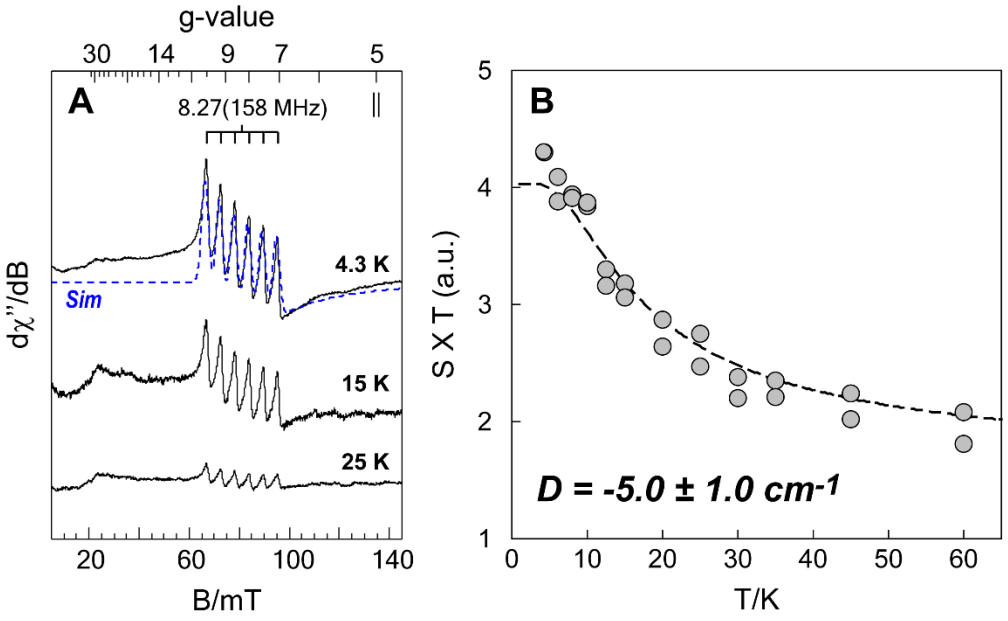

Figure 6.4. A. Parallel mode CW-EPR spectra (*black traces*) of $Mn(III)_2$-Tf at selected temperatures (4.3, 15, and 25 K). The intensities of all spectra are normalized for temperature to correct for Curie Law. For comparison, quantitative EPR simulation (*dashed line*) is overlaid on the data. Instrumental parameters: microwave frequency, 9.41 GHz; microwave power, 21.12 mW; modulation amplitude, 0.9 mT. Simulation parameters: S = 2; I = 5/2 (100% abundance); D = -5.0 cm^{-1}; E/D, 0.08; $g_{1,2,3}$ (2.01, 2.01, 2.02); $\sigma_{E/D}$ = 0.007; $A_{1,2,3}$(155, 155, 160) MHz; σ_B, 0.6 mT. B. Temperature normalized signal intensity (S × T) of the Mn(III) g ~ 8.3 resonance as a function of temperature. The axial zero field splitting (D = -5.0 ± 1.0 cm^{-1}) for Mn(III) was modeled by fitting the temperature normalized data to a Boltzmann population distribution (*dashed line*) for a transition within the ground | ±2 > doublet of a S = 2 spin system.

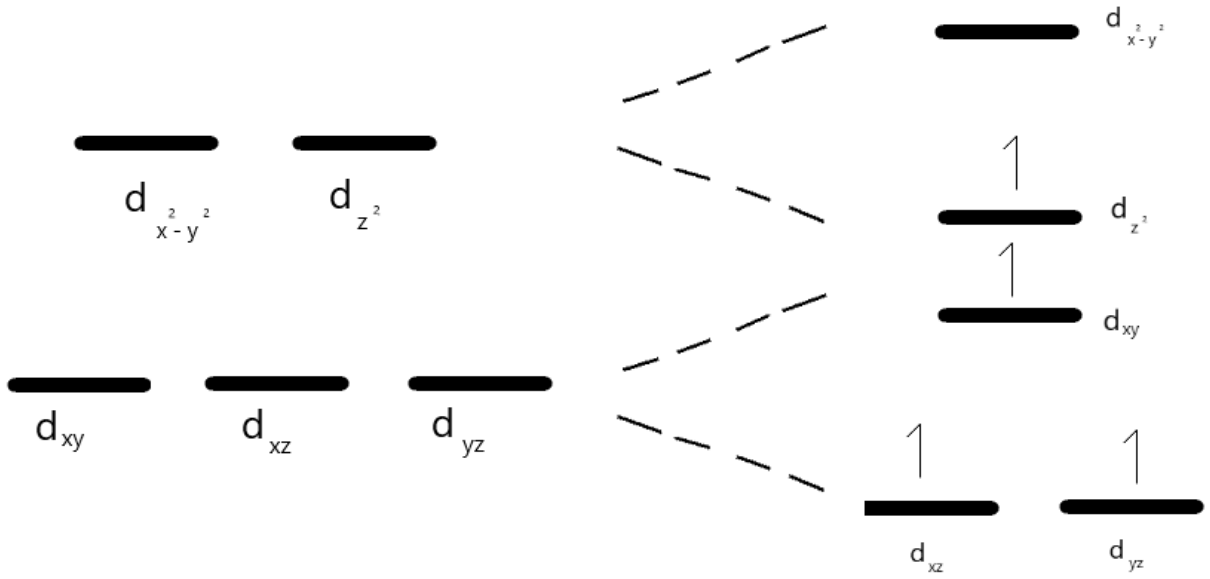

Figure 6.5. Representation of the d-orbital splitting in Mn(III)-Tf.

CONCLUSIONS

Accurate understanding of Cr(III)'s biochemistry is critically important for designing experiments probing its potential therapeutic effects. Many previous studies investigating Cr(III)'s action in glucose metabolism and body mass composition are inconsistent in their findings due in large part to their inconsistent methodologies. The duration of the studies, amount of Cr(III) administered, and forms of Cr(III) administered vary widely with poor consensus on appropriate standards. The mechanism of transport of Cr(III) from blood into cells and bioactive forms of Cr(III) have been speculated, but only a few studies have tested the purposed mechanism's plausibility. In this dissertation, several experiments testing the plausibility of a mechanism for Cr(III) transport utilizing the endosome-mediated transferrin (Tf) pathway are presented providing evidence as to the identity of the physiological transporter of Cr(III) into cells. The binding and release of metals by Tf, factors effecting Tf's ability to bind and release the metals, and possible ligands for removal of Cr(III) from Tf are examined.

In Chapter 2, the ability for Cr(III) to be lost from Tf under endosomal conditions was examined. CW-EPR was used to examine the status of the Cr(III) throughout the experiment. CW-EPR spectra of human Cr_2-Tf at pH 7.4 allowed for Cr(III) bound at the metal binding site of the two different lobes, C-Lobe and N-Lobe, to be distinguished as their EPR features have unique g-values and shapes. Cr_2-Tf was acidified in the presence or absence of ascorbic acid, EDTA, or citric acid to pH 4.5 and 5.5, and aliquots were taken to monitor the status of the Cr(III). Cr(III) bound to the C-lobe of Tf was found to be lost rapidly at both pH 4.5 and pH 5.5, with a small enhancement of rate occurring at pH 4.5. The presence or absence of a potential

chelating ligand had no effect on the rate of this loss of Cr(III) from the C-lobe. The loss of Cr(III) from the N-lobe of Tf was significantly slower. The loss of Cr(III) from this lobe of Tf was sensitive to pH being twice as rapid at pH 4.5 compared to pH 5.5. The presence of a potential chelating ligand did have an effect on the rate of loss of Cr(III) from the N-lobe. The rate of loss of Cr(III) was accelerated ~2 fold by the presence of a potential chelating ligand; however, the identity of the ligand did not have an effect on the enhancement of the rate of loss of Cr(III). The ligand, therefore, appears to be helping to displace the synergistic bicarbonate or binding to an allosteric site on the protein, rather than directly competing with the binding site for binding Cr(III). Loss of Cr(III) from the C-lobe of Tf was concluded to be feasible for Cr(III) transport via Tf-mediated endocytosis to occur, but N-lobe Cr(III) loss would only deliver a fraction of the loaded Cr(III) under these conditions.

The receptor protein, transferrin receptor (TfR), has a known effect in modulating the rate of Fe(III) loss from the acidified Fe_2-Tf-TfR complex. The loss of Cr(III) from the Cr_2-Tf-TfR complex was subsequently investigated in Chapter 3. Isolation and purification of TfR in its soluble portion (sTfR) was outlined, using a slightly modified procedure from literature. Because a bovine source was used to isolate the sTfR, loss of Cr(III) from bovine Tf alone was measured to establish if the Cr(III) loss from bovine Tf was similar Cr(III) loss from human Tf. Cr(III) loss from the Cr_2-Tf-sTfR complex was found to be very rapid compared with loss from Cr_2-Tf alone. This loss of Cr(III) from the complex indicated that Cr(III) could reasonably be transported by Tf-mediated endocytosis; however, the loss of Cr(III) from the complex indicating that some unknown ligand would likely be required to bind Cr(III) was followed by non-specific Cr(III) binding to Tf as it was lost from the complex. Additionally, the conformation of the bovine Tf

had an effect on the CW-EPR features of Cr-Tf and might be the cause of the accelerated loss of the Cr(III) from bovine Tf compared to human Tf. This was investigated in detail in Chapter 4.

The binding of Cr(III) to Tf had previously been investigated, which demonstrated a first order dependence of the concentration of bicarbonate, but whether the protein undergoes any conformational changes during the binding of Cr(III) was unknown. In Chapter 4, a combination of UV-Vis, CW-EPR, and pulsed EPR experiments were utilized to demonstrate that subsequent to the binding of Cr(III) ions to Tf, the Cr_2-Tf undergoes conversion into several conformations. The formation of the first conformation involves the binding of Cr(III), is complete in ~ 15 min, and is accompanied with a large change in the 245 nm absorbance resulting from binding of Cr(III) to tyrosine residues. The three-pulse ESEEM spectra of Cr_2-Tf incubated for 5 min had a feature at 4 MHz corresponding to coupling between the Cr(III) and a nearby ^{14}N, likely from the histidine residue in the binding pocket, indicating that both the tyrosine and histidine are bound in the first conformer and that changes in ligand about the Cr(III) were not occurring between this and subsequent conformers. Conformer 2 is characterized by distinct EPR features in the g ~5.42 region that resemble those of Cr_2-Tf when complexed with its receptor. Conformer 2 reaches a maximum at ~120 min and can be considered the most physiologically relevant conformer given the half-life of circulating holo-Tf (~90 min). After the EPR feature at g ~ 5.42 from conformer 2 reaches its maximum intensity, the feature decays with the simultaneous appearance of EPR features at g ~ 5.66 and 5.08 typically ascribed to Cr(III)-bound in the N-lobe of Tf. These new features are attributed to the third conformer of Tf that is generated when Cr(III) is incubated with Tf for more than 24 hr in 25 mM bicarbonate or for two weeks in ambient bicarbonate. Loss of Cr(III) from Tf in conformer 2 proceeds more rapidly than from the

previously used conformer 3, but not as rapidly as the Tf-TfR complex demonstrating the significance of conformation of Tf in the release of metals following acidification.

In earlier chapters, the loss of Cr(III) from Cr_2-Tf was shown to result in the formation of non-specifically bound Cr(III) to the surface of Tf. Efforts were undertaken to identify a potential ligand that could bind Cr(III)-Tf under endosomal conditions and compete with this non-specific binding as described in Chapter 5. The oligopeptide low-molecular-weight chromium-binding substance (LMWCr) is known to bind up to 4 Cr(III) ions with high affinity and is known to carry Cr(III) from the bloodstream to the urine. The rate of Cr(III) loss from Cr_2-Tf under endosomal conditions and the rate of formation of Cr(III) bound to LMWCr were found to be slow in respect to an endosomal cycle; however, these rates were found to be sufficiently accelerated in the presence of sTfR to feasibly occur during endocytosis. These results suggest that LMWCr may function to bind Cr(III) released in the endosome for transport into the cell.

Tf is known to bind metals other than Fe(III) and is suspected to play a potential role in their transport similar to the apparent case of Cr(III). The transport of Mn(III) is thought to be accomplished by Tf, but studies investigating this are limited by available spectroscopic tools to probe Mn(III)-Tf interactions. In Chapter 6, the first parallel mode EPR signal of Mn(III) bound to Tf as is reported. The EPR signal at $g \sim 8.3$ exhibits the characteristic 6-line hyperfine splitting of Mn and can be attributed to Mn(III) in the metal binding site of Tf. Temperature dependence and simulation of the EPR features indicate the Mn(III) is in an elongated tetragonal environment, corroborating that the Mn(III) is in the metal binding site of Tf and indicating that the coordination number and active site geometry do not differ significantly relative to native $Fe(III)_2$-Tf. The EPR signal presents an useful tool for future studies investigating the

physiological significance of Mn(III)-Tf, as well as acting as a spectroscopic model for other Mn(III)-dependent proteins.

This dissertation provides evidence the Tf-mediated endosomal pathway is the process by which Cr(III) moves from blood into cells. Transport of Cr(III) throughout the body was known to include several steps, but a comprehensive pathway had not been elucidated. A working model which shows steps in Cr transport known from Cr(III)'s absorption to its ultimate excretion in urine is shown in Figure 7.1. The story is not complete however, for example, how Cr-LMWCr formed in the endosome exits into the cell cytosol is not known. Whether LMWCr acts as an ionophore is an area worthy of investigation. Another question is whether mixed Cr/Fe-Tf can deliver Cr(III) in a similar fashion to Cr_2-Tf as monoferric Tf is the major form of Tf in the bloodstream. The techniques developed in this dissertation should be directly applicable to studying metal release from Cr/Fe-Tf species. Lastly, how LMWCr interacts with Fe(III) under endosomal conditions as to whether it binds in acidic media and its plausibility as a transient species in the endosome could be explored with techniques outlined in this dissertation.

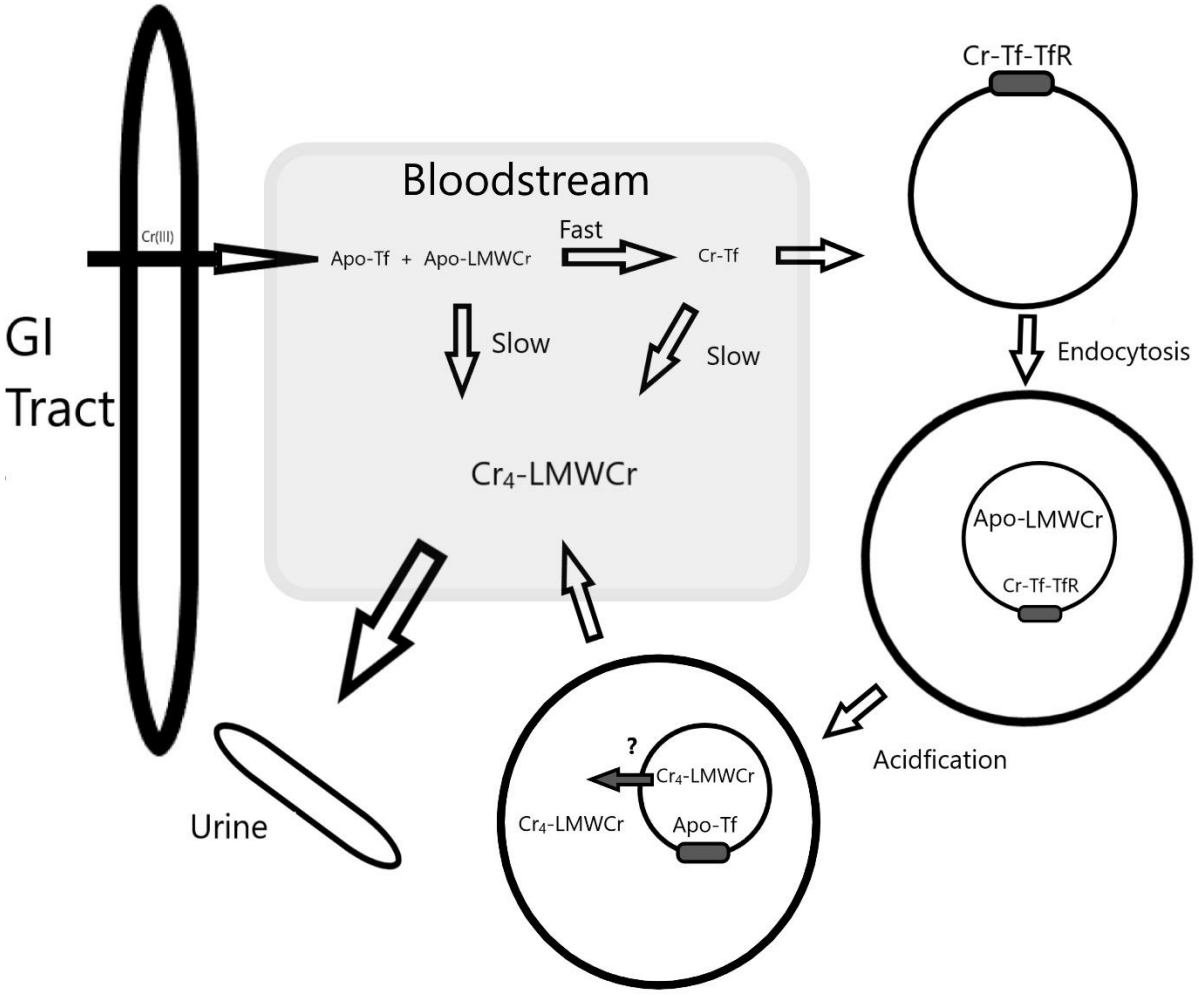

Figure 7.1. Purposed pathway of Cr(III) from gastrointestinal track to urine. Unknown step is shown as grey arrow.